



UNIVERSITÀ DI PISA

FACOLTÀ DI INGEGNERIA

Relazione per il conseguimento della Laurea Magistrale in
Ingegneria Meccanica

ALTERNATIVE 3D MODELING THROUGH THE USE OF ULTRASOUND TECHNOLOGY: ANALYSIS AND TESTS

Relatori

Dott. Ing. Gualtiero Fantoni

.....
Ing. Jacopo Tilli

Il Candidato

Dott. Sergio Currenti

Dipartimento di Ingegneria Civile e Industriale

Anno accademico 2013-2014

INDICE

1	INTRODUCTION.....	7
2	STATE OF THE ART	9
2.1	Ultrasound technology	9
2.2	Ultrasonic impact grinding (UIG)	10
2.3	Micro-motion devices technology.....	12
2.4	Vitrectomy probe	12
2.5	Fixation of bone fractures	14
2.6	Manufacturing of polymer micro parts.....	15
2.7	Ultrasonic soldering in electronics.....	16
2.8	Processing of mica/epoxy nanocomposites by ultrasound mixer.....	17
2.9	Spray head	18
2.10	Cleaning devices	20
2.11	Reducing and eliminating foaming of liquid products	20
3	SHAPING OF FOAM-LIKE MATERIALS	24
3.1	Introduction.....	24
3.2	State of the art	25
3.3	Experimental setup	26
3.4	Ultrasound technology	26
3.5	Parameters measurement	26
3.6	Sample analysis	27
3.7	Experimental results	29
3.8	Working principle	29
3.9	Polystyrene.....	30
3.10	Polyurethane	33
4	UNDERWATER DRILLING OF FOAM-LIKE MATERIALS AND WAX.....	38
4.1	Introduction.....	38
4.2	State of the art	39
4.3	Experimental setup	40
4.4	Ultrasound technology	40
4.5	Parameters measurement	40

4.6	Input parameters	42
4.7	RESULTS.....	42
4.8	Foam-like materials	43
4.9	Wax.....	47
5	OBJECT SHAPING WITH A SONOTRODE	51
5.1	Introduction.....	51
5.2	State of the Art.....	52
5.3	Methodology	53
5.4	Milling	56
5.5	Turning	57
5.6	Analysis of the results.....	59
5.7	Dimensional Analysis.....	59
5.8	Material Analysis	66
6	ULTRASOUND PROPAGATION IN WATER.....	70
6.1	Problem analysis	70
6.2	Problem modeling.....	71
6.3	Enhancements of focused ultrasound.....	71
6.3.1	State of the art: HIFU.....	72
6.3.2	HIFU mechanisms and bioeffects	74
6.4	Sonotrode horn shaping	76
6.5	FEM analysis	78
6.6	Results	79
7	Conclusion and future works.....	85
7.1	Conclusion.....	85
7.2	Future works.....	86
8	BIBLIOGRAFIA.....	87
8.1	References	90

INDICE DELLE FIGURE

Figure 1.1. Polyurethane applications.	7
Figure 1.2. Ultrasonic Vibrations produced by a converter and transmitted by a sonotrode.....	8
Figure 2.1. Ultrasonic machining.	11
Figure 2.2. A sketch of a head assembly of a magnetostrictively driven UIG machine.	11
Figure 2.3. Cross-sectional view of an eye in which a cutter of a vitrectomy probe extends into a posterior segment of the eye.....	13
Figure 2.4. Vitrectomy probe having a cutter with an adjustable-sized cutting port.....	13
Figure 2.5. Section view of a bone screw.....	14
Figure 2.6. Plasticization with ultrasound: course of the process.....	16
Figure 2.7. Exemplary spray device.	18
Figure 2.8. Schematic diagram of one embodiment of an ultrasonic cleaning device.	20
Figure 2.9. Perspective view of an example of realization of a sonotrode device.	22
Figure 3.1. Top view of the experimental setup: (a) the translation stage, (b) load cell, (c) sonotrode and (d) power supply (d). The sample (e) is fixed on the load cell.....	28
Figure 3.2. Graphs of the average force exerted on Polystyrene sample, varying the feed rate value at the amplitude 100 μm	30
Figure 3.3. Force exerted by the sonotrode on polystyrene samples ($v = 5 \text{ mm/s}$, amplitude 100 μm).	31
Figure 3.4. Maximum force exerted by the sonotrode on Polystyrene samples ($v = 1 \text{ mm/s}$), varying the amplitude.	32
Figure 3.5. Samples of Polystyrene obtained with the same set of input parameters ($v = 1 \text{ mm/s}$, amplitude 60 μm).	33
Figure 3.6. Force exerted by the sonotrode on polyurethane samples ($v = 5 \text{ mm/s}$, Amplitude = 100 μm).	34
Figure 3.7. Maximum force exerted by the sonotrode on polyurethane samples ($v = 1 \text{ mm/s}$), varying the amplitude.....	35
Figure 3.8. Samples of Polyurethane obtained with the same set of parameters ($v = 1 \text{ mm/s}$, amplitude 60 μm).	36
Figure 4.1. Scheme of the holding structure of the sonotrode.	41
Figure 4.2. Frontal picture of the experimental setup.....	41
Figure 4.3. Comparison between the force exerted for the same machining parameters ($v = 1 \text{ mm/s}$, amplitude 80 μm) on Polystyrene samples.	43
Figure 4.4. Comparison between the force exerted for the same machining parameters ($v = 1 \text{ mm/s}$, amplitude 80 μm) on Polyurethane samples.....	44
Figure 4.5. Comparison between the force exerted on Polystyrene samples with different working parameters.	45
Figure 4.6. Comparison between the force exerted on Polyurethane samples with different working parameters.	45
Figure 4.7. Differences between (a) the sample of Polystyrene machined in in-air configuration and (b) the underwater machined sample ($v = 1 \text{ mm/s}$, amplitude 100 μm).	46
Figure 4.8. Differences between (a) the sample of Polyurethane machined in in-air configuration and (b) the underwater machined sample ($v = 1 \text{ mm/s}$, amplitude 100 μm).	47
Figure 4.9. Different behavior of Wax when machined (a) in air and (b) underwater.	48

Figure 4.10. Screenshots of Wax underwater machining video.	49
Figure 4.11. Force exerted for the same machining parameters ($v = 1 \text{ mm/s}$, amplitude $80\mu\text{m}$) on Wax samples.	50
Figure 5.1. The three operations that can be performed with the sonotrode: axial removal operation (a), the longitudinal removal translation (b) and their combination (c).	54
Figure 5.2. Comparison between the milling operation with the sonotrode (left) and with a traditional cutter (right).	55
Figure 5.3. The picture shows the material that is undergoing to the deformation process (a) and the same material after the machining process (b).	55
Figure 5.4. Difference between the CAD theoretical design (a) and the object shaped with the ultrasound technology (b).	57
Figure 5.5. Scheme of the setup for the ultrasound machining on lathe (a) and the real setup (b). Because of the dimensions of the sonotrode, the only operation possible was the face grooving. ..	57
Figure 5.6. Shapes created on Polystyrene: circles (a), cylinder (b) and spiral (c).	58
Figure 5.7. Shapes created on Polyurethane samples: cylinders (a) and spiral (b). The quality of the machined piece is coarse.	58
Figure 5.8. Scheme of the assembled optical dental scanner (a) and real setup (b).	60
Figure 5.9. Spiral on Polystyrene block with highlighted significant points and measures [mm]: center of rotation (O), initial point (A), point where the material has been torn (B) and point from which the machining operation is fully satisfactory (C).	61
Figure 5.10. Spiral on Polyurethane block with highlighted significant points: center of rotation (O), initial point (A), point where the material starts melting even if not in contact with the sonotrode (B) and point from which the machining quality worsens (C).	62
Figure 5.11. Comparison between the manufactured pyramid and the CAD model: top (a), side (b) and isometric (c) views.	63
Figure 5.12. Deviation of the specimen from the CAD model versus percentage of points for the grooved cylinder.	63
Figure 5.13. Comparison between perfectly cylindrical surfaces and the real machined surface for the section of the specimen indicated on the left.	64
Figure 5.14. Deviation of the specimen from the CAD model versus percentage of points for the grooved circles for the section illustrated in Figure 5.13.	64
Figure 5.15. Deviation of the bottom surface of the grooved cylinder from an ideal planar surface.	65
Figure 5.16. Deviation of the specimen from the CAD model versus percentage of points for the grooved circles for the section illustrated in Figure 5.15.	65
Figure 5.17. Comparison of the whole bottom surface of the grooved cylinder. The blue areas indicate where the axis of the sonotrode has passed. The deviation values are in millimeters.	66
Figure 5.18. Polystyrene SEM analysis: (a) untreated, (b) thermal altered, (c) in-air machined and (d) underwater machined Polystyrene samples.	68
Figure 5.19. Polyurethane SEM analysis: (a) untreated, (b) thermal altered, (c) in-air machined and (d) underwater machined Polyurethane samples.	69
Figure 6.1. Focus point deriving from different geometrical conditions.	72
Figure 6.2. HIFU working principle.	72
Figure 6.3. HIFU as an alternative treatment for localized prostate cancer.	74

1 INTRODUCTION

Polyurethanes are one of the most versatile plastic materials. The nature of the chemistry allows polyurethanes to be adapted to solve challenging problems, to be molded into unusual shapes and to enhance industrial and consumer products. The market for polyurethanes is large and growing; it is estimated that recently around 20 million tons were produced per year and the sector was worth ca. \$50 billion per annum.

In facts, polyurethanes can be used in different kinds of industrial productions, from automotive to footwear applications, or even as an adhesive or a building material. Finished products containing polyurethane are mattresses and seats, home insulation, shoes, packaging materials, glues and coatings for wires, piping and many other surfaces.



Figure 1.1. Polyurethane applications.

The aim of our work is to study and investigate drilling operation on Polyurethane blocks, using ultrasound technique.

This kind of usage is by now an unexplored field for ultrasonic devices, therefore we believe that great developments could be realized, analysing the process and making experiments directed to evaluate which process inputs, like speed, amplitude or even the sonotrode shape, have a significant impact on the final manufacturing.

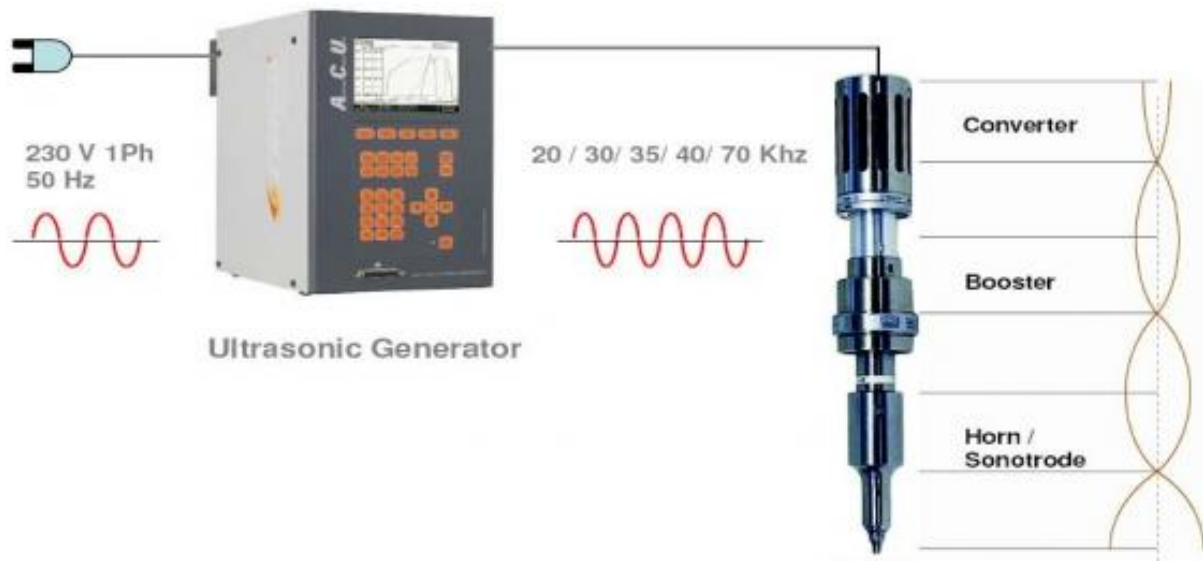


Figure 1.2. Ultrasonic Vibrations produced by a converter and transmitted by a sonotrode.

We will try to drill Polyurethane workpiece first in air and then in water, with different process parameters: force, speed, temperature, frequency, amplitude.

Afterwards we will evaluate the result of our tests, with visual measures (optical, SEM, TEM, etc..) and with traction and flexion testing.

Finally we will reproduce the process using a CAD program, in order to validate and improve our studies. This includes changes in alimentation (H_2O) as well as redesign of the head of the sonotrode.

We will finally discuss the conclusion of the work and possible future developments.

2 STATE OF THE ART

2.1 Ultrasound technology

Ultrasonic machining is traditionally employed to machine hard and brittle materials (both electrically conductive and non conductive material), with the use of a vibrating sonotrode. The process was first developed in 1950s and was originally used for finishing EDM surfaces. Afterwards a new technique has been developed: ultrasonic impact grinding (UIG) (*Section 2.2*), which can be used to fabricate small, even ornate patterns in brittle materials such as silicon, glass and ceramics. In UIG the tool head vibrates vertically at the resonance frequency (in the range of 20–28 kHz) of the compound system, which comprises the transducer, transmitting cone, tool cone and tool head. Abrasive slurry (typically silicon carbide or boron carbide abrasive grit mixed with water) is passed over the working material and is thus squeezed in between the work piece and the tool, and the minute ultrasonic pounding is responsible for the grinding.

Ultrasound is a technology used to create actuators, too. In fact, ultrasonic motors belong to a category of micro-motion devices (*Section 2.3*), characterized by the absence of noise during operation, with high torque-weight ratio, highly accurate speed, and position control. Typical applications of this kind of devices are chip assembly in the semiconductor industry, cell manipulation in biotechnology, and automatic surgery in medicine.

In ophthalmology in cataract surgery an ultrasonic probe is used to break up and remove a clouded crystalline lens from the eye (*Section 2.4*), another use in surgery is a device for fixation of bone fractures (*Section 2.5*).

There are also processes where a material is cyclically deformed at ultrasonic frequencies, that is an alternative approach to process small amounts of a thermoplastic material (*Section 2.6*). The generated melt can be filled into micro cavities, so that the system can produce micropolymer parts in one process step. In January 2014 an ultrasonic welding device for components in power electronic modules has been patented.

In electronics ultrasonic soldering (*Section 2.7*) ensures local and mainly contactless effect of the heating source, besides there is the advantage of creating new possibilities of joining materials with different chemical structures and properties.

There are many other fields in which ultrasound technology is used, some are for example ultrasound mixing, a way to process Mica/Epoxy Nanocomposites (*Section 2.8*) and active micromixer for microfluidic systems, a method using ultrasonic vibration.

Recently many other kind of devices were patented: in 2005 an apparatus for applying adhesive onto a joining surface of an adherend, which eliminates laborious clearing and surface-pretreatment steps; in 2013 a spray head including a sonotrode has been assigned to L'Oreal (*Section 2.9*), the sonotrode having an end collar defining an ejection surface for ejecting particles of Composition; a method and a device for a mechanical dewatering process of a fiber web using ultrasound has been patented; enhanced ultrasonic cleaning devices have been invented (*Section 2.10*), in order to remove soils using ultrasonic waves; in January 2014 a de-foaming device has been patented (*Section 2.11*), a sonotrode for generating an ultrasonic field in industrial production processes such as chemical, food, petroleum, pharmaceutical, beverage or mining-related processes for reducing and eliminating foaming of liquid products.

2.2 Ultrasonic impact grinding (UIG)

Ultrasonic impact grinding (UIG) is an old but virtually unknown technique which can be used to fabricate small, even ornate patterns in brittle materials such as silicon, glass and ceramics. Although suited primarily for brittle materials, UIG has been used to prepare metallic foils and metal composites.

The tool head vibrates vertically at the resonance frequency (in the range of 20–28 kHz) of the compound system, illustrated in Figure 2.1, which comprises the transducer, transmitting cone, tool cone and tool head. Abrasive slurry (typically silicon carbide or boron carbide abrasive grit mixed with water) is passed over the working material and is thus squeezed in between the work piece and the tool, and the minute ultrasonic pounding is responsible for the grinding.

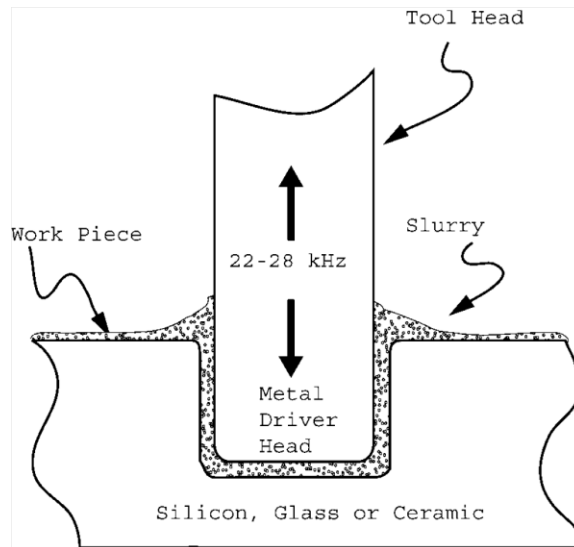


Figure 2.1. Ultrasonic machining.

The heart of the machine used is a magnetostrictive ultrasonic transducer (Figure 2.2). Feeding electrical current to the exciting coil at an ultrasonic frequency will induce an alternating magnetic field in the stack of nickel laminates, which in turn will minutely alter the physical dimensions of the stack at the ultrasonic frequency.

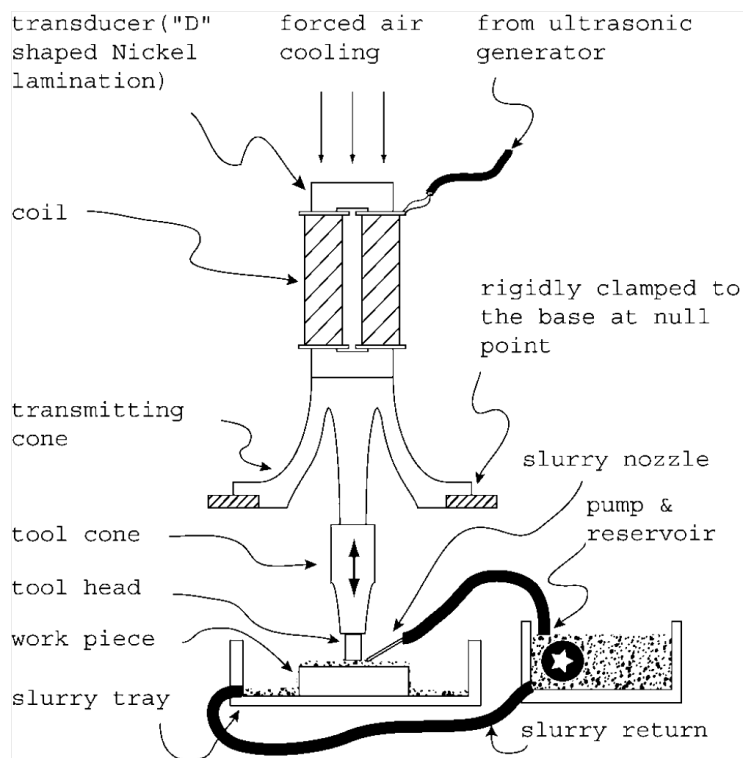


Figure 2.2. A sketch of a head assembly of a magnetostrictively driven UIG machine.

By using UIG one can achieve such structures, up to millimeters in depth in virtually no time. Furthermore, in silicon substrates, the orientation or any other physical dimension of the feature will no longer be constrained as in anisotropic etching by the crystallographic planes and directions; and in amorphous glass or ceramic substrates, features with vertical walls can be achieved, otherwise usually accomplished only by expensive laser ablation.

2.3 Micro-motion devices technology

Nowadays, industry is quite interested in using precision manufacturing and assembly for small parts with a size ranging from very few millimeters down to micrometers. Also, there exists a worldwide interest in micro tools. Micro-motion devices [2] that can perform very small motions with very high positioning accuracy potentially have wide application in industry. Typical applications are chip assembly in the semiconductor industry, cell manipulation in biotechnology, and automatic surgery in medicine.

Micro-motion systems technology is classified into three major systems: actuators, manipulator systems for micro motion, and compliant mechanisms for micro motion. The main goal of actuators for micro motion is to create a linear motion between the input and output signals. The main goal of the manipulator systems for micro motion is to create a non-linear motion between the input and output signals, in addition to a long motion range with small resolution. Finally, the main goal of compliant mechanisms is to provide a relatively new paradigm for generating micro motion.

2.4 Vitrectomy probe

Vitrectomy probes are used during vitreoretinal surgery to remove ocular tissues [3], such as vitreous humor and membranes covering the retina. These probes have a port for drawing in and dissecting tissues. The port opens a fixed amount, tissue is drawn into the port, the port closes, severing the tissue, and the tissue is aspirated. This action may be repeated to remove desired tissues.

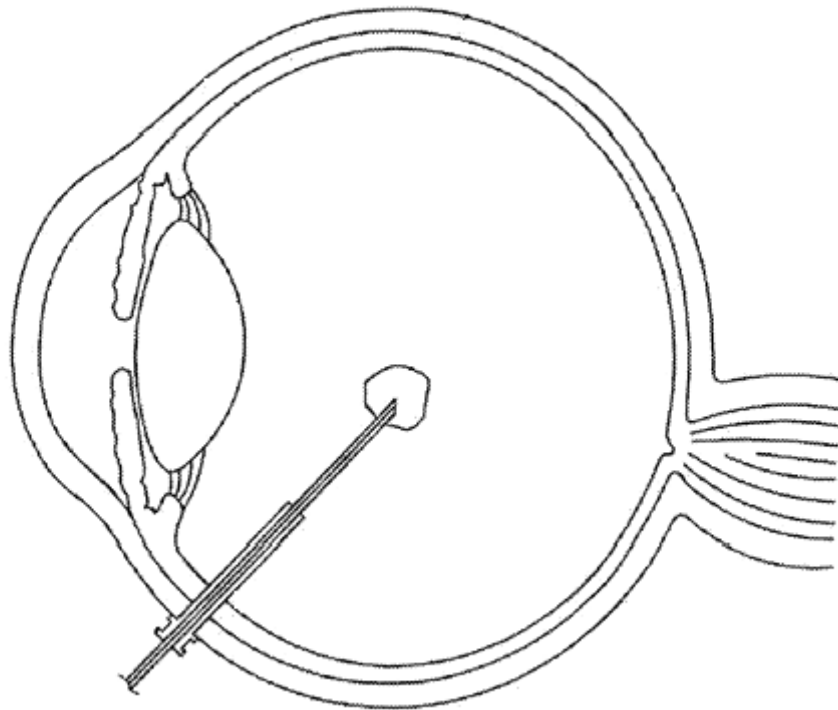


Figure 2.3. Cross-sectional view of an eye in which a cutter of a vitrectomy probe extends into a posterior segment of the eye.

The vitrectomy probe includes a housing, a cutter extending longitudinally from a first end of the housing, an oscillator, and a stroke limiter. The cutter may include an outer cutting member coupled to the housing, an inner cutting member slideable within the outer cutting member, the inner cutting member slideable between a retracted position and an extended position, and an adjustable port.

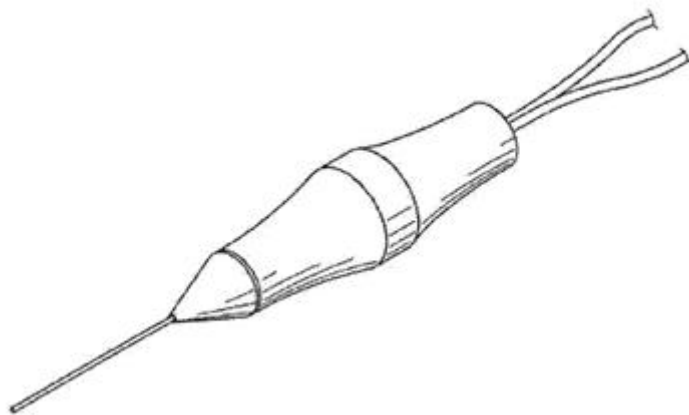


Figure 2.4. Vitrectomy probe having a cutter with an adjustable-sized cutting port.

A size of the adjustable port may be defined by an edge of an opening formed in the outer cutting member and an end surface of the inner cutting member when the inner cutting member is in a fully retracted position. The stroke limiter may include a moveable member threadably retained within the housing. The moveable member may be moveable in a first longitudinal direction in response to a rotation a first rotational direction, and the moveable member may be moveable in a second longitudinal direction opposite the first longitudinal direction in response to a rotation in a second rotation direction. The moveable member may contact the inner cutting member at a location defining the fully retracted position.

2.5 Fixation of bone fractures

A device and method for fixation of bone fractures [4] has a bone screw comprising a shank with a threaded end portion, on the outer surface. The screw has a through bore with two bore portions differing in diameter. A step in the diameter is formed between these bore portions and is located within the end of the screw having the thread. This step in diameter can support a metal insert which in turn supports a polymer pin when the latter is pressurized with a sonotrode in the bone screw. Together with an applied ultrasonic vibration the pressure fluidizes the polymer pin and presses the material through holes configured in the wall of the bone screw and into surrounding bone.

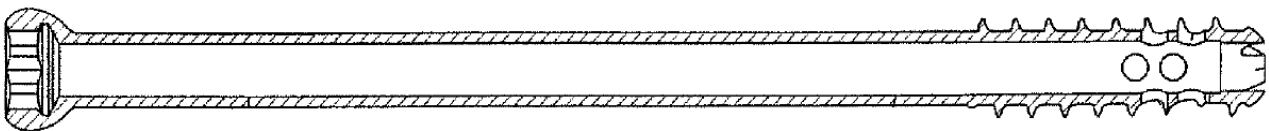


Figure 2.5. Section view of a bone screw.

This apparatus relates in general to sonic fusion technology, it relating more particularly to a device and a method for the fixation of bone fractures, with a bone screw for augmenting within a bone. According to this mechanism a fixation cement is introduced through a bone screw into a portion of a bone afflicted by osteoporosis. Femoral neck fractures as well as distal femoral fractures can be fixated by means of this device.

The system in accordance with prior art comprises a bone screw having a flow cavity, i.e. an axial through bore through which bone cement can be introduced into the portion at the tip of the screw.

The bone cement is advanced by a device which is releasably attached to the trailing end of the screw. This device is similar to a commercially available syringe in comprising substantially a cylindrical barrel and a plunger. The barrel forms a cavity in which the plunger is movable to and fro.

In use of this prior art device the fixation cement is filled into the barrel, after which the plunger is urged against the cement. By applying manual compression force the fixation cement is jetted into the axial through bore of the bone screw. Due to the pressure the fixation cement is adequately fluidized so that it can pass through the proximal end of the bone screw into the bone, as a result of which the bone screw is augmented in the bone.

This system has the drawback that the manual pressure applied to the fixation cement varies, not only basically from application to application but also during the application itself so that the distribution of the fixation cement within the portion of the bone at the tip of the bone screw is neither reliable nor even.

2.6 Manufacturing of polymer micro parts

Plasticizing polymers with energetic ultrasound [5] is an alternative approach to process small amounts of a thermoplastic material.

In ultrasonic plasticizing, energetic ultrasound is used to heat and to plasticize thermoplastic polymers.

The basic idea of the process is to deform a material cyclically at ultrasonic frequencies.

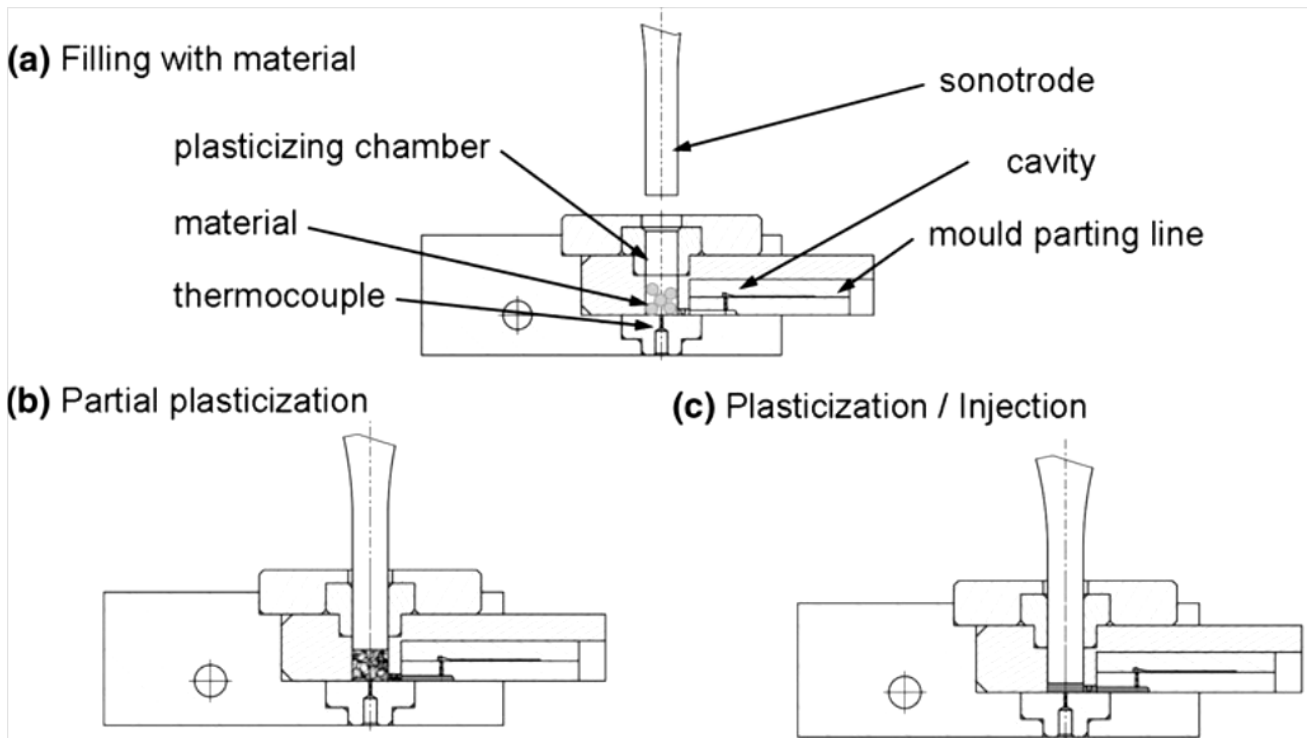


Figure 2.6. Plasticization with ultrasound: course of the process.

The deformations are applied on the material by a common ultrasound sonotrode; the plasticization takes place in a plasticizing chamber.

The generated melt can be filled into micro cavities. Hence, the system can produce micro polymer parts in one process step. A main advantage of the plasticization with ultrasound is that the process offers the possibility of delivering just that small amount of melt that is required for the next cycle in micro injection moulding.

2.7 Ultrasonic soldering in electronics

Soldering problems in modern electronics have been widely developed for a number of reasons:

- the microminiaturization of components and functionally complicated microelectronic devices
- soldered connections have found wide applications in mounting electronic equipment; however, they are not reliable enough;

- environmental matters of soldering have increased recently.

Recent processes developed for mass soldering in electronics are activated by concentrated energy flows deriving from ultrasonics [6] , ensuring local and mainly contactless effect of the heating source on the parts to be soldered. In addition activation of physical-chemical processes creates new possibilities of joining materials with diverse chemical structures and properties.

Applying modern electronic US oscillation sources makes US soldering a reliable, environmentally friendly process eliminating flux application.

2.8 Processing of mica/epoxy nanocomposites by ultrasound mixer

Polymer-layered silicate nanocomposites have attracted a great deal of attention in both academic and industrial fields [7] , since many potential improvements are waited by introducing a small amount of nanosize clay particles in polymers: increase of mechanical properties, improvement of barrier properties and flame retardation, and better dimensional and thermal stability. Among polymers, epoxy resins find many industrial applications in adhesives, construction materials, composites, laminates, coatings, and air craft because of their high strength, low viscosity, low volatility, low shrinkage during cure, low creep, and good adhesion to many substrates. Therefore, epoxy resins are one of the most commonly studied polymers in the preparation of nanocomposites with layered silicates, because the polar epoxy monomers can easily diffuse into the clay galleries. In fact, the matrix/filler type system, the extent of filler adhesion to the matrix, and the levels of dispersion of the filler throughout the matrix degree are among the parameters which highly determine any enhancement of a particular property of nanocomposites. Moreover, the nature of the curing agent as well as the curing conditions, especially the temperature is expected to play a role in the exfoliation process.

Ultrasonicator is used as a means of applying external shearing forces to disperse the silicate clay layers in the epoxy matrix. The first step of the nanocomposite preparation consists of swelling the mica in a curing agent, i.e., aliphatic diamine based on polyoxypropylene backbone having a low viscosity for better diffusion into the intragalleries. Then, the epoxy prepolymer is added into the mixture. It guarantees better dispersion and intercalation of the nanoclay in the matrix.

The organomodification of mica with octadecylammonium ions leads to an increase in the initial d-spacing ($[d_{001}]$ peak) from 12.3 to 28.1 Å , determined by WAXS, indicating the occurrence of an

intercalation. The addition of 5 per hundred resin (phr) of MICAC18 into the epoxy matrix results in finer dispersion as evidenced by both the disappearance of the diffraction peak in the WAXS pattern and TEM images. The mechanical and viscoelastic properties are improved for both MICA and MICAC18 nanocomposites, however, more pronounced for the modified ones.

2.9 Spray head

Exemplary embodiments provide a device for spraying a cosmetic composition, the device including a sonotrode, the sonotrode having an end collar defining an ejection surface for ejecting particles of composition, the collar being suitable for bending under the effect of vibration of the sonotrode.

It is possible to obtain a spray that gives rise to satisfactory results, obtaining relatively high spraying efficiency.

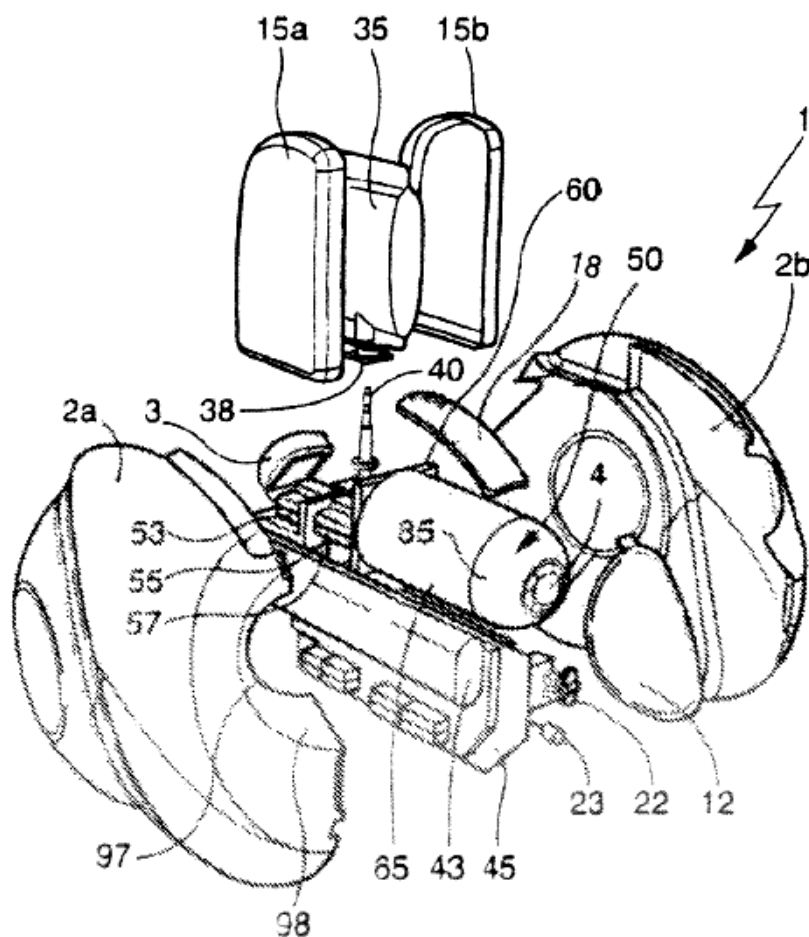


Figure 2.7. Exemplary spray device.

While oscillating the collar may be deformed by changing the shape of the ejection surface, which may for example pass from being a plane at rest to being concave or convex towards the front. The amplitude of bending towards the front or towards the rear may be greater than or equal to 5 micrometers from the rest position, e.g., lying in the range 5 μm to 25 μm relative to the rest position, giving a total amplitude of 10 μm to 50 μm .

Droplets of composition may be ejected over the entire circumference of the end collar, thereby contributing to obtaining a spray that is substantially uniform.

Other exemplary embodiments also provide a device for spraying a cosmetic or dermatological composition, the device comprising a sonotrode and a transducer coupled to the sonotrode, the sonotrode presenting an end collar defining an ejection surface for projecting particles of composition, the sonotrode also including a portion of decreasing diameter that is extended by a cylindrical portion (or “ejector”) that is connected to the end collar, the ratio of the transducer diameter divided by the diameter of the cylindrical portion being less than or equal to 4.5, and possibly greater than or equal to 3.

These geometrical characteristics may lead to results that are particularly satisfactory. The collar may extend along a plane perpendicular to a longitudinal axis of the sonotrode.

The presence of the narrow portion may result in easier fabrication of the remainder of the channel, which may be of relatively large section. Such a design may assist in limiting head losses.

The narrow portion may provide a certain amount of capillary retention when the device is not in use, thereby enabling exchange with air to be reduced. The use of a shutter for the feed channel can thus be avoided.

The term “hair agent” is used to mean any ingredient for a composition that serves to provide cohesion to a piece of hair by depositing a material that limits relative movement between individual hairs for example any polymer.

It is possible to use any hair agent and it is also possible to use mixtures containing a plurality of such agents.

2.10 Cleaning devices

Ultrasonic cleaning devices comprise a sonotrode and a power supply adapted to supply current to the sonotrode, and further include one or more features which facilitate use of the ultrasonic cleaning devices by consumers, improve the safety of the ultrasonic cleaning devices when used by consumers, and/or improve the cleaning efficiency of the ultrasonic cleaning devices when used by consumers.

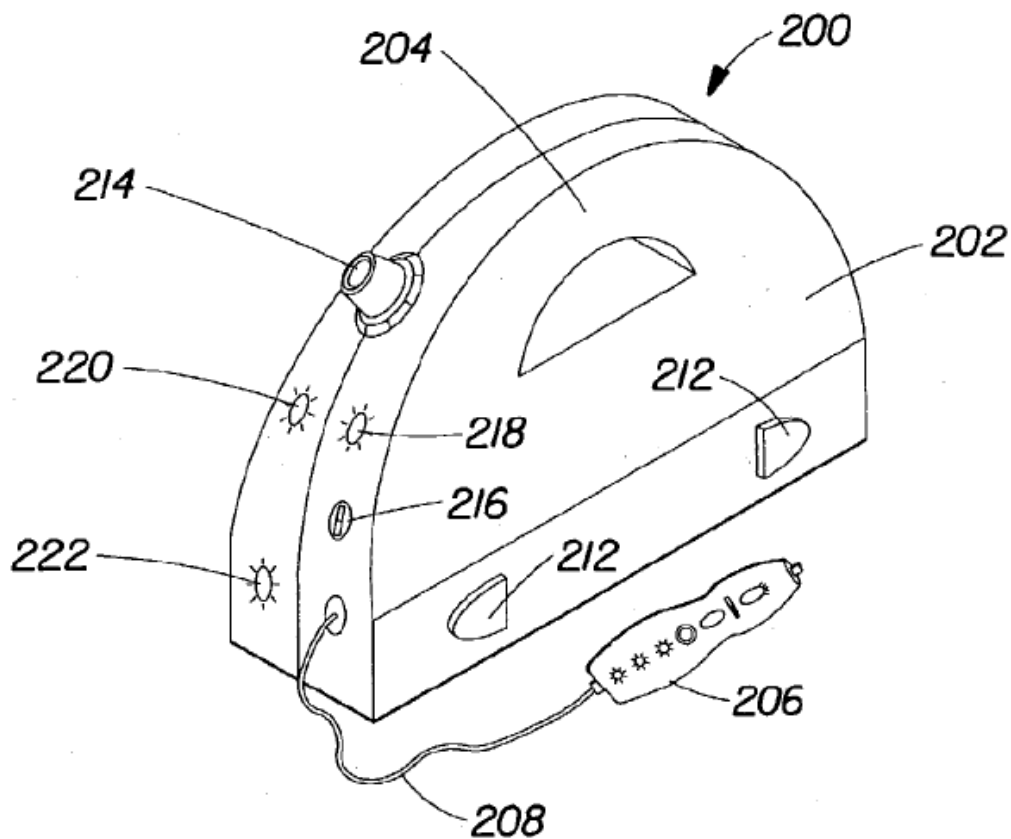


Figure 2.8. Schematic diagram of one embodiment of an ultrasonic cleaning device.

2.11 Reducing and eliminating foaming of liquid products

In different fields of industry, the foam generation of a product to be processed is an inherent problem. In the field of beverage industry, for example, mainly with carbonated products such as cola and beer, but also with non-carbonated products such as fruit juices, etc., there exists during the production process, but also during the filling of the product into bottles or the like the problem that

the product generates a large amount of foam. The generation of foam often results in an undesired loss of product, and also the contamination of the containers, into which the product is to be filled, is a big problem in these industries. During the filling process, the generation of too much foam leads to problems with regard to the sealing of the containers, and furthermore the filling line process is considerably slowed down due to the foam on top of the product. However, also in other industries, the foam generation of liquid products is a problematic issue.

Examples of other industries are the chemical, petroleum, pharmaceutical and mining industries. Foam can form in tanks, open vessels or in containers or bottles, into which the product is filled. Due to the foam, there exists also a problem with regard to the vessel capacity/volume, the downstream processing equipment such as pumps, homogenizers, pasteurizers, filling lines and the filtration equipment.

In the prior art, conventional technologies used to reduce or to act against the generation of too much foam have for several years involved the use of anti-foam chemicals.

However, in the food industry, the use of chemicals is not possible, and in other industries the use of such chemicals for reducing the generation of foam is rather cost-intensive. Also,

the chemicals may change the characteristics of the liquid product, which is processed in the production line.

A further solution to this type of problem consists in anti-foam devices using ultrasound waves for the destruction of foam on top of the liquid product.

Such sonotrode for de-foaming are provided with a main body part having connecting means for the connection of the sonotrode with a high-frequency generator, and has a front face, from which the ultrasonic field is directed to the desired spot or area of the product or on top of the product to be de-foamed. The sonotrode is characterized in that the main body part has a shape of a compact block element, and that the front face is concave in shape in relation to a product surface such that the ultrasonic field is focused and directed to a specific area of a product foam to be treated in a concentrated form compared to a non-focused ultrasound.

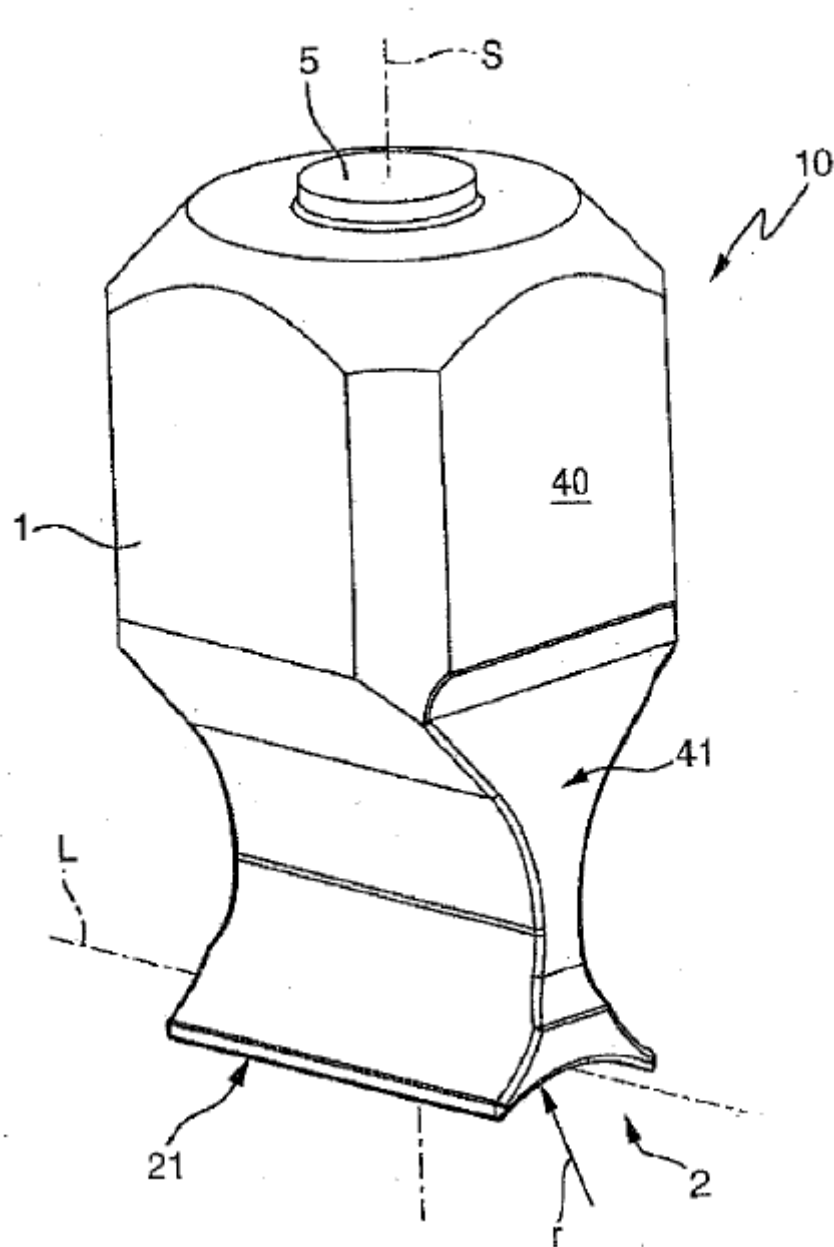


Figure 2.9. Perspective view of an example of realization of a sonotrode device.

As a result of the concave form of the front face, the ultrasonic field is concentrated compared to a flat or a convex front face. The concavity of the front face according to the invention is formed such that an increased effect for the de-foaming of a liquid product is achieved. The concave front face of the sonotrode according to the invention may in particular be formed like a rounded groove or channel with an especially optimized curvature.

The ultrasonic high amplitude frequency, which is introduced into the sonotrode by means of a connecting part, is effectively transmitted by the block-shaped main body part to the concave front

face such that the generation of foam during the processing of the liquid product can be effectively eliminated and reduced.

The sonotrode is provided with a high power output. According to an advantageous form of realization, the sonotrode is provided with a high-amplitude ratio, in particular with an ultrasonic amplitude of peak to-peak displacement preferably from 30 to 120 microns. Through extensive search, it was found out that with these ranges of a high-amplitude ratio a highly effective foam destruction and reduction is possible. Surprisingly, these high-frequency ratios have turned out to be most effective for the purpose of de-foaming liquid products.

3 SHAPING OF FOAM-LIKE MATERIALS

Shaping of Polystyrene and Polyurethane with traditional machining operations may create dust and debris, which are undesired consequences of the manufacturing techniques adopted. The proposed technology makes use of an ultrasound probe that compresses and heats the foam-like material and forms the desired shape. The chapter presents the preliminary tests as a first step toward a full feasibility analysis of the new proposed technology.

3.1 Introduction

Expanded Polystyrene and Polyurethane are largely used by hobbyists for manufacturing lightweight model planes, surfboards, but also by artists to create masks, costumes, statues etc. From an industrial point of view surf manufacturers during the design and prototyping phase shape expanded polystyrene blocks by using hot wires and then by milling. They use 3axes NC milling machines with mills tailored for cutting wood. Unfortunately the process of milling creates a lot of dust and debris that, owing to tribological charges, stick to the milled surfboard.

In order not to affect the following operations (coating with primer and painting), an accurate cleaning operation to remove dust and debris is required. This operation may result high time consuming and often not easy owing to the electrostatic charges on the debris that sticks on the workpiece. Thus, the simplification of the cleaning process would be highly desirable.

It is hereafter investigated the possibility of using an instrument often used for joining plastic components (e.g. plastic automotive covers), or for including metal elements like bolts and screws in a plastic matrix for a different field. A sonotrode originally used for the mixing of chemical solutions was used for the drilling operation on Polystyrene and Polyurethane blocks.

The following sections of the paper present (i) an overview of the state of the art of ultrasound technology uses, (ii) the design of experiment and the measurement procedures of the samples and (iii) the results of the tests. Finally (iv) a brief conclusion of the work and possible future developments is presented.

3.2 State of the art

Ultrasound technology is largely used to detect objects and measure distances. Ultrasonic imaging is used in human medicine, in nondestructive testing of products and structures (e.g. to detect invisible flaws). However ultrasounds are also used as actuators, not only as sensing media.

In oral care ultrasonic cleaners are used to loosen and remove plaque and tartar from teeth, in ophthalmology in cataract surgery an ultrasonic probe is used to break up and remove the clouded crystalline lens from the eye. Of course ultrasound scalpels found many uses in surgery even in bone cutting e.g. in maxillofacial surgery (Eggers et al, 2004). Recently, a piezoelectric vitrectomy probe able to liquefy the humor vitreous for eye surgery has been patented (Underwood et al, 2011) and the number of patents exploiting ultrasound wave is continuing growing year by year.

Industrially, ultrasound technology is widely used in several fields: from micromotion (Ouyang et al, 2008) to cutting of materials (Moriwaki et al, 1992), from cleaning to foundry, from joining and soldering (Lanin, 2001) to hard material machining (Benedict, 1987), from mixing (Yang et al, 2000) to chemical processes acceleration (Suslick and Gareth, 1999) and material dispensing (Springall, 1994). Examples, working principles and video material can be found in many websites of OEMs (Original Equipment Manufacturers). Even if the scientific level is not often high, such sources provide insight of processes that now are no more considered as “non-conventional processes”.

Focusing on manufacturing technology, ultrasounds are used with hard slurries in the so called ultrasonic impact grinding, both for macro and micro machining (Medis and Henderson, 2005). The process consists in a vibrating tool oscillating at ultrasonic frequencies used to compress an abrasive slurry between the workpiece and the tool thus inducing small cracks on the workpiece and removing the material from the workpiece itself. This machining process suits perfectly for hard and brittle materials, such as glass, titanium, sapphire, ruby, diamond and ceramics (Benedict, 1987).

In ultrasonic welding of plastics, high frequency (15 kHz to 40 kHz) low amplitude vibration is used to create heat by way of friction between the materials to be joined. The interface of the two parts is specially designed to concentrate the energy for the maximum weld strength.

In investment casting (known as lost-wax casting in art) (Marty, 1971) reported that solidified parts are broken from the sprue thanks to ultrasonic vibrations.

Recently (in the last 20 years) ultrasonic blades found many applications in food industry since US are suitable for almost all kind of food cutting. Actually, ultrasonic assisted food cutting offers good performance in precision, uniformity and hygiene, and is the perfect cutting technology for a wide range of industries.

Other ultrasonic instruments relates to the cleaning systems, both for industrial or private use (Duval et al, 2006).

3.3 Experimental setup

The investigation proposes the use of ultrasound tools for drilling and milling operations of polymeric foam-like materials. The aim of this study is to analyze the force-displacement behavior and to examine the profile of the samples obtained with this technique in case of different input parameters and materials.

The following subsections present the technology adopted for the machining operations and for the data acquisition.

3.4 Ultrasound technology

The main apparatus of the experimental setup is the sonotrode. The machine used is the Vibra Cell VCX 130 PB from Sonics & Materials, Inc.. The vibration frequency is constant and it is 20 kHz, while the amplitude can be set within a range from 0 μm to 100 μm . The tip of the sonotrode is cylindrical with a diameter of 6 mm.

3.5 Parameters measurement

The system acquisition experimental setup includes: (i) a PhidgetBridge 4-Input, (ii) a Wheatstone Bridge based sensor acquisition board from Phidgets, Inc, (iii) an off center load cell, modified with shelves for acquisition of compression load, with a maximum nominal load of 3 kg from CELMI s.r.l. and (iv) a translation stage VT-80 from Micos USA having an allowed maximum force of 49.0 N. Force acquisition and the stage control were done using Labview 8.5 using a sample period of 20 ms. The load cell was calibrated using a series of weights starting from 100 g up to 600 g.

Figure 3.1 shows a top view of the experimental apparatus. It is possible to clearly observe the translation stage (a) on the left, with the load cell (b) mounted on it. The sonotrode (c) is powered by the Vibra Cell power supply (d). A Polystyrene sample (e) is fixed on the load cell.

Output data from LabView 8.5 were processed in Microsoft Excel files, allowing the comparison of force exerted by the sonotrode during the drilling operations in different working conditions and different materials.

3.6 Sample analysis

Samples were sectioned along the axis of the machined hole to analyze the features of the produced profile. White samples (polystyrene) were gold sputtered in a S150B gold sputtering instrument for better resolution.

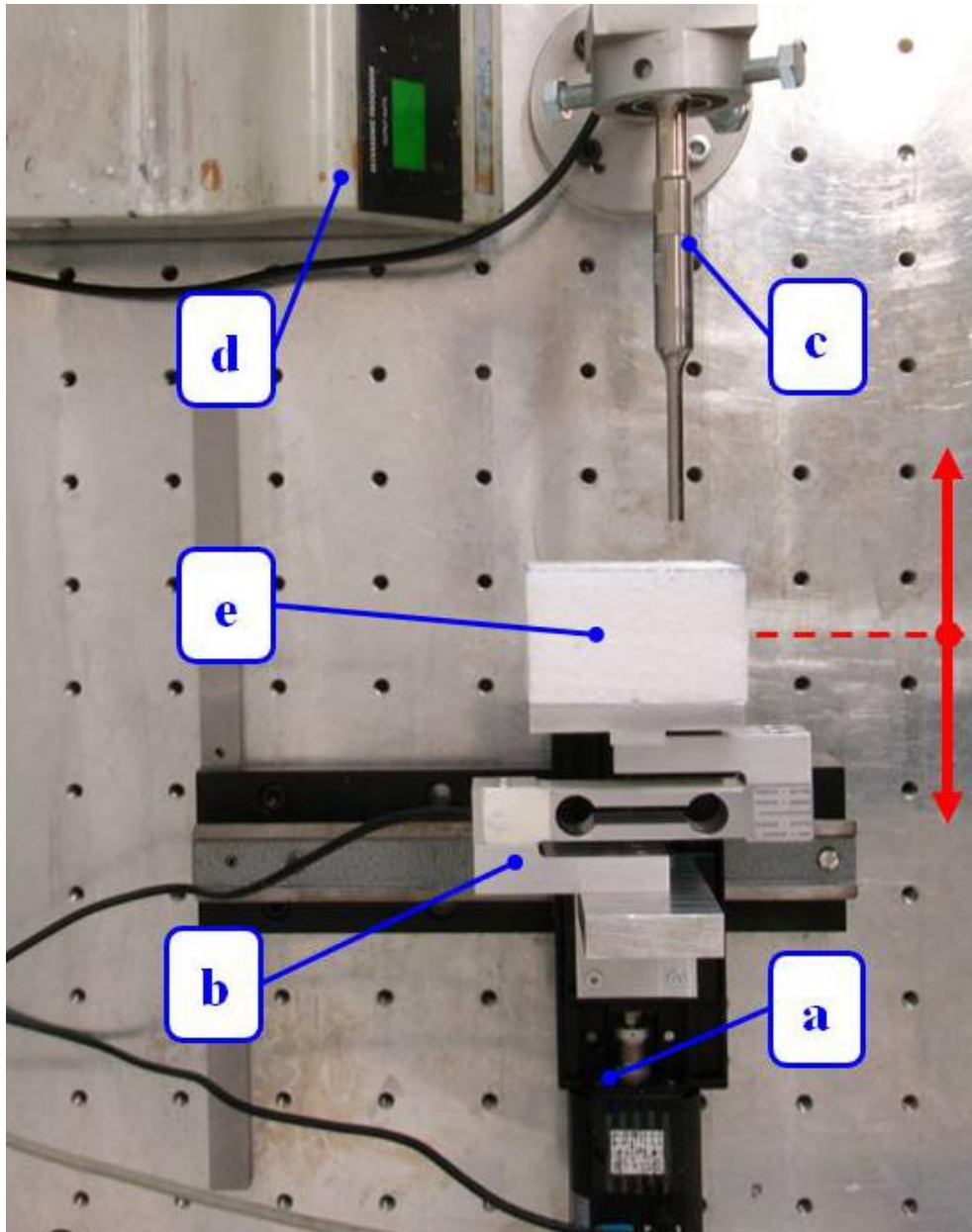


Figure 3.1. Top view of the experimental setup: (a) the translation stage, (b) load cell, (c) sonotrode and (d) power supply (d). The sample (e) is fixed on the load cell.

Samples were then examined under a stereomicroscope Wild M3Z in reflected light. Images were recorded using a digital camera directly mounted on the microscope. Images show differences between the investigated features of the sample by using the contrast between the different areas.

3.7 Experimental results

The aim of the study is to analyze how input parameters affect the drilling operation in terms of maximum force exerted and quality of the profile of the hole.

In order to analyze the effects of input parameters on the drilling operation, experiments were performed using three constant feed rate values (1 mm/s, 2 mm/s and 5 mm/s), and three amplitude of the sonotrode (60 μm , 80 μm and 100 μm) on two different materials. The materials considered for the experiments were polystyrene with a density of 13.5 kg/m³ and polyurethane with a density of 30.5 kg/m³.

Because of the lower homogeneity of the structure of polystyrene, five polystyrene samples for each input set were tested, while only three samples of polyurethane for each set were tested owing to the higher homogeneity of polyurethane foam. Thus a total number of 45 samples for Polystyrene and 27 samples for Polyurethane were analyzed. For the sake of synthesis, not all the experiments are shown in the paper, but significant data and samples are presented hereinafter.

Pictures of samples both for Polystyrene and Polyurethane are illustrated in Figure 3.5 and **Figure 3.8** for different set of parameters. As a remark we have to underline that tests at amplitude of 60 μm and 5 mm/s speed have not been performed owing to the high expected forces on the sample, which might have had damaged the translation stage.

3.8 Working principle

When the tip of the sonotrode is pressed against the workpiece, two main effects occur: the first one is the compression of the material in front of the sonotrode, the second one is heat generation. The tip and the workpiece heat up (the maximum temperature measured during the tests was 47°C) because of friction between the side of the sonotrode and the wall of the hole. One more effect seems to occur, that is cavitation, but more detailed research has to be carried out regarding this aspect. The absence of dust and debris is related to a combination of the pressure and heat generation. In fact pressure is the main responsible of shape forming at least in the first phase of the machining operation, while heat creates a shell around the walls of the hole, having higher density and different mechanical properties.

3.9 Polystyrene

The data analysis shows the force displacement behavior and the maximum force required to the sonotrode to perform the drilling operation for each set of parameters.

It is interesting to note that force increases rapidly during the initial part of the experiment, then decreases to a lower value. The peak is to be attributed to the elastic deformation of material, while the decrement happens in correspondence of the heat generation due to contact between material and sonotrode.

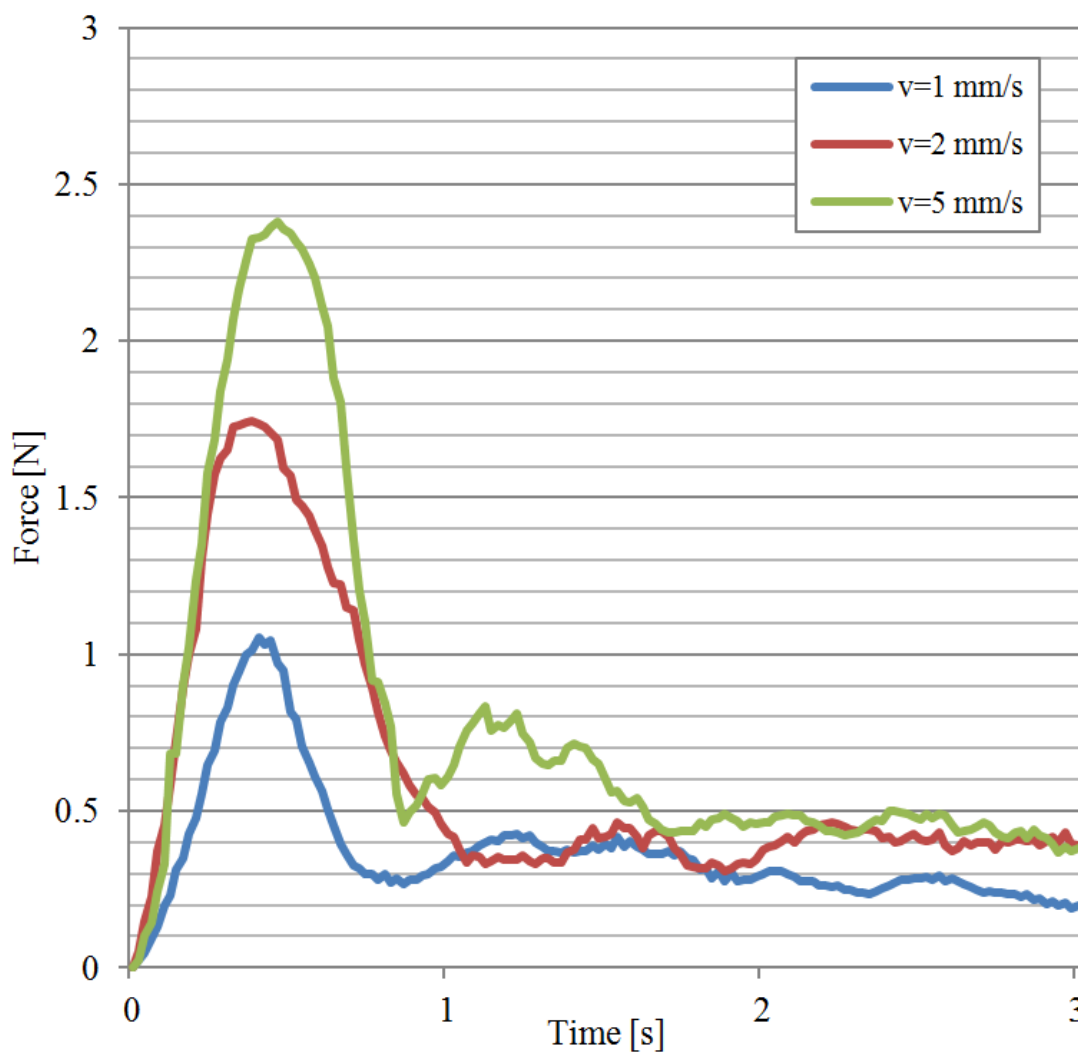


Figure 3.2. Graphs of the average force exerted on Polystyrene sample, varying the feed rate value at the amplitude 100 μm .

One of the most remarkable results emerging from the data analyzed is the strict dependence of the maximum force exerted from the material structure. Polystyrene macroscopic structure shows the high non-homogeneity level of the material, thus revealing scattered results of maximum exerted

force, even using the same working parameters. This is clearly shown in **Figure 3.3**, where the maximum load varies from 3.34 N of Sample 1 to 0.73 N of Sample 3 for a feed rate of 5 mm/s and an amplitude of 100 μm .

Considering the sample with the highest load value, given a certain feed rate, graphs can be compared varying the amplitude (**Figure 3.4**). It is interesting to note that the force value decreases when the amplitude is increased. On the other hand, comparing graphs of force exerted at a given amplitude, and varying the feed rate values (**Figure 3.3**), it is evident that maximum load decreases when the feed rate is reduced.

The analysis of samples obtained with the same working parameters highlighted the variability of surface finish. This is shown in **Figure 3.5**, where three Polystyrene samples obtained with 1 mm/s feed rate and 60 μm amplitude are compared.

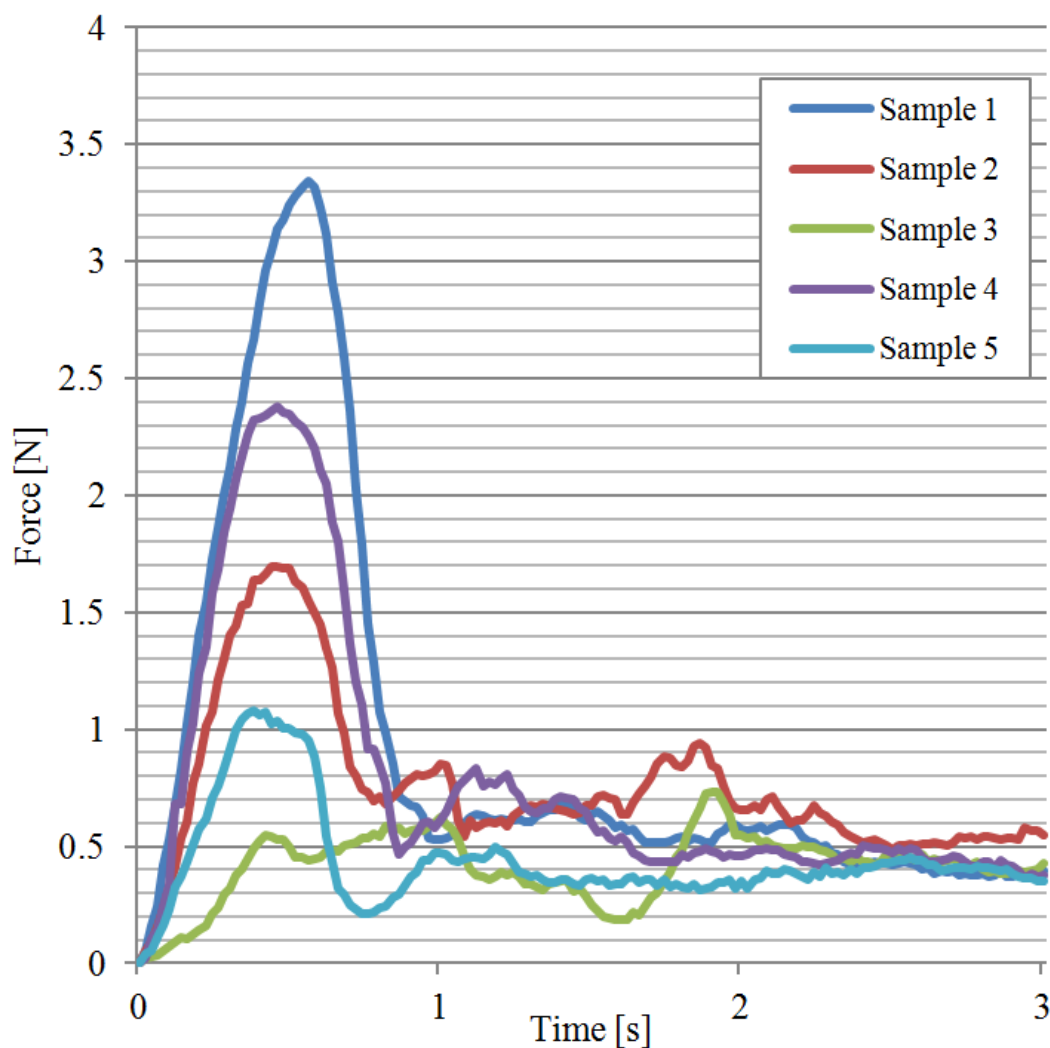


Figure 3.3. Force exerted by the sonotrode on polystyrene samples ($v = 5 \text{ mm/s}$, amplitude $100 \mu\text{m}$).

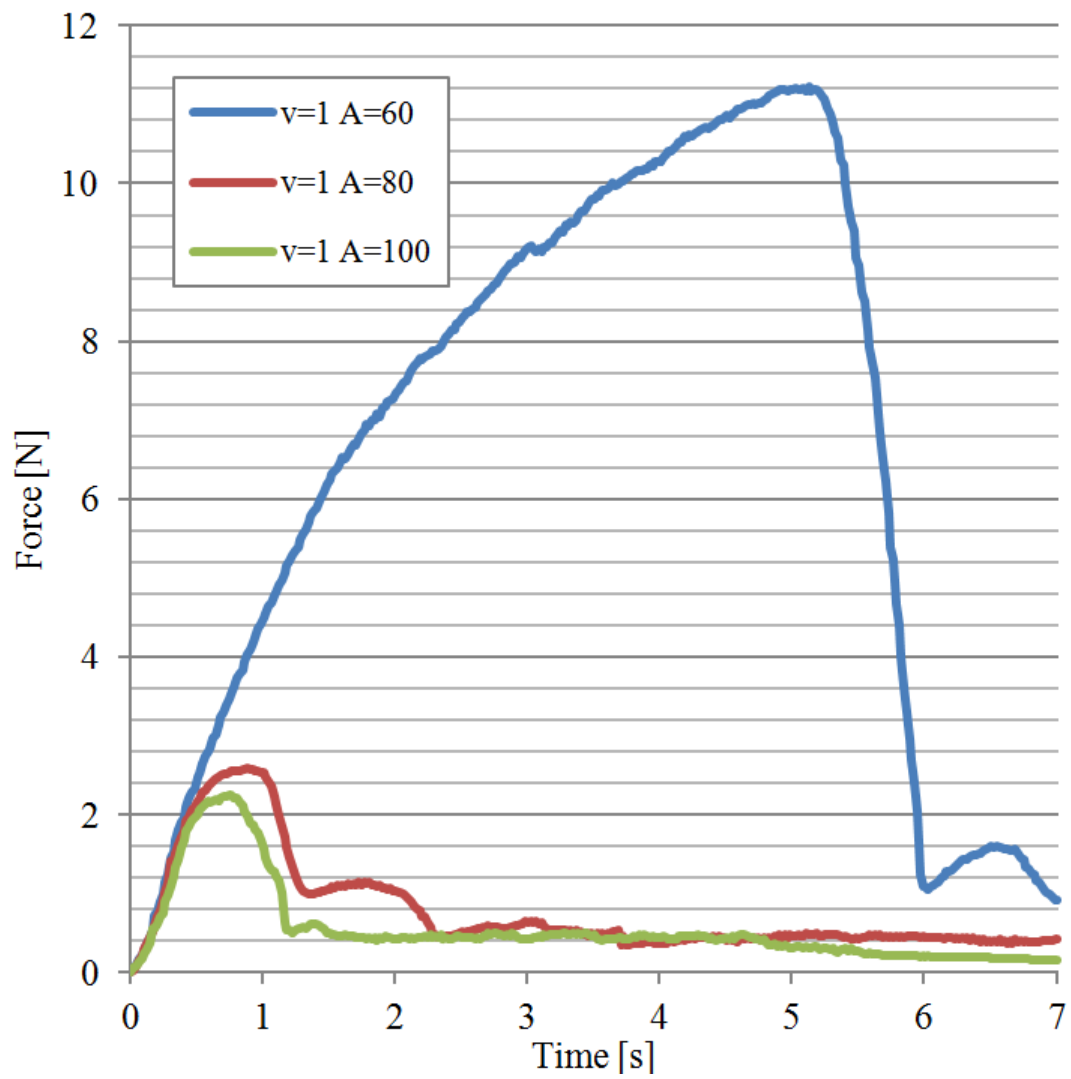


Figure 3.4. Maximum force exerted by the sonotrode on Polystyrene samples ($v = 1$ mm/s), varying the amplitude.

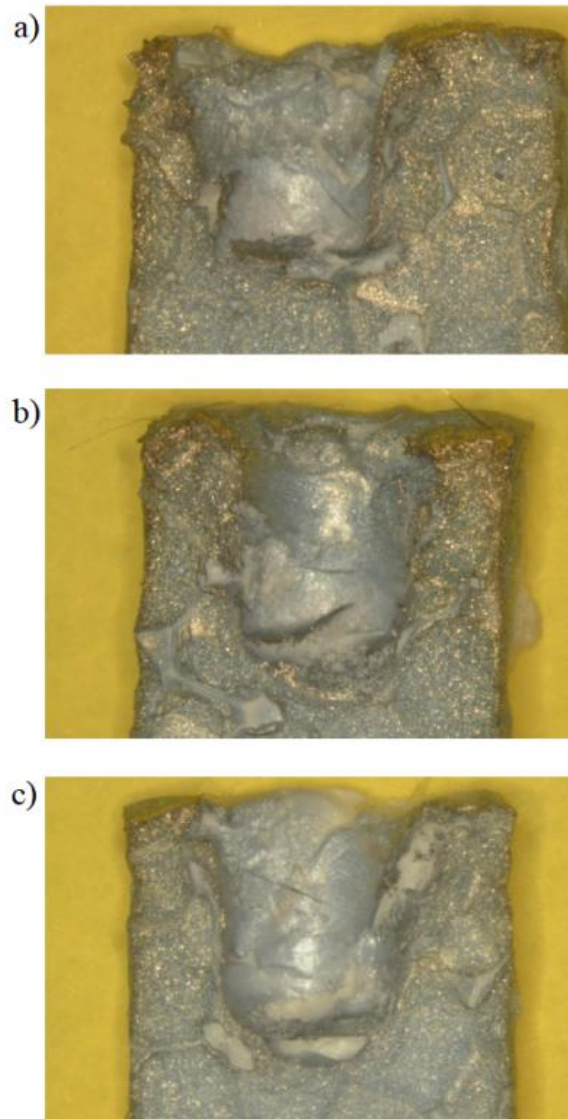


Figure 3.5. Samples of Polystyrene obtained with the same set of input parameters ($v = 1$ mm/s, amplitude $60 \mu\text{m}$).

However, it is important to note that, even if variable, the average surface quality is almost the same for the same set of working parameters. The tests revealed that no dust or debris are produced during the manufacturing process.

3.10 Polyurethane

Polyurethane has a completely different behavior. Actually Polyurethane foam has a homogeneous distribution of material, thus resulting in a good repeatability of experiments, as shown in **Figure 3.6**.

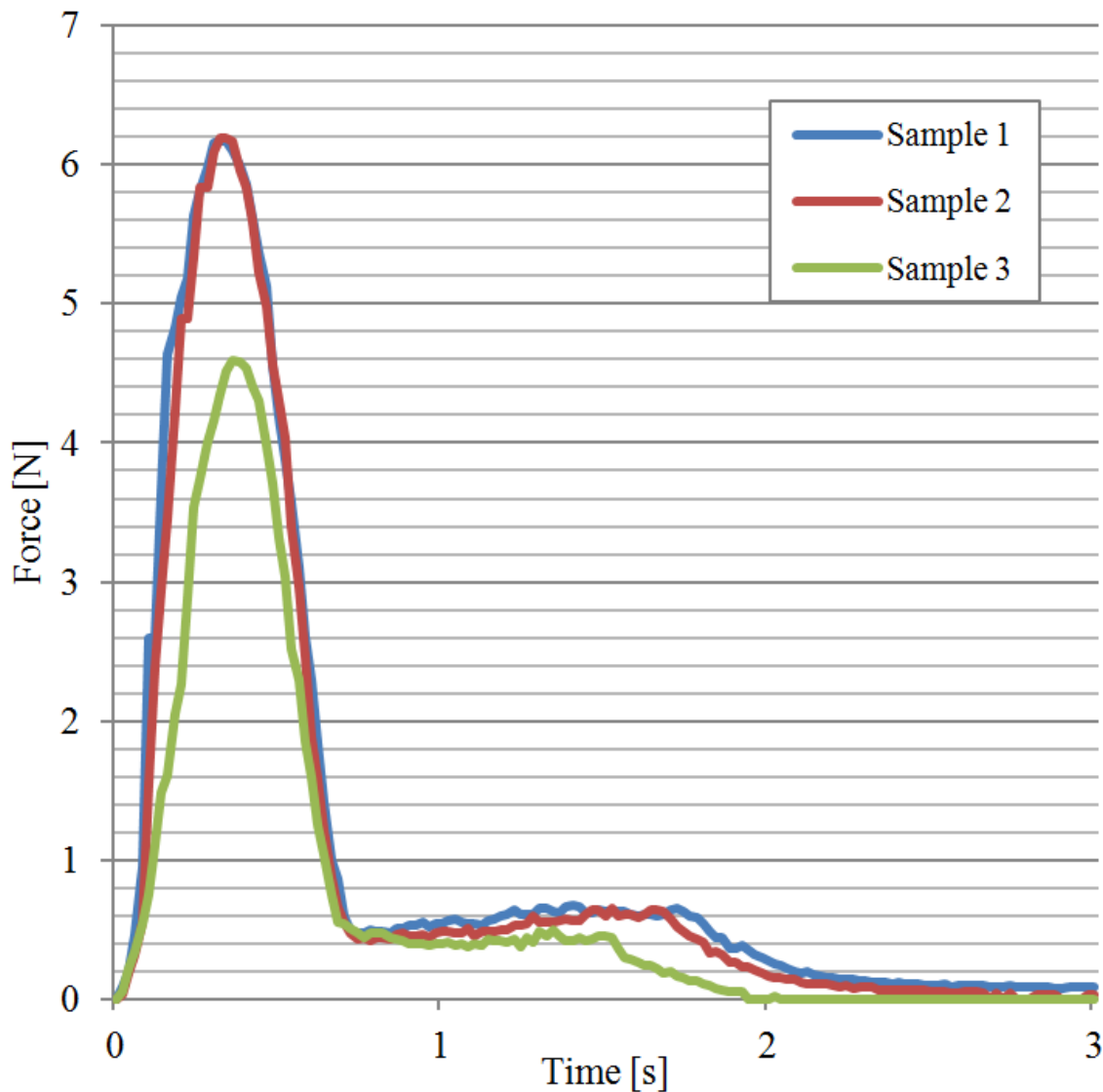


Figure 3.6. Force exerted by the sonotrode on polyurethane samples ($v = 5 \text{ mm/s}$, Amplitude = $100 \text{ }\mu\text{m}$).

This fact is confirmed also by the analysis of surface finish for samples obtained with the same working parameters (**Figure 3.8**) used in case of polystyrene. The analysis of the plots reported in Figure-6 for a given speed confirms the results already obtained for Polystyrene samples. The maximum force exerted by the sonotrode decreases from a value of 5.72 N of the sample obtained with 1 mm/s and an amplitude of $60 \text{ }\mu\text{m}$, to the value of 1.92 N of the sample obtained with the same speed and with an amplitude of $100 \text{ }\mu\text{m}$. Like in the manufacturing of Polystyrene samples, no dust or debris are produced during the drilling operations.

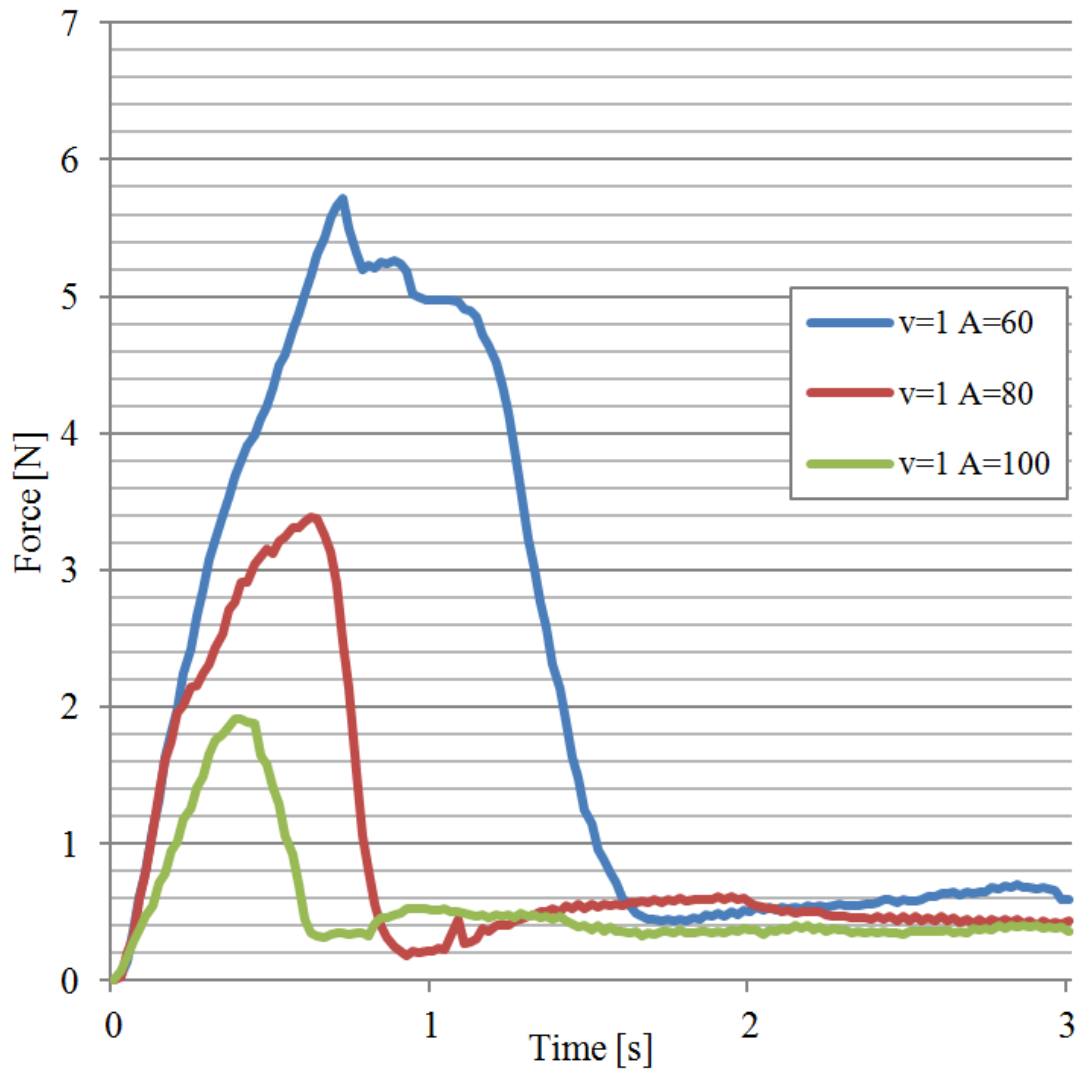


Figure 3.7. Maximum force exerted by the sonotrode on polyurethane samples ($v = 1$ mm/s), varying the amplitude.

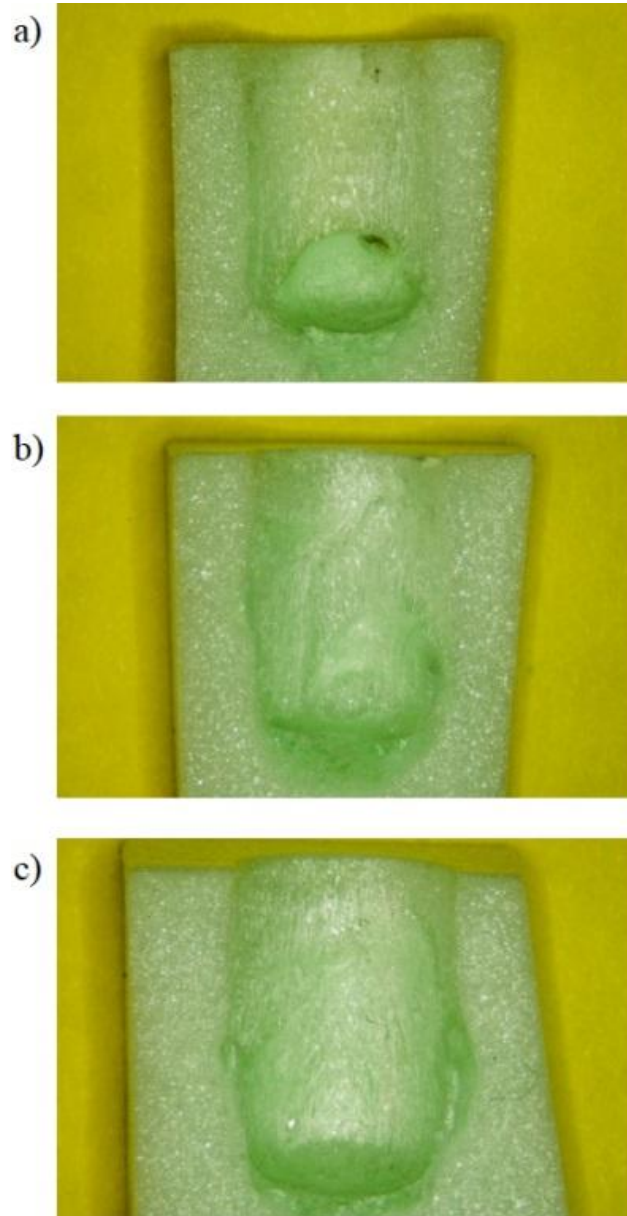


















Figure 3.8. Samples of Polyurethane obtained with the same set of parameters ($v = 1$ mm/s, amplitude $60 \mu\text{m}$).

Table 1. Pictures of Polystyrene and Polyurethane samples obtained varying the feed rate and the amplitude.

		60 μm	80 μm	100 μm
V=1 mm/s	Polystyrene			
	Polyurethane			
V=2 mm/s	Polystyrene			
	Polyurethane			
V=5 mm/s	Polystyrene	Test not performed owing to the force that exceeds the maximum allowed.		
	Polyurethane	Test not performed owing to the force that exceeds the maximum allowed.		

4 UNDERWATER DRILLING OF FOAM-LIKE MATERIALS AND WAX

The chapter presents the results related to ultrasound machining of several materials as foam-like materials (i.e. Polystyrene and Polyurethane) and wax in underwater conditions. The study also shows the comparison with in-air ultrasound machining performed on the same materials. The comparison demonstrates an enhancement mainly in terms of surface finish, overcut and heat altered zone. Such enhancements are due to the capability of water to decrease the influence of high temperatures on the tool-surface interface and to facilitate the removal of the machined material. The underwater conditions make it possible to successfully drill and mill wax, too: in air the molten wax tends to refill the manufactured features, while in water wax immediately solidifies and a chip is formed. Another possible machining benefit is given by the cavitation effect which happens underwater and facilitates also chip removal.

4.1 Introduction

The use of sound and ultrasound waves has become common in the last decades for many industrial sectors, including manufacturing processes, health care, food industry and many other fields. However, while in health care research is continuing pushing the boundaries of their use and adoption (see for example the case of the High Intensity Frequency Ultrasound® technology for cancer treatment), in manufacturing the development curve seems to have reached the asymptote.

The chapter starts from a previous work of Fantoni et al., 2014, where the possibility of manufacturing foam-like materials through the use of a sonotrode was investigated. A mix of effects, as the heat generated in the contact between the sonotrode and the workpiece and the sound wave pressure, make the foam melt and the machining operation is thus performed. The new methodology combines the effect of heat with cavitation, which occurs when an ultrasound tool is submerged in a fluid (under certain conditions).

While the above mentioned paper investigated the manufacturing of foam like materials in air, the present work focuses on the machining underwater that presents interesting novelties and

peculiarities. The heat specific capacity of water reduces the effect of thermal melting and promotes the cavitation, but also “freezes” the molten material in a rigid structure immediately after it is generated (thus reducing the heat altered zone and temperature increase of the tool). This effect is particularly interesting for the machining of wax: this material is not machinable with the in-air ultrasound technology, because wax melts and is not removed from the machining area. When the drilling or milling operation is accomplished, wax solidifies again, thus making the operation unusable.

This work begins by examining the state of the art of ultrasound technology, focusing the attention on the effects of water influence on the operations performed.

4.2 State of the art

There is a considerable amount of literature on the use of sonotrodes in liquid solutions, but the major part is related to chemical processes. Many authors investigated the possibility of using the ultrasound technology for disinfection of water, both combined with other principles, e.g. electrochemically assisted (Kraft et al., 2002), and alone (Mason et al., 2003 and Phull et al., 1997).

Other uses of sonotrodes in liquid solution refer to preparation of emulsions (Jafari et al., 2007) and preparation of liquid samples for chemical analysis (Zhou et al., 2009).

Liquids have also been used to prevent the sonotrode from sticking on the welding surfaces by Skogsmo (2004), or even to cool down the temperature of the tip of the sonotrode to avoid problems with the operation performed. This type of operation is not limited to industrial manufacturing, but is also used in oral care ultrasonic cleaning, where ultrasonic instruments are used to loosen and remove plaque and tartar from teeth (Bianchetti, 2000), or in oral implantology (Cardoni, 2010).

Another application of sonotrodes with a water-based solution is the micro ultrasonic machining (Boy et al., 2010) and ultrasonic machining (Singh and Khamba, 2005), where the slurry (hard particles plus water) has both abrasive and cooling functions. A vibrating tool oscillates at ultrasonic frequencies, compressing the abrasive particles between the workpiece and the tool. Small cracks are created on the workpiece and material is removed from the workpiece itself. This machining process suits perfectly for hard and brittle materials, such as glass, titanium, sapphire, ruby, diamond and ceramics (Benedict, 1987).

In addition to the manufacturing processes involving the ultrasound technology, the use of a sonotrode for shape modelling of foam like materials has already been investigated by Fantoni et al. (2014) with encouraging results. As far as we know, till now nobody investigated the possibility of using a sonotrode for the underwater manufacturing of foam-like components.

4.3 Experimental setup

In this test polymeric foam-like materials and wax samples will be drilled using ultrasound tools. While in air experiments have already been conducted for Polyurethane and Polystyrene (Fantoni et al., 2014), now the goal of the experiment is to test the same ultrasound process, working underwater. The investigation will concern force-displacement behavior and the analysis of the profile of the samples obtained with this technique under different input parameters.

In the following paragraphs the technology and the set up, the data acquisition method, the input parameters and the results concerning foam-like material and wax are described.

4.4 Ultrasound technology

The foam-like/wax drilling and milling is obtained by using a sonotrode, in particular the Vibra Cell VCX 130 PB from Sonics & Materials, Inc.. The tip of the sonotrode is cylindrical with a diameter of 6 mm. The sonotrode adopted vibrates at the constant value of 20 kHz, while the amplitude can be regulated from 0 μm up to 100 μm .

4.5 Parameters measurement

Output data are acquired using the following devices: (i) a PhidgetBridge 4-Input, (ii) a Wheatstone Bridge based sensor acquisition board from Phidgets, Inc., (iii) an off center load cell, modified with shelves for acquisition of compression load, with a maximum nominal load of 3 kg from CELMI s.r.l. and (iv) a translation stage VT-80 from Micos USA. Labview 8.5 is used to collect force acquisition and stage control with 20 ms as a sample period.

In order to compare the force exerted by the sonotrode during the drilling operations under different working conditions and different materials, Microsoft Excel for the final processing of data.

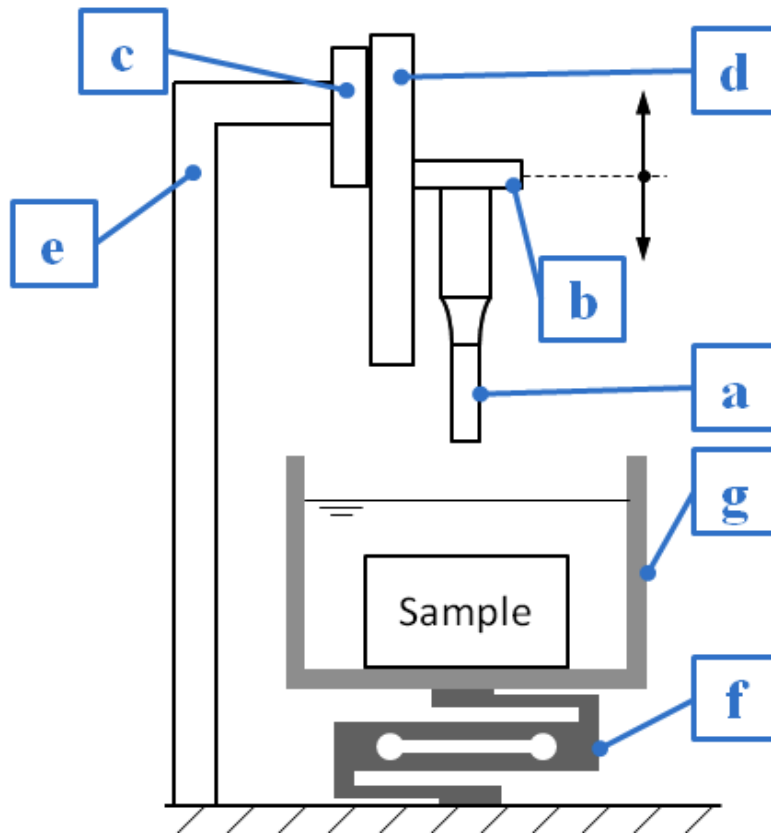


Figure 4.1. Scheme of the holding structure of the sonotrode.

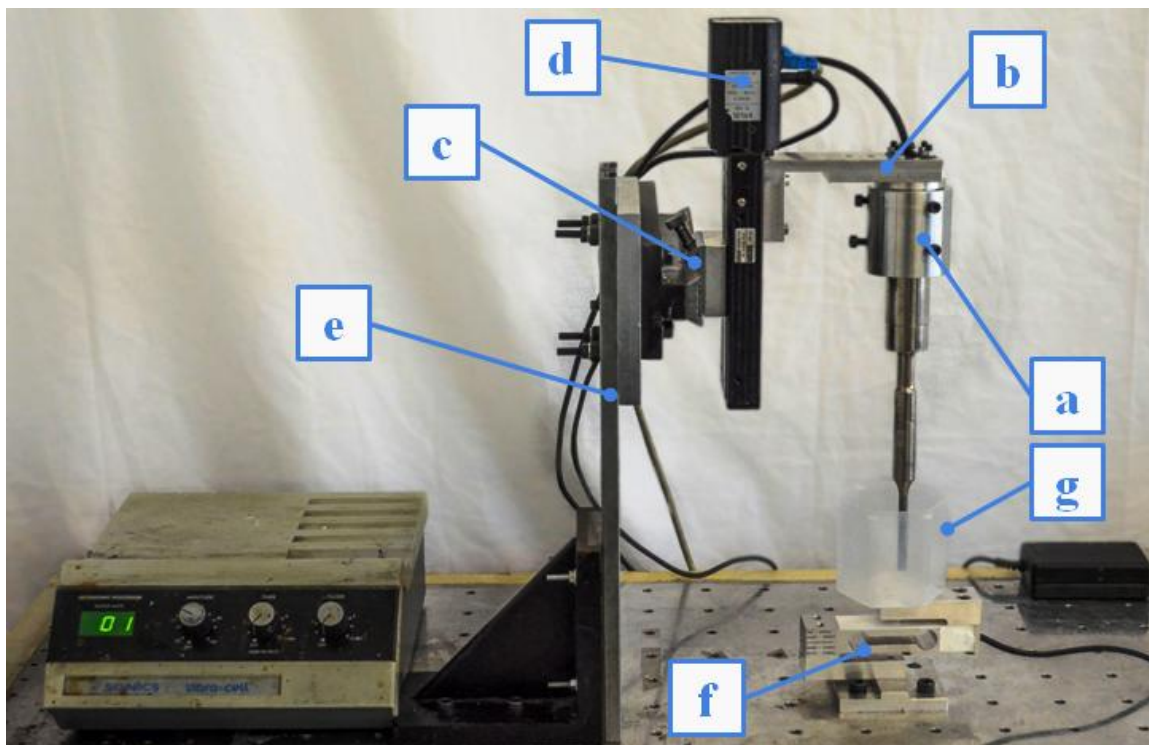


Figure 4.2. Frontal picture of the experimental setup.

A model of the experimental setup is shown in Figure 4.1. The sonotrode (a) is maintained vertically and linked to the translation stage (d) thanks to a specific support (b). A horizontal guide (c) links the stage the vertical structure (e), which is firmly fastened to the frame. A transparent container (g) is located upon a load cell (f). The workpiece is blocked in the container (g) where water is poured until the workpiece (sample) is completely submerged. The real setup is shown in Figure 4.2.

4.6 Input parameters

Because of the contact between the sonotrode and the workpiece, heat is generated during the operation. The presence of water is the main responsible of heat removal from the machining area. In many applications this effect would be desirable, and one of the goals of this study is to investigate if heat removal improves the surface finishing of the machined areas. On the other hand, since the quasi-absence of heat effects, the expected loads are higher than the ones obtained without heat removal. This is the reason why experiments were performed with low feed rate (1 mm/s and 2 mm/s) and high amplitudes (80 μm and 100 μm).

4.7 RESULTS

As mentioned above, because of the higher forces expected, the experiment was done only over four different combinations of speed and amplitude, not including neither high feed rate, nor low amplitude of the sonotrode (Table 1). Each combination was repeated over three samples. 2 mm/s feed rate experiments were not done on wax because of its fragility.

Table 2. Working parameters adopted for the experiments and number of samples analyzed for each material.

	v = 1 mm/s	v = 2 mm/s
A = 80 μm	3 Samples	3 Samples
A = 100 μm	3 Samples	3 Samples

4.8 Foam-like materials

It is interesting to note that both for Polystyrene and for Polyurethane, force increases rapidly during the initial part of the experiment, then decreases to a lower value, like when these materials are machined in air. The main difference is the force decrement during the second part of the graph: while the peak is to be attributed to the elastic deformation of material, the decrement happens in correspondence of the heat generation in case of in-air machining, and because of a combination of heat generation, cavitation effect (Moussatov et al., 2003) and direct contact between sonotrode and workpiece in case of underwater machining.

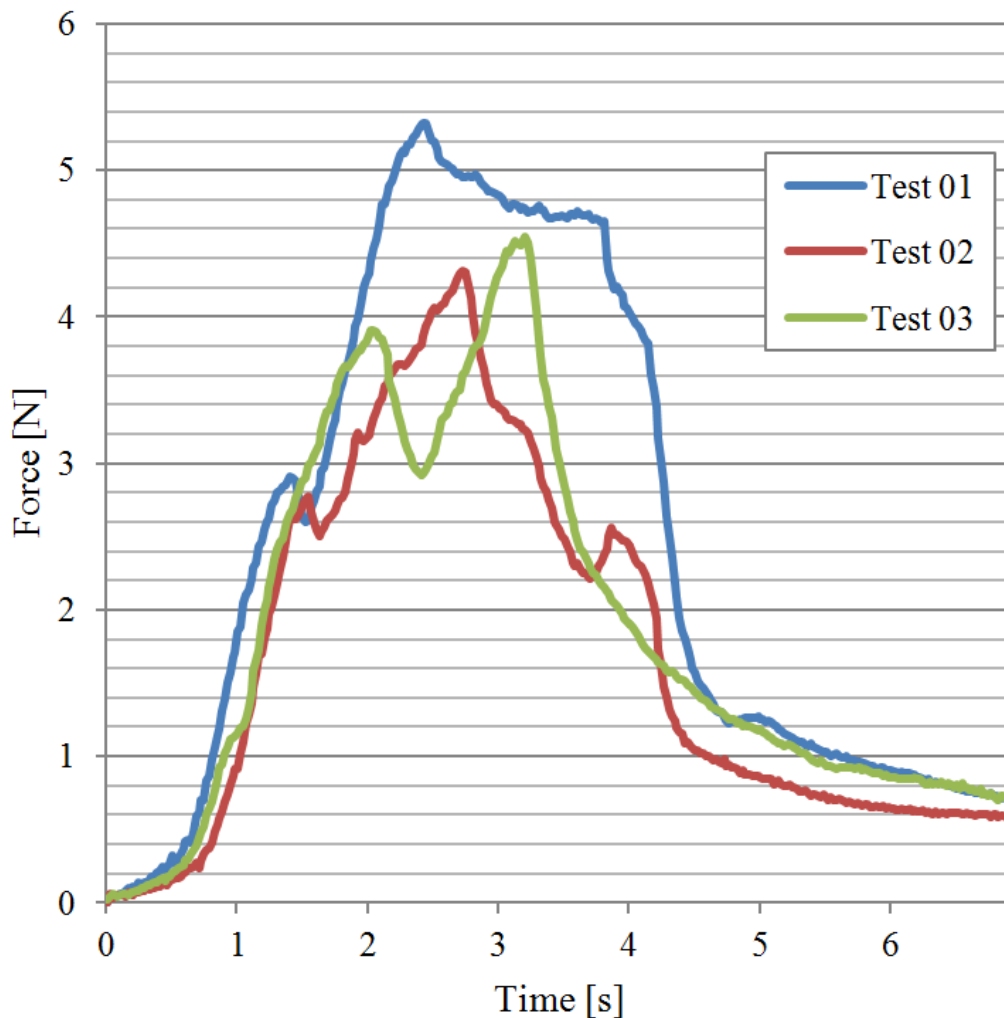


Figure 4.3. Comparison between the force exerted for the same machining parameters ($v = 1 \text{ mm/s}$, amplitude $80\mu\text{m}$) on Polystyrene samples.

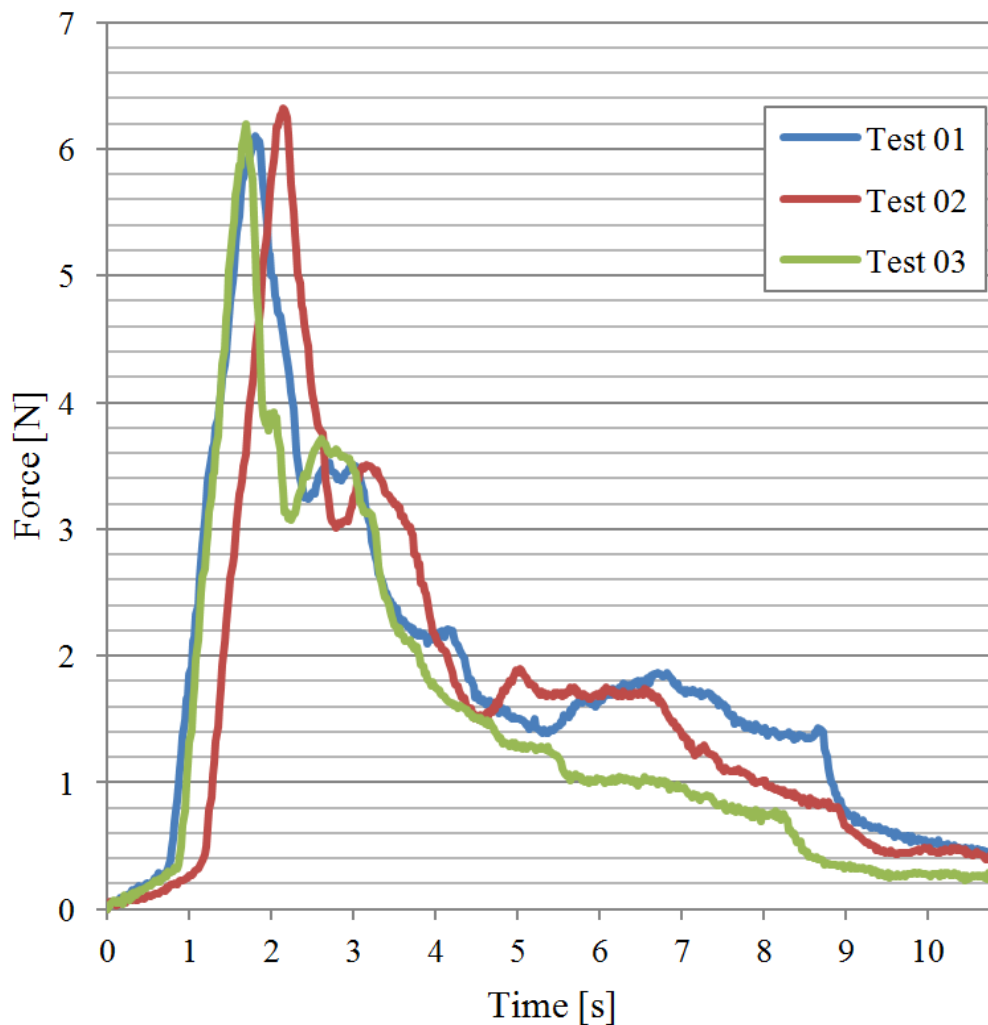


Figure 4.4. Comparison between the force exerted for the same machining parameters ($v = 1 \text{ mm/s}$, amplitude $80\mu\text{m}$) on Polyurethane samples.

The data analyzed here seem to confirm one of the results emerged from the in-air machining studies: the maximum force exerted is highly dependent on the material structure. Polystyrene high non-homogeneity significantly influences the profile of the graph and the maximum force exerted, since they vary within the samples machined with the same working parameters (Figure 4.3). Polyurethane has a more homogeneous structure, thus resulting in a lower variability of experimental data within samples machined with the same parameters (Figure 4.4).

Considering the effects of working parameters, from the graphs shown in **Figure 4.5** (Polystyrene) and **Figure 4.6** (Polyurethane), it is clear that both speed and amplitude influence the force exchanged between the workpiece and the sonotrode. Given a feed rate value, when amplitude is increased, force decreases. On the contrary, given an amplitude value, the maximum force exerted decreases when feed rate is reduced.

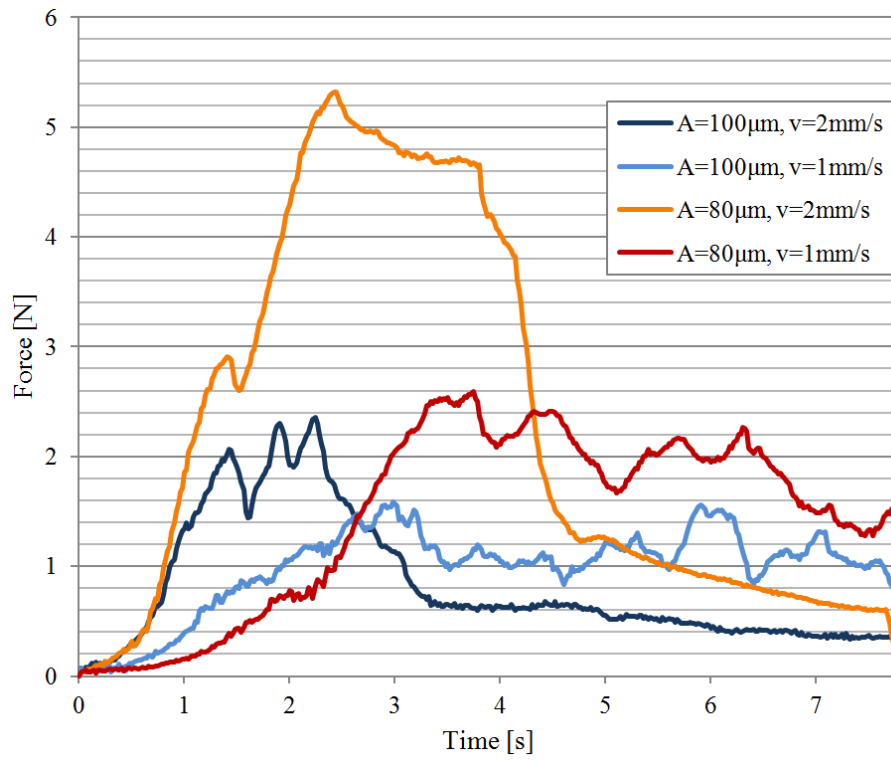


Figure 4.5. Comparison between the force exerted on Polystyrene samples with different working parameters.

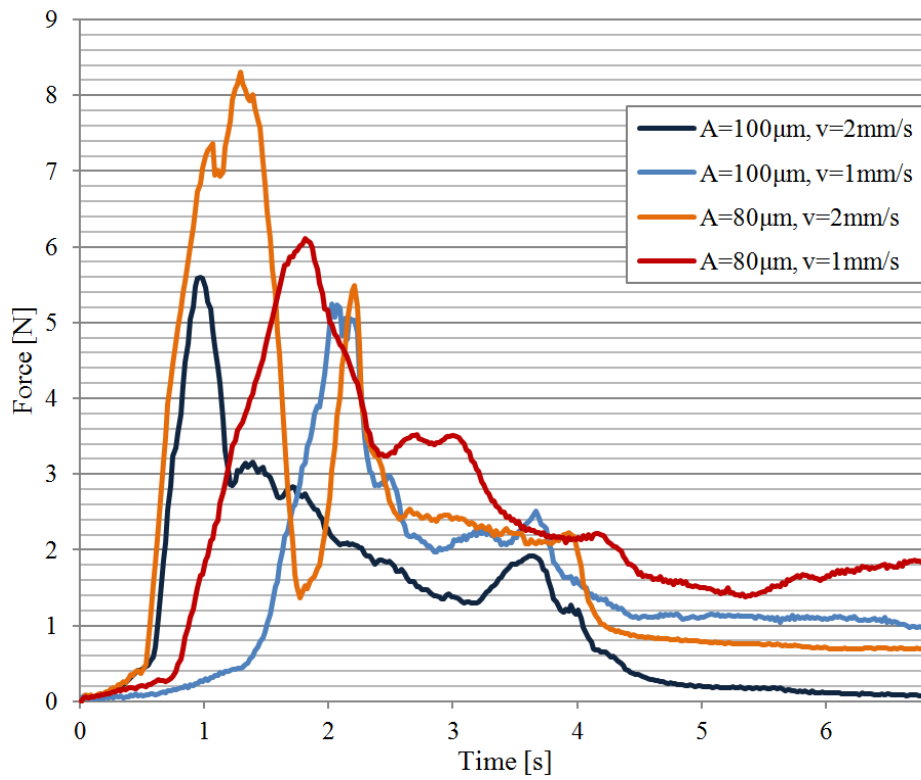


Figure 4.6. Comparison between the force exerted on Polyurethane samples with different working parameters.

An important comparison has to be done about the surface finishing of materials, if compared with in-air samples. Considering for instance Polystyrene (**Figure 4.7**), the dimensional precision of the hole does not change significantly, or is even improved. The single most marked observation to emerge from the comparison between in-air (**Figure 4.7a**) and underwater samples (**Figure 4.7b**) is the difference of the heat affected material distribution. In both cases there is a shell-like material surface with altered properties (gray area in **Figure 4.7a**), but comparing under water with in in-air machining, the properties of this heat affected area are more homogeneously distributed. This effect is also evident from the analysis of Polyurethane samples (**Figure 4.8**). The observation of in-air samples (**Figure 4.8a**) highlighted the presence of highly heat affected zones (lower part of the hole), while is evident the absence of this area in underwater machined samples obtained with the same working parameters (**Figure 4.8b**). The main difference between in-air and underwater machining is not the dimensional precision, that is comparable, but the influence of heat affected zone. For both Polystyrene and Polyurethane the pattern of the walls is different, because of the different working principle responsible for the operation.

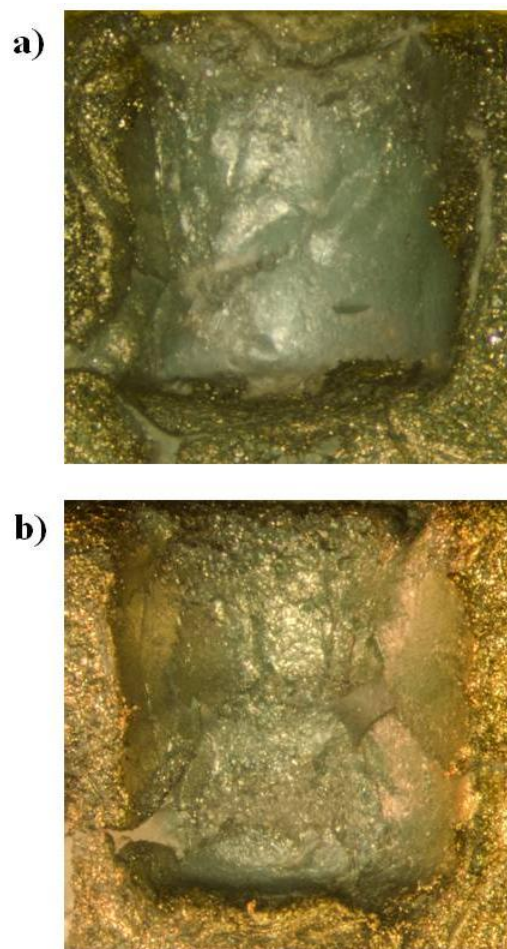


Figure 4.7. Differences between (a) the sample of Polystyrene machined in in-air configuration and (b) the underwater machined sample ($v = 1 \text{ mm/s}$, amplitude $100\mu\text{m}$).

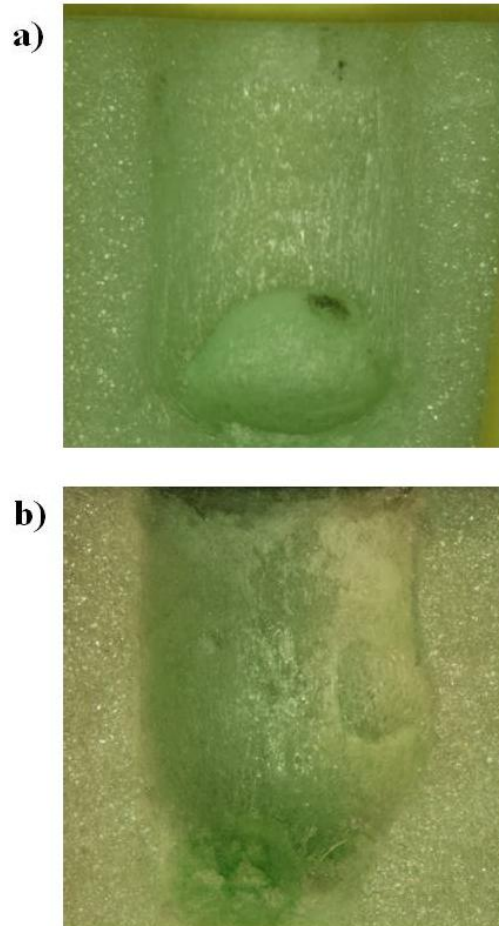


Figure 4.8. Differences between (a) the sample of Polyurethane machined in in-air configuration and (b) the underwater machined sample ($v = 1 \text{ mm/s}$, amplitude $100\mu\text{m}$).

4.9 Wax

Machining of Wax has also been analyzed. In-air machining of this type of material is possible, but comparing the holes shown in **Figure 4.9**, underwater machined hole (b) is much well defined than the in-air machined one (a). By analyzing the videos of the experiment (screenshots shown in **Figure 4.10**), the different phases of the process are evident.

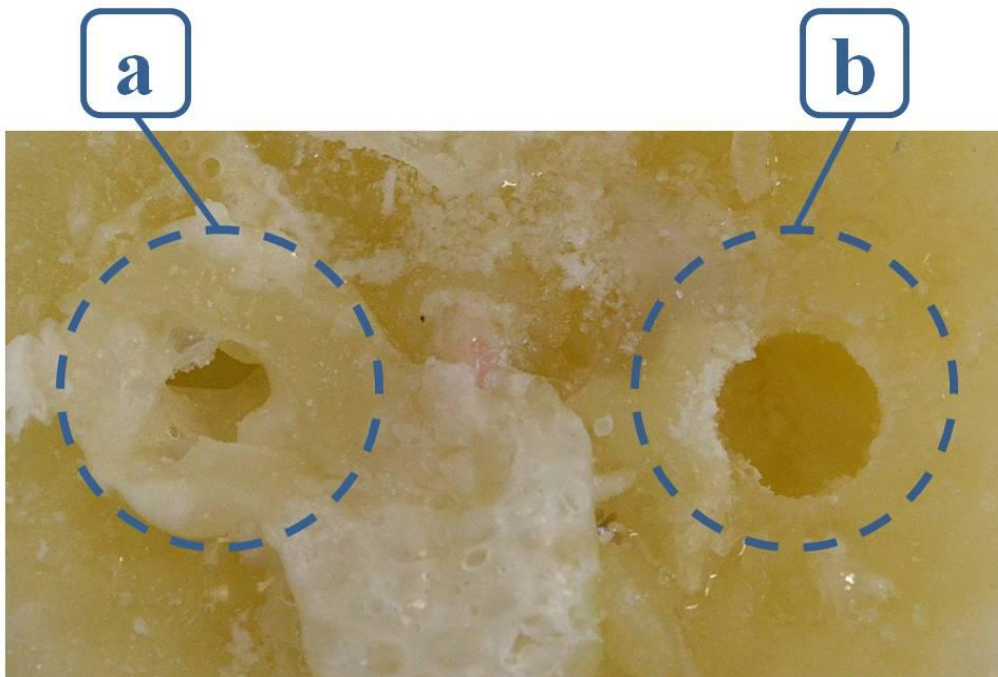
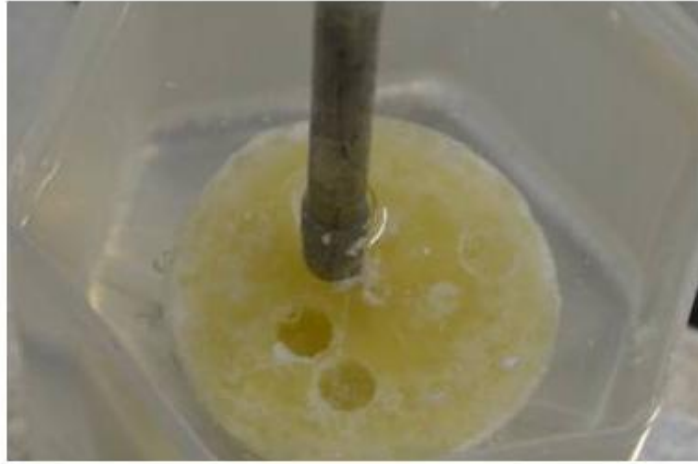


Figure 4.9. Different behavior of Wax when machined (a) in air and (b) underwater.

The sonotrode is positioned over the workpiece (a), then the drilling operation starts and wax starts melting (b). Finally wax solidifies and is removed from the working area (c).

Experiments were done only for 1 mm/s feed rate, because of the fragility of wax samples, but the data analysis revealed an unexpected low force exchanged between the sonotrode and the workpiece. This is most probably because of the low melting temperature of wax, that makes heat the main working principle also for underwater machining. In fact, the measured temperature at the interface wax-sonotrode was 43°C, thus allowing the authors to conclude that heat has a big influence on wax working conditions. **Figure 4.11** shows the experimental results for samples obtained with an amplitude value of 80µm. Output data have been filtered to remove the load cell noise, that for the values obtained is visible. The in-air tests have not been performed because of the unacceptable quality of holes created.

a)



b)



c)

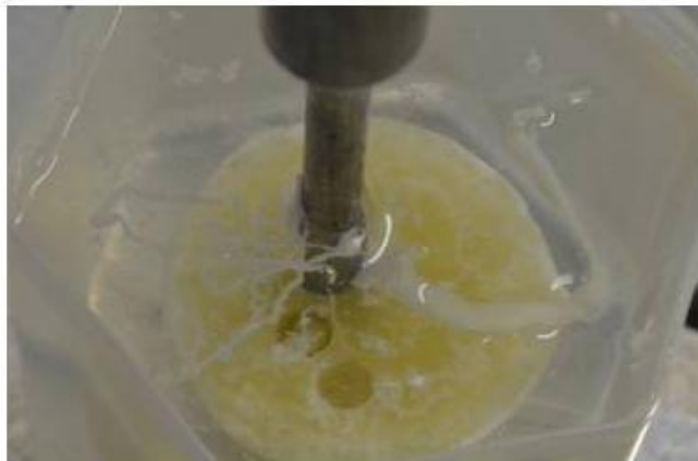


Figure 4.10. Screenshots of Wax underwater machining video.

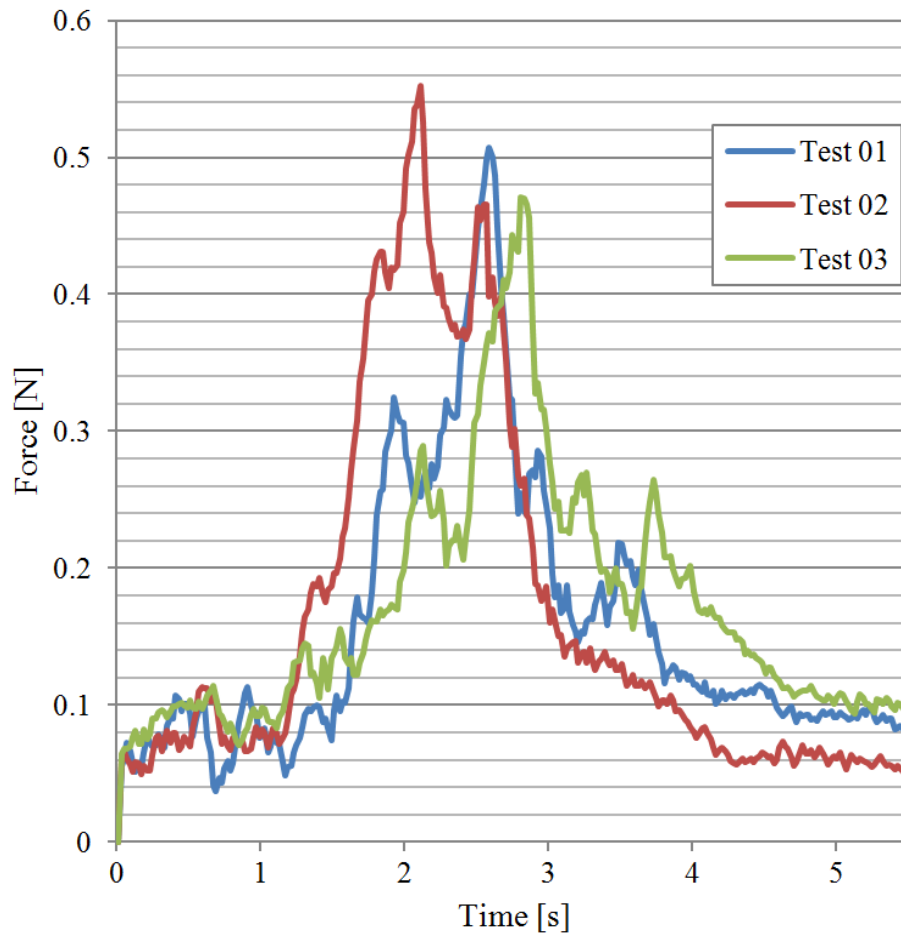


Figure 4.11. Force exerted for the same machining parameters ($v = 1$ mm/s, amplitude $80\mu\text{m}$) on Wax samples.

5 OBJECT SHAPING WITH A SONOTRODE

Rapid Prototyping methods are often based on additive manufacturing strategies. Depending on the application, it can also be considered the use of a removal manufacturing rapid prototyping methodology. In this chapter it is investigated the possibility of using the ultrasound technology for the shaping of materials that can be considered as a final object, or as a rapid manufactured mold for the creation of products. Free-form objects can be manufactured starting from foam like materials and model the foam thus shaping the desired features.

The possibility of implementing the technology onto automated systems was tested, allowing considering the use of this system on automated manufacturing lines. Geometrical deviations from the 3D model are measured and material morphology before and after machining is analyzed.

5.1 Introduction

The intent of this study is to operate some traditional machining operation, like lathe-shaping and milling, on samples made of polystyrene, using a sonotrode instead of a traditional tool. Industrially, some operations can be performed on polystyrene blocks using traditional machining operations, but as a main difference if compared to ultrasound machining, many chips are created when using cutting tools to shape the material with traditional operations. Furthermore, because of the structure of polystyrene, it can happen that entire elements are removed when machined with traditional machining tools.

The chapter analyses the possibility of using a sonotrode as shaping tool for milling and lathe-shaping operations, evaluating the differences between theoretical shapes and real surfaces. In addition to this first analysis, the presence of debris will be evaluated, and the structural composition of the machined material will be analyzed. The accuracy of shapes created with ultrasound shaping is important to recognize the benchmark the technology aims at, evaluating its suitability in one field of application more than another one.

The work is organized as follows: Section 5.2 presents an overview of the application fields of the ultrasound technologies. The following Section 5.3 explains the design of experiment for the achievement of the shaped objects, while results are analyzed in Section 5.4.

5.2 State of the Art

Ultrasound technology has been widely exploited in several fields in the last decades. Recently (in the last 20 years) ultrasonic blades found many applications in food industry. Ultrasonic assisted food cutting offers good performance in precision, uniformity and hygiene, and is the perfect cutting technology for a wide range of industries. Other ultrasonic instruments relates to the cleaning systems, and the interest of industry in this field is clear from the high number of patents relating both to industrial devices and appliances for private use.

From the initial results of an ongoing research activity at the University of Pisa about the uses of ultrasound technologies in manufacturing process, it appears that ultrasounds are becoming always more and more exploited also in the biomedical field. For instance, there are many patents regarding the use of ultrasounds are for the creation of holes in porous tissues, for energizing foams that can be used for pain relief, or even for the manufacturing of biomedical devices like garments.

Focusing on manufacturing technology, ultrasounds are commonly used with hard slurries in the so called ultrasonic impact grinding, both in the macro and micro machining fields. The process consists in a vibrating tool oscillating at ultrasonic frequencies used to compress an abrasive slurry between the workpiece and the tool, thus inducing small cracks on the workpiece and removing the material from the workpiece itself. The main working principle is mechanical, even if the slurry has some thermal functions. This machining process suits perfectly for hard and brittle materials, such as glass, titanium, sapphire, ruby, diamond and ceramics.

Ultrasonic probes are also used for welding plastics. Nowadays, this technology cannot be considered innovative any more, since there are many papers dating back in the 70s, e.g. the excellent review of industrial application conducted by Shoh. Usually a high frequency (from 15 kHz to 40 kHz) and low amplitude vibration is used to create heat by way of friction between the materials to be joined. The interface of the two parts is specially designed to concentrate the energy for the maximum weld strength.

Other uses of sonotrode in manufacturing operations are in investment casting, where solidified parts are broken from the sprue thanks to ultrasonic vibrations. Furthermore the possibility of using ultrasound technology with foam-like materials has already been explored both from academics and from industry.

5.3 Methodology

The possibility of using a sonotrode for the shaping of foam-like materials was already tested, with encouraging results. While the work mentioned above analyzes the use of a sonotrode for drilling operation, the present chapter aims at combining also lateral motion. An axial translation is required for the drilling operation (Figure 5.1a), while there are two more possibilities for shaping materials with the ultrasound technology: the first one is represented in Figure 5.1b, and consists of a longitudinal translation of the sonotrode, and it can be assimilated to a traditional milling operation. Figure 5.1c shows a combination of both axial and longitudinal translation, that is an operation common in the facing operation of a lathe.

The study explores the possibility of implementing the work procedures represented in Figure 5.1b and Figure 5.1c, thus mounting the sonotrode on a milling machine and on a lathe. The sonotrode has been fixed on traditional machines available at the workshop of the Department of Civil and Industrial Engineering at the University of Pisa, and on a robot made available from Gruppo Scienza Machinale.

For the present work, the ultrasound technology has been used only for shaping operations of Polystyrene samples. The aim of this study is to validate the possibility of using the ultrasound technology for shaping operations of foam like materials, and specifically of polystyrene blocks. Other materials have been considered for shaping, but experiments are still ongoing at the present moment.

Two different setups have been created for testing the sonotrode both in milling and in turning operations. Different interfaces have been created to mount the end effector both on the lathe and on the robot. One more setup aimed at showing the differences between a traditional milling operation with a milling machine and the ultrasound milling in terms of quantity of chips created.

The sonotrode is the core of the ultrasound machining operation. The system used for experiments is the Vibra Cell VCX 130 PB from Sonics & Materials, Inc.. The data sheet reports that the vibration frequency is constant and it is 20 kHz, while the amplitude can be adjusted. The probe mounted on the sonotrode is an exponential one made of Titanium alloy, having a tip with a diameter of 6 mm. The sonotrode has been used at the maximum value of its amplitude for all the tests.

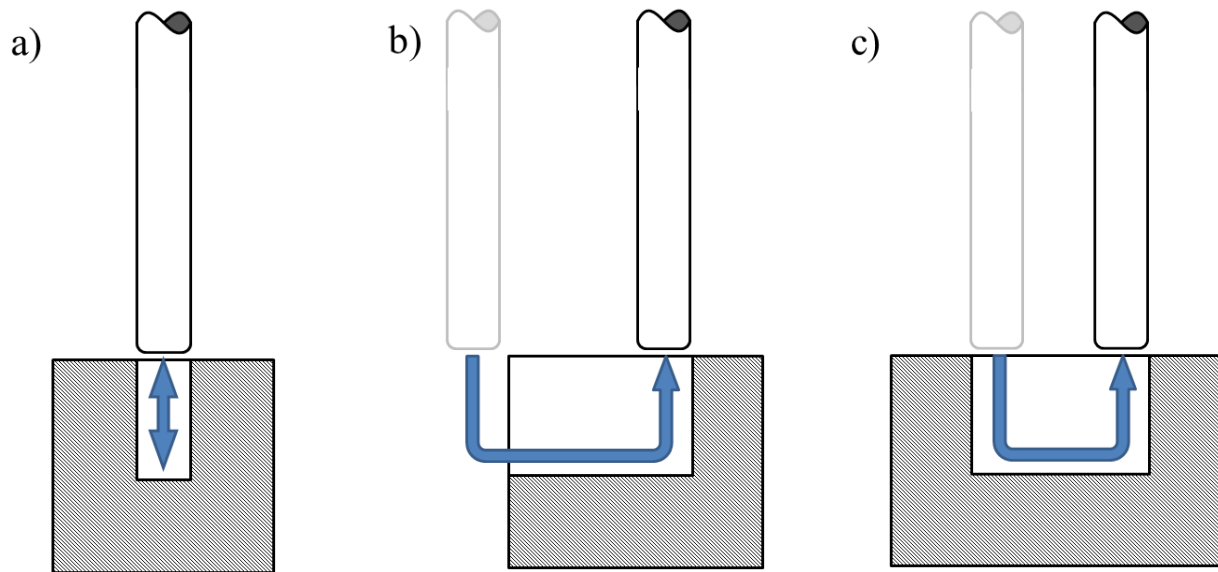


Figure 5.1. The three operations that can be performed with the sonotrode: axial removal operation (a), the longitudinal removal translation (b) and their combination (c).

The working principle of the machining operation comprises both mechanical and thermal effects. The thermal effect is evident also from the presence of a small amount of chips generated: Figure 5.3 explains how material is deformed and where the machined material goes. The portion of material painted in blue (Figure 5.3a) is the part that is undergoing the deformation process. When heated, Polystyrene softens and the blue volume of Figure 5.3a is spread on the lateral surfaces of the machined hole or groove, as shown in Figure 5.3b. Not all the deformed material is spread inside the groove, so some chips and debris are generated. However, the quantity of chips generated by the sonotrode is considerably lower than the one generated by a traditional tool (see Figure 5.2).

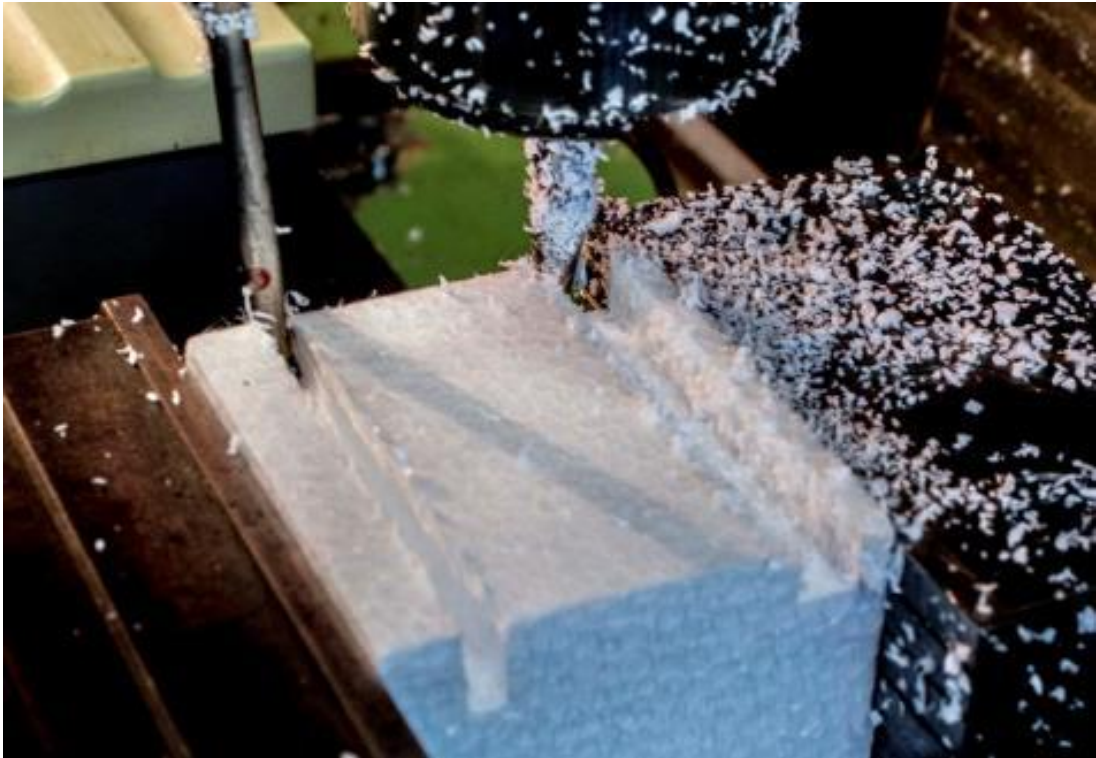


Figure 5.2. Comparison between the milling operation with the sonotrode (left) and with a traditional cutter (right).

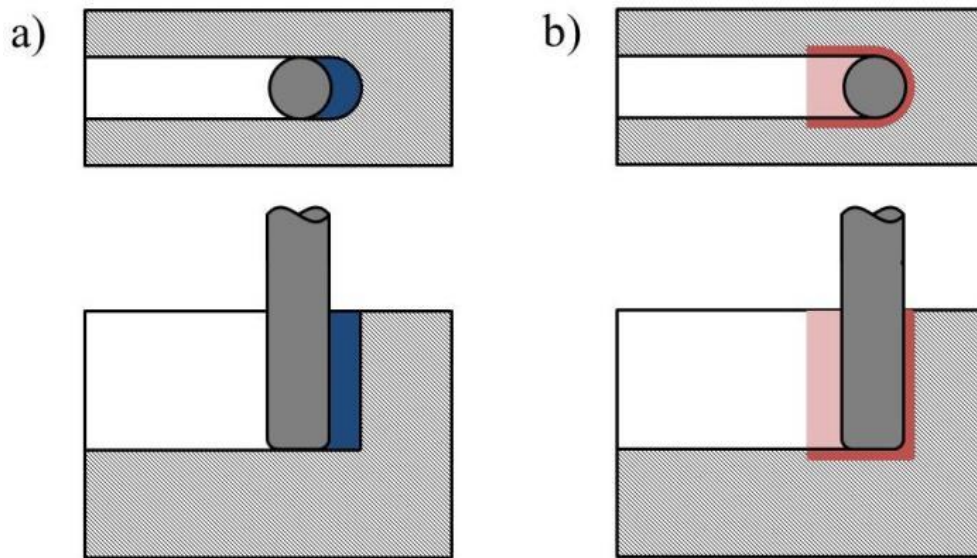


Figure 5.3. The picture shows the material that is undergoing to the deformation process (a) and the same material after the machining process (b).

5.4 Milling

The sonotrode was mounted on 6-axis ABB robot. The robot has been controlled in speed along the trajectories calculated with the specific software ARPP[®], with a set of speeds from 5 mm/s to 20 mm/s. The software is used for the calculation of trajectories for machining operations using conventional manufacturing tools. This consideration is not trivial, since the shaping trajectory has a significant influence on the working principle of the ultrasound technology. When used as a drilling instrument, the sonotrode uses both the mechanical and thermal effect, while for the milling operations heat becomes more important. During the machining operations, the probe of the sonotrode reached 52°C, that is a significantly higher temperature if compared with the maximum one measured during the simple drilling operation (41°C).

A pyramid has been created as benchmark test for the milling operation on a polystyrene block. The initial block is approximately a parallelepiped having a square-shaped base, each side sizing 70 mm, and height 50 mm. The levels are alternatively circles and square shapes. The desired final surface is shown in Figure 5.4a, while the real object obtained is shown in Figure 5.4b. As mentioned above, some surfaces have a coarse precision due to the trajectories assigned by the software. Moreover it is evident how the surface quality is also affected by the working parameters, especially by the feed ratio. More detailed analysis on the surface will be discussed in Section 5.4.

One more shaping experiment was conducted on Polyurethane samples, but because of the material properties and of the high temperatures generated during the machining process, the result was not considered positive. As explained in “Fantoni, G., et al., Shaping of foam-like materials through the use of a sonotrode”, when machined in-air, the friction between the sonotrode and the workpiece generates a heat. While for drilling operations the process lasts few seconds, in the shaping of materials it can last long. In Polyurethane machining temperatures rose the 120°C, and heat became the only working principle, with Polyurethane becoming soft and deforming itself also without being in touch with the sonotrode (the softening point of Polyurethane varies significantly depending on the specific type of Polyurethane used). At the present moment there are ongoing experiments on different types of Polyurethane, especially on the Polyurethane known as *Blue Foam*, that is widely used in design modeling and in augmented reality.

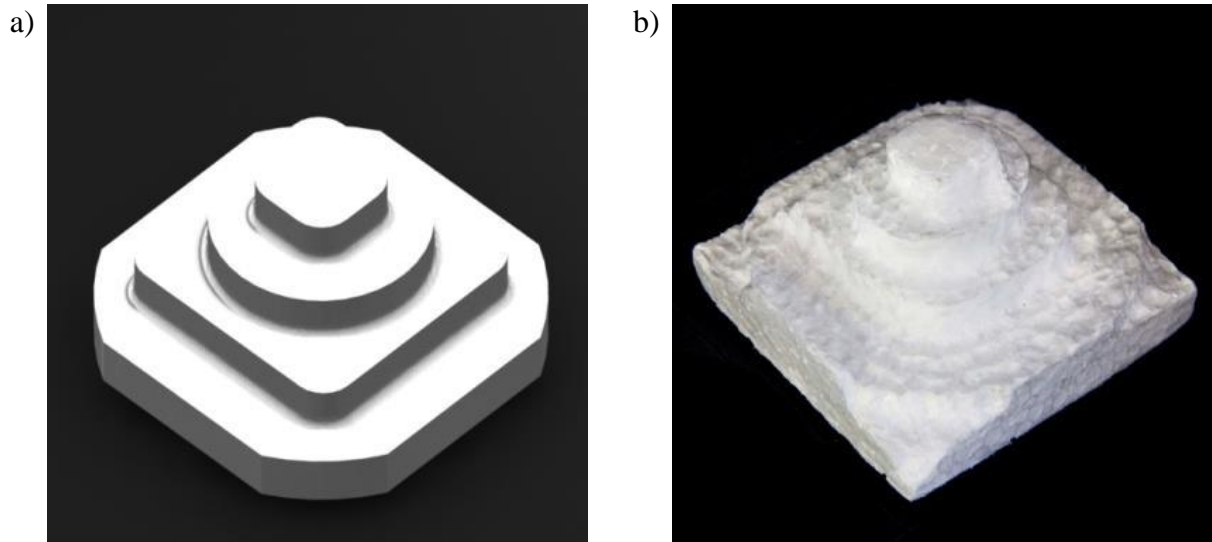


Figure 5.4. Difference between the CAD theoretical design (a) and the object shaped with the ultrasound technology (b).

5.5 Turning

In order to accomplish the turning machining operation, the sonotrode was fastened to the turret-head. The workpiece, shaped as a prism with a constant square section of 70 mm and a height of 50 mm, was fixed to the turning machine through a combination chuck. The scheme of the setup is illustrated in Figure 5.5. Because of the geometry of the sonotrode and the limited excursion range of the turret head in the z-axis, only face grooving operations were possible.

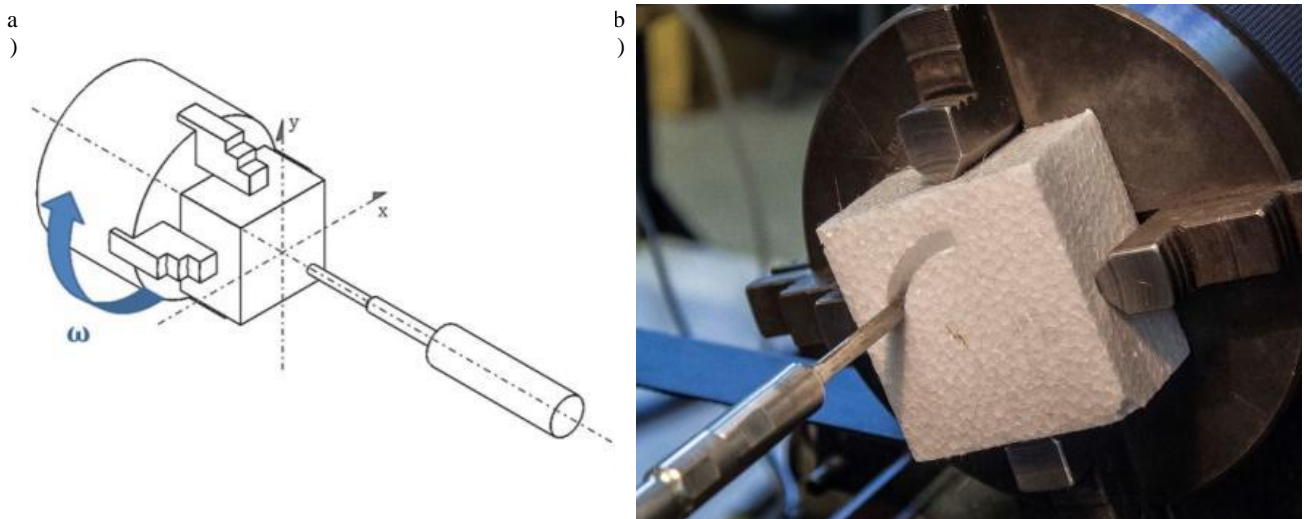


Figure 5.5. Scheme of the setup for the ultrasound machining on lathe (a) and the real setup (b). Because of the dimensions of the sonotrode, the only operation possible was the face grooving.

The shapes created in the face grooving operation on Polystyrene were circles, cylinders and spirals (Figure 5.6). The shapes created on Polyurethane samples were cylinders and spirals (Figure 5.7). The goal of the test was to evaluate the possibility of shaping material with this type of operation. The samples created on Polystyrene have been dimensionally analyzed, in order to understand how the working parameters can influence the precision and the surface finish. Results on Polyurethane have been analyzed only at a qualitative level, since the coarse quality of results make the process unsuitable for machining on the type of Polyurethane analyzed. As for the milling process, there are ongoing experiments on different types of Polyurethane.

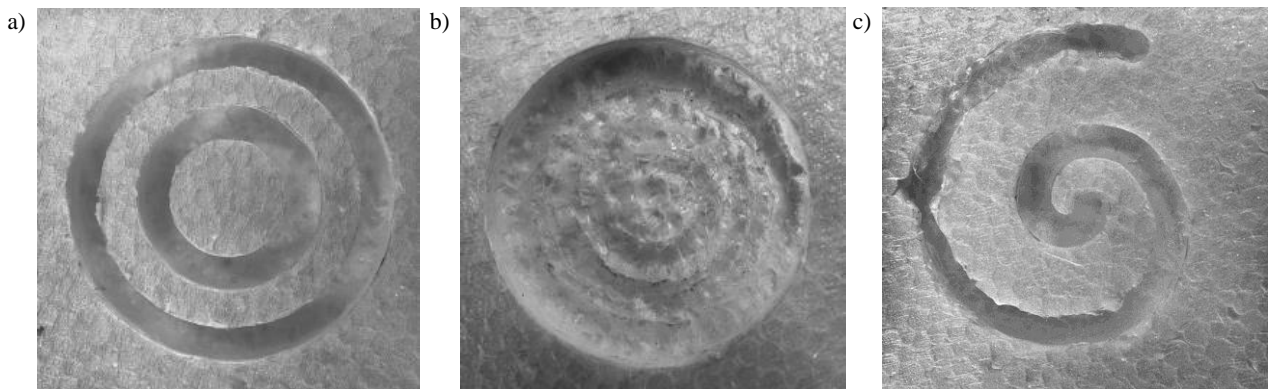


Figure 5.6. Shapes created on Polystyrene: circles (a), cylinder (b) and spiral (c).

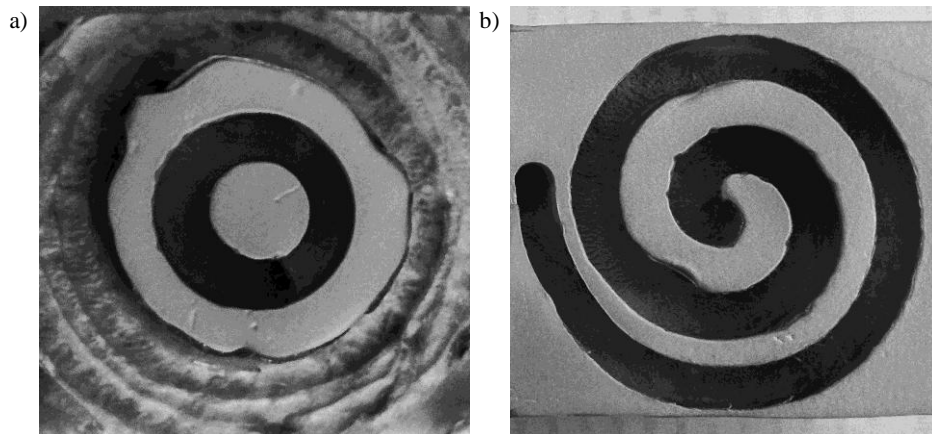


Figure 5.7. Shapes created on Polyurethane samples: cylinders (a) and spiral (b). The quality of the machined piece is coarse.

5.6 Analysis of the results

The following subsections present the technology adopted for data acquisition and for the analysis of material after the machining operations. Both dimensional and material analyses are conducted. The first ones help in understanding the precision gathered with the ultrasound machining, while the material analyses focus on the physical principle that is suited for the process.

5.7 Dimensional Analysis

In this work, an optical scanner based on an active stereo vision approach (Figure 5.8) has been designed in order to acquire manufactured sample models. A two-axis platform structure, including rotating and tilting movements, has been assembled by using two stepper motors having a resolution of 400 steps per round. The optical sensor (Figure 5.8) is composed of a monochrome digital CCD camera ($1,280 \times 960$ pixels) and a multimedia white light DLP projector ($1,024 \times 768$ pixels). A multi-temporal Gray Code Phase Shift Profilometry (GCPSP) method is used for the 3D shape recovery. A sequence of vertical light planes is projected onto the model to be reconstructed. The planes are defined by black and white fringes with time variable period. Each acquired pixel by the camera is characterized by a light intensity that can be either bright or dark, depending on its location in the respective projected image. A binary code (0, 1 with n bit) is assigned to each pixel, where n is the number of the projected stripe patterns, and the values 0 and 1 are associated to the intensity levels, i.e., 0 = black and 1 = white. This encoding procedure provides $l = 2^n - 1$ encoded lines. The 3-D coordinates of the observed scene point are then computed by intersecting the optical ray from the camera with the projected plane. The geometry of the hardware set-up, the camera ray direction and the plane equation of the corresponding stripe are known by a preliminary calibration step. The methodology provides $n_p = l_h \times l_v$ encoded points, where l_h is the horizontal resolution of the projector while l_v is the vertical resolution of the camera. The whole measurement is obtained by collecting 3D surface data of sample models from various directions. Different views are automatically aligned with reference to a common coordinate system on the basis of the controlled rotating axes, exploiting a calibration procedure which relate turntable positions with respect to the common reference system. The combination of two distinct controlled axes allows a reliable acquisition of shape details, since different viewing directions better handle occlusion problems and undercut areas. The vision system has been configured for a working distance of 300 mm and a working volume of $100 \text{ mm} \times 80 \text{ mm} \times 80 \text{ mm}$ (width \times height \times depth). The scanner is capable of measuring about 1 million 3D points with a spatial resolution of 0.1 mm and an overall accuracy of 0.01 mm.

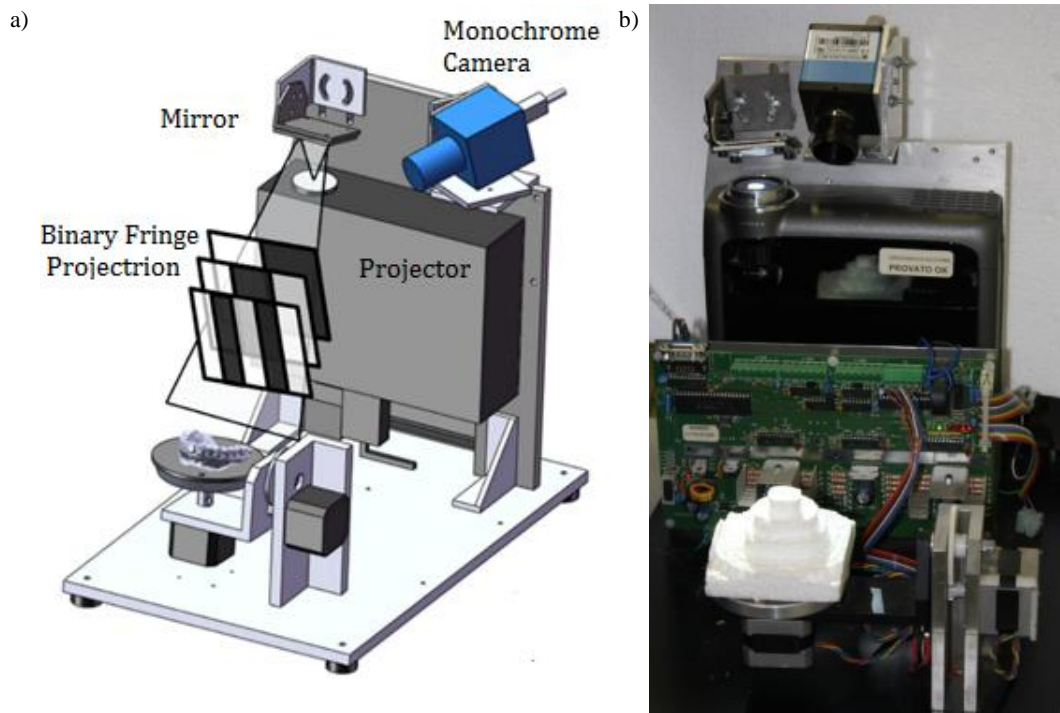


Figure 5.8. Scheme of the assembled optical dental scanner (a) and real setup (b).

Data have been acquired and a comparison was made based on the results of interest. Some analyses are at quantitative and qualitative level: the milled pyramid (Figure 5.4b) was analyzed to compare the overall machining quality, the milled circles (Figure 5.6a) are helpful to evaluate the lateral precision, while the grooved cylinder (Figure 5.6b) can be considered to evaluate the precision of the bottom surface.

Other types of analyses were only at a qualitative level, like the spiral sample both on Polystyrene and Polyurethane. The spiral (Figure 5.6c and Figure 5.7b) allows understanding how heat and speed of the sonotrode can affect the quality of the surface. The rotational speed around the center of rotation O (Figure 5.9) was kept constant and was 0.5 rpm for both the samples. As in all the turning operations, the closest the tool is to the center of rotation, the lower the tangential speed is. Considering the spiral on Polystyrene, and referring to Figure 5.9 and Table III, it is evident that when the tangential speed decreases, the surface quality is improved. On the other hand, also the contribution of heat has to be taken into account, since when the machining operation starts, the temperature of the sonotrode is the ambient temperature, and increases during the manufacturing process. In Figure 5.9, the part of spiral from A (initial point) to C creates poor quality borders, even if the quality progressively increases while getting closer to the point C. From the point C to

the final point of the machining process, the quality of the borders can be considered fully satisfactory.

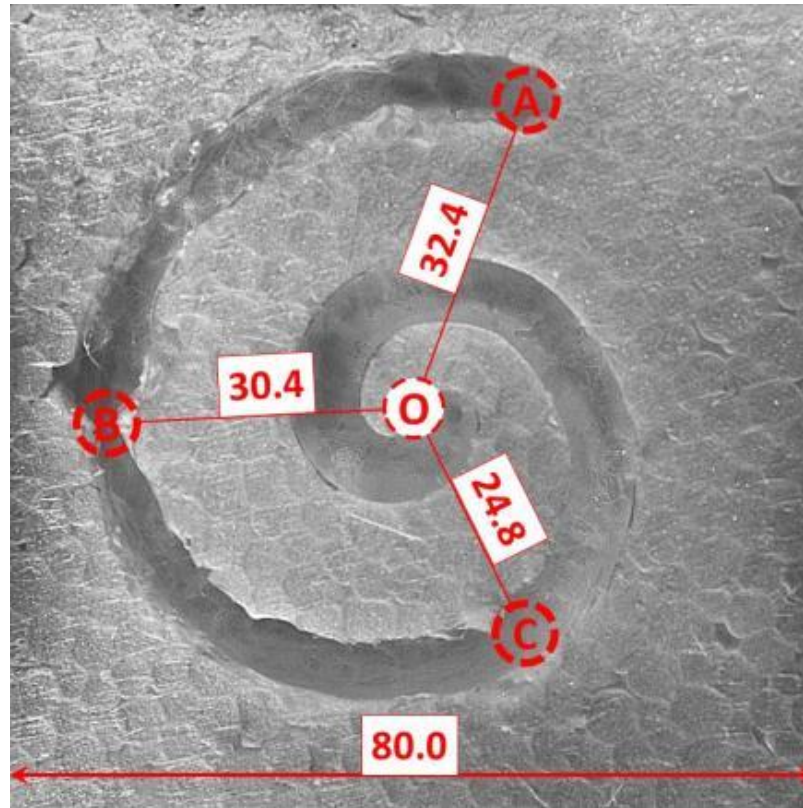


Figure 5.9. Spiral on Polystyrene block with highlighted significant points and measures [mm]: center of rotation (O), initial point (A), point where the material has been torn (B) and point from which the machining operation is fully satisfactory (C).

Table III. Measures and values of machining parameters, referring to Figure 5.9.

Point (Figure 5.9)	Rotational speed [rad/s]	Distance from the Center (O) [mm]	Tangential speed [mm/s]
A	π	32.4	101.8
B	π	30.4	95.5
C	π	24.8	77.9

Considering the spiral created on the Polyurethane block (Figure 5.10), it appears that during the initial part of the machining process (part from A to B) the quality of the machined part is good, but it significantly gets worse in the point C. This is due to the high temperature reached by the sonotrode, that makes material melting even if it is not in contact with the sonotrode.

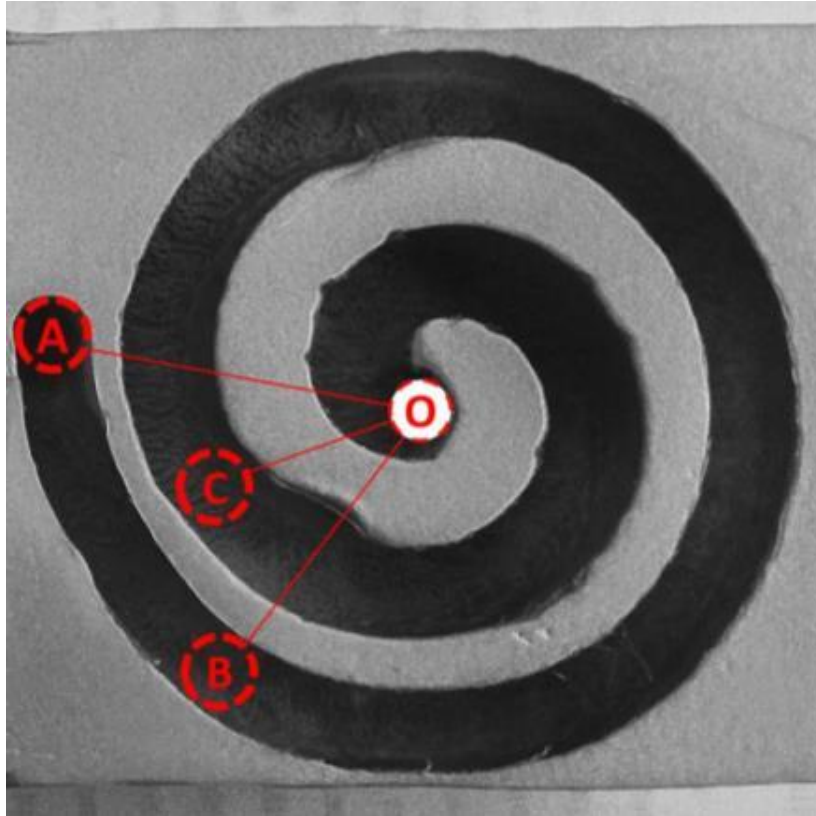


Figure 5.10. Spiral on Polyurethane block with highlighted significant points: center of rotation (O), initial point (A), point where the material starts melting even if not in contact with the sonotrode (B) and point from which the machining quality worsens (C).

About the pyramid, the comparison between the CAD model and the manufactured object is shown in Figure 5.11. If compared with traditional machining operations on conventional materials, the results appear to be unsatisfying. There are few considerations to take into account: the first one, and most important, is that the interface between the sonotrode may have not been connected in a tough way to the robot. This was necessary not to damage the instrument, which does not belong to the department. The second matter is the calculation of trajectories: as already mentioned, the software is used for the calculation of trajectories for machining using conventional manufacturing operations. Also the fillet radius was not considered in the CAD model, but the software created it because of conventional setting parameters. The fillet radius has been created starting from the reverse engineering analysis, but these areas lose their importance in the comparison analysis. The last consideration regards the machined material itself, since its intrinsic structure causes a high level of non-homogeneity and a low surface precision level, even when the material is not machined. The percentage of measured points versus deviation values are plotted in Figure 5.12, and clearly show that the maximum precision that can be gathered is coarse. However, because of the problems explained above, more experiments with different interfaces and different trajectories have to be done before a conclusion can be made.

The circular groove shown in Figure 5.6a has been used to evaluate the lateral precision of the ultrasound machining process. The comparison between perfectly cylindrical surfaces and the real machined surface is shown in Figure 5.13, where a section of the specimen is analyzed. Figure 5.14 presents the deviation of the specimen from the CAD model versus percentage of points for the section shown in Figure 5.13.

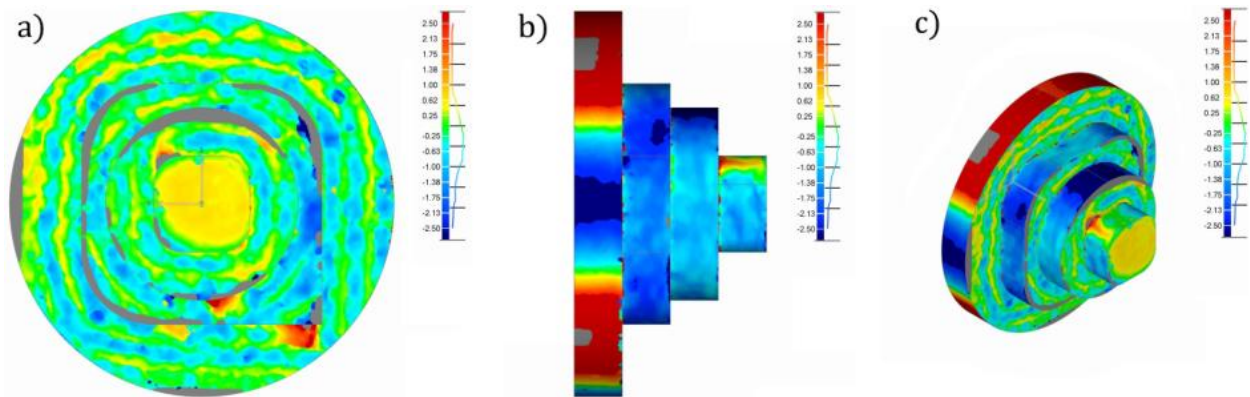


Figure 5.11. Comparison between the manufactured pyramid and the CAD model: top (a), side (b) and isometric (c) views.

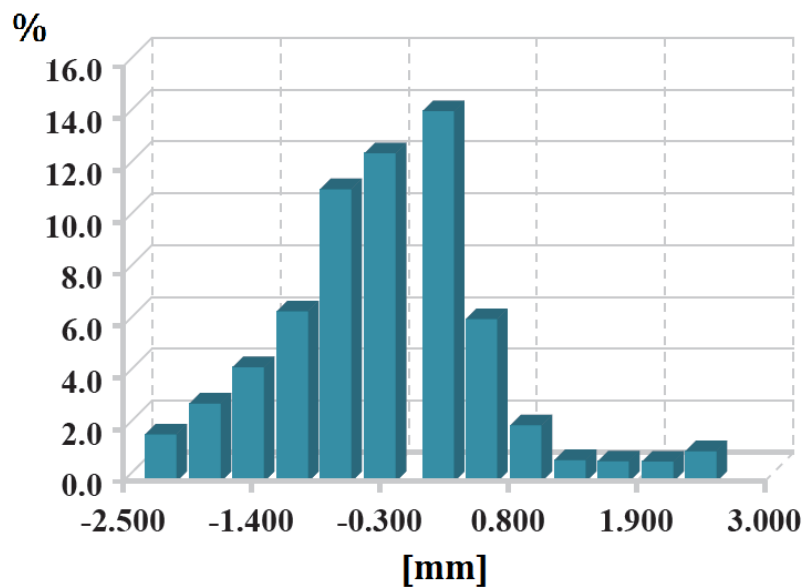


Figure 5.12. Deviation of the specimen from the CAD model versus percentage of points for the grooved cylinder.

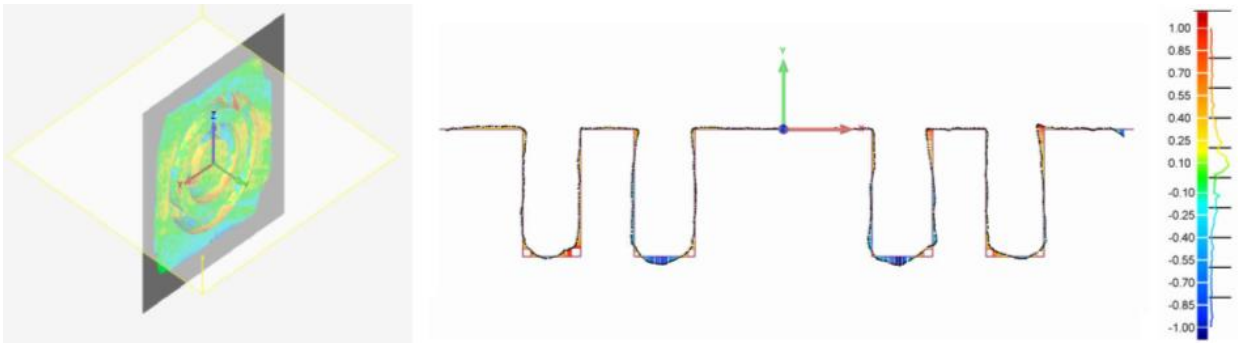


Figure 5.13. Comparison between perfectly cylindrical surfaces and the real machined surface for the section of the specimen indicated on the left.

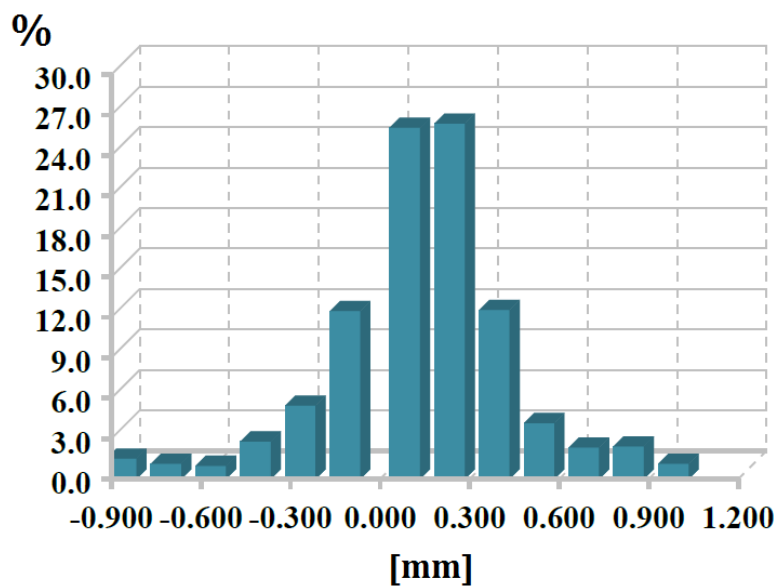


Figure 5.14. Deviation of the specimen from the CAD model versus percentage of points for the grooved circles for the section illustrated in Figure 5.13.

Considering now the cylinder, the comparison between the ideal cylindrical surface and the manufactured object is used to evaluate how the working parameters, especially the feed ratio, affect the bottom surface. The results are shown in Figure 5.17, and together with the results shown in Figure 5.15 for a section of the cylinder, highlight the trajectories of the axis of the sonotrode. The blue areas refer in fact to the planar part of the probe, while the red parts have not been properly machined. This test has to be considered only for a shape evaluation purpose, since it has been compared with a fitting ideal surface. Figure 5.16 presents the deviation of the specimen from the CAD model versus percentage of points for the section shown in Figure 5.15.



Figure 5.15. Deviation of the bottom surface of the grooved cylinder from an ideal planar surface.

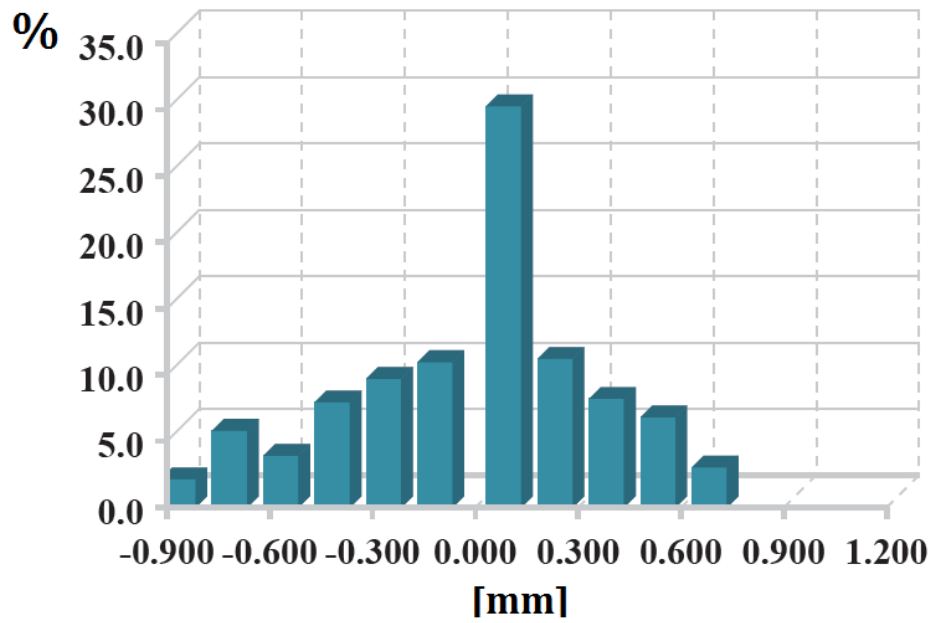


Figure 5.16. Deviation of the specimen from the CAD model versus percentage of points for the grooved circles for the section illustrated in Figure 5.15.

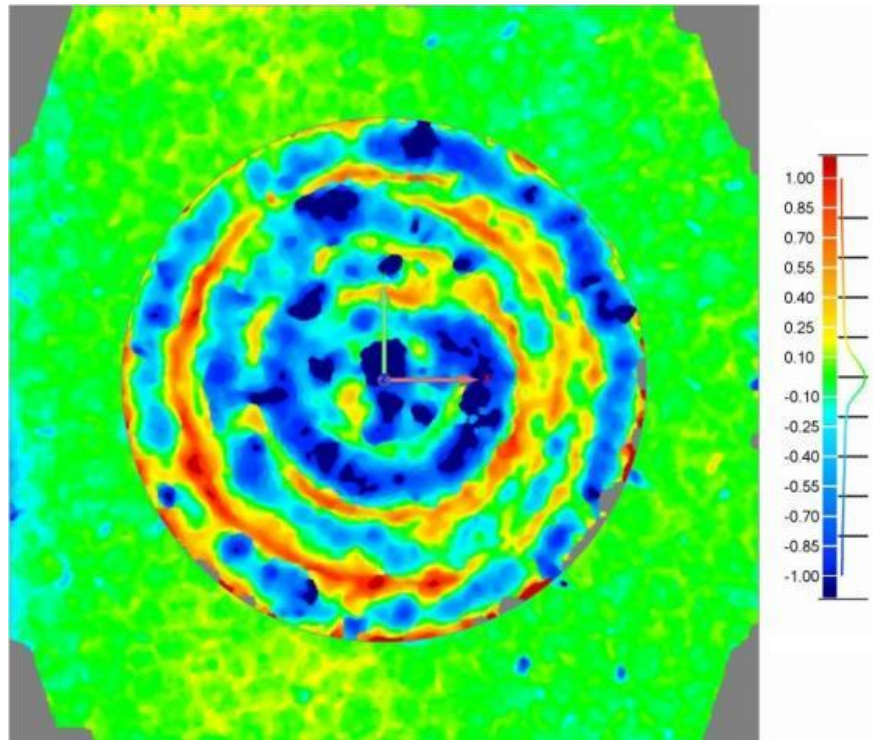


Figure 5.17. Comparison of the whole bottom surface of the grooved cylinder. The blue areas indicate where the axis of the sonotrode has passed. The deviation values are in millimeters.

Before concluding this section, it is important to highlight how the comparative analysis values significantly vary between the shape machined with the milling manufacturing and the ones obtained using the lathe. In fact, while the deviation of the pyramid from the CAD model presents a high number of points significantly distant from their ideal position, the percentage and the maximum error decrease significantly for the lathe-machined workpieces. This allows the authors to consider that the working parameters affected significantly the results of the machining process, and encourage to continue the experimental activity.

5.8 Material Analysis

Control of polystyrene and polyurethane surface properties is very important for the characteristics and the performance of the material. Without altering the bulk properties of the polymers, surface modification of these polymers becomes important, since the external morphology of Polystyrene and Polyurethane, together with an ultrasonic induced compaction near the surface, can determine a variation of stiffness and resistance properties. The aim of this work is to analyze the modification of polymer surface, as a consequence of a thermal alteration and an ultrasonic machining. Also underwater machined surfaces are analyzed, even if this working principle was not applied in the

manufacturing processes presented in this paper. However, it could be an important result, since it is exploited for ongoing research activities.

The Scanning Electron Microscope (SEM) used to analyze the difference between standard and machined surfaces is a JEOL JSM 5600LV. This is a high vacuum and partial vacuum (10^{-4} Pa- 10^{-6} Pa) SEM with secondary electron detector based on the scintillator-photomultiplier design of Everhardt and Thornley. Also fitted; solid state backscattered electron detector for compositional and topographical information. It is to be used at accelerating voltages between 1 and 30 kV. Images are stored digitally and/or on film.

The SEM provides an image of surfaces and is capable of both high magnification and good depth of field. Unlike a light microscope, the SEM uses electrons instead of white light to view the specimen, so that you can magnify over 100,000 times. In SEM, the electron beam scans across the specimen surface point by point. The signal collected from each point is used to construct an image on the display, with the cathode ray tube beam and the column beam following a synchronized scanning pattern. This means the displayed image is the variation in detected signal intensity as the column beam is scanned across the sample.

Images shown in Figure 5.18, thanks to the signals that derive from electron-sample interactions, reveal information about the external morphology of the samples of Polystyrene:

- a) *untreated Polystyrene* presents a regular structure, with spherical profiles;
- b) *thermal altered Polystyrene* shows a stretched structure, with pseudo-circular holes;
- c) *in-air machined Polystyrene* has a spread texture, in consequence of the fact that polystyrene begins to melt;
- d) *underwater machined Polystyrene* shows a squamous structure, due to the rapid solidification of melted material in contact with water.

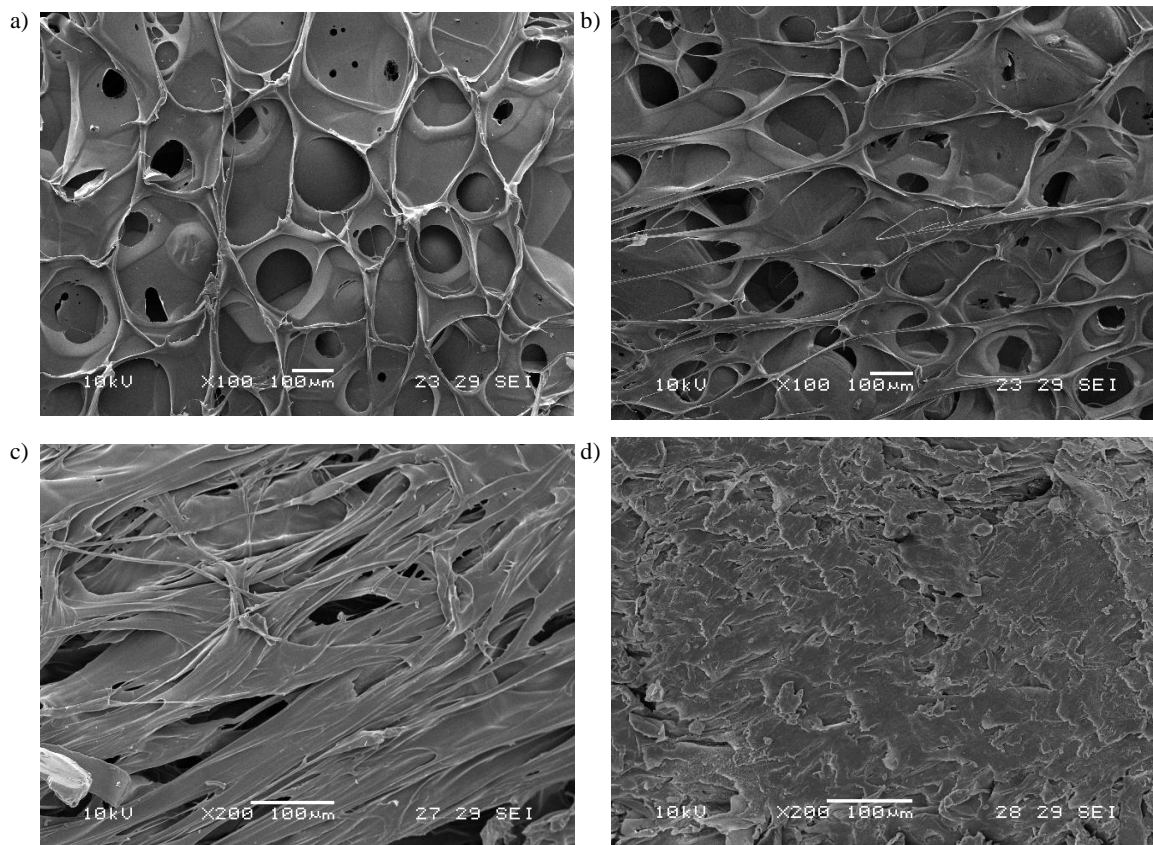


Figure 5.18. Polystyrene SEM analysis: (a) untreated, (b) thermal altered, (c) in-air machined and (d) underwater machined Polystyrene samples.

Conducting the same analyses for Polyurethane samples, Figure 5.19 reveal information about their texture:

- a) *untreated Polyurethane* presents a smoothed face, with few irregular holes;
- b) *thermal altered Polyurethane* presents a regular hexagonal structure;
- c) *in-air machined Polyurethane* has a sorded texture, due to the solidification of melted polyurethane;
- d) *underwater machined Polyurethane* reveals an indented structure, by reason of the rapid solidification of underwater processed material.

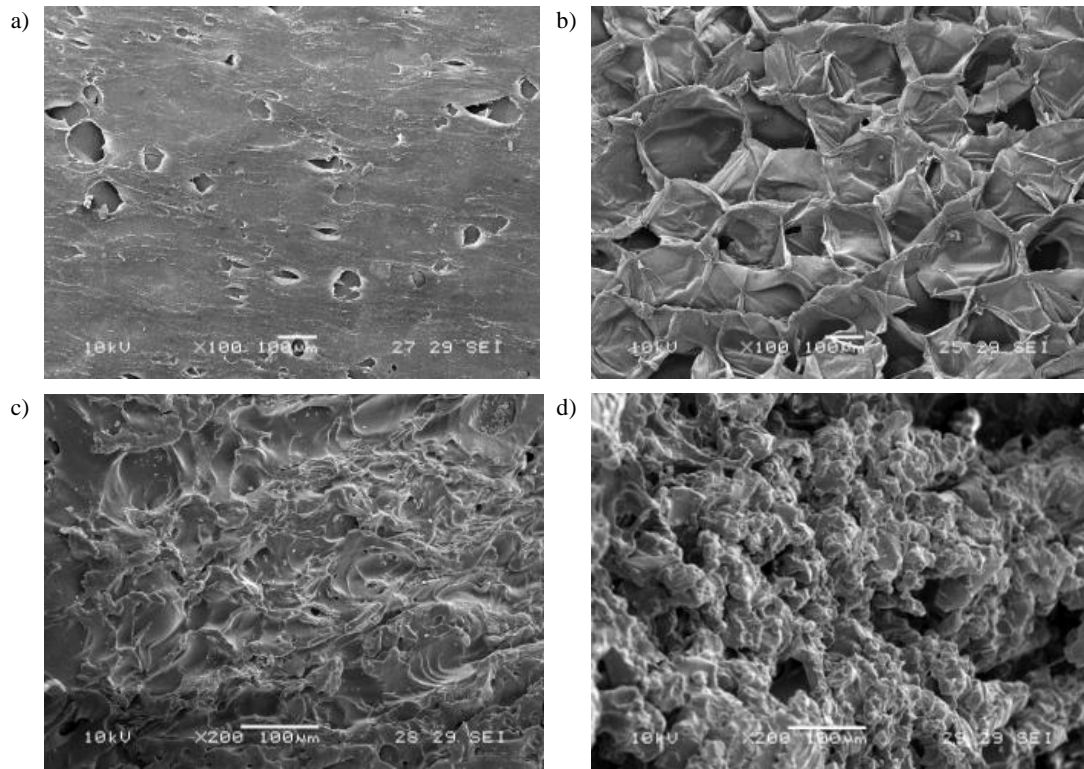


Figure 5.19. Polyurethane SEM analysis: (a) untreated, (b) thermal altered, (c) in-air machined and (d) underwater machined

Polyurethane samples.

6 ULTRASOUND PROPAGATION IN WATER

As shown in the previous chapters, high power acoustic waves can affect the structure of polystyrene and poliurethane. Due to the acoustic processing the grain structure becomes finer and more isotropic, leading to changes in the material properties.

Implementation of this technique can be represented by underwater ultrasound machining; the effective enhancement of underwater high power acoustic waves is the occurrence of mechanically violent cavitation bubbles, which activate and multiply the crystallization nuclei in the melt. Besides cavitation, a second process occurring is the acoustic streaming. It acts as a stirring mechanism, causing an increased part of the liquid volume to be treated by the local cavitation zone. The acoustic streaming is affected by the presence of cavitation.

Hereafter will be analyzed the acoustic streaming in liquid, in particular in the jet-flow region and the cavitation zone.

6.1 Problem analysis

Acoustic streaming below the cavitation threshold, but at a sufficient driving power, applied through an acoustic point source is known to form a flow pattern equal to that of a turbulent free jet (J. Lighthill, Acoustic streaming, Journal of Sound and Vibration 61 (3) (1978) 391–418).

Here the minimum driving power, P , is related to the minimum squared Reynolds number as: $\rho c^{-1} P \mu^{-2} = Re^2 > 4 * 10^3$, with ρ the density, c the speed of sound and μ the dynamic viscosity of the liquid.

In general the cavitation zone is a very small region with respect to the total volume.

Furthermore it is adopted that the treatment effectivity of the cavitation zone is perfect, that is, once a fluid volume passes through the cavitation zone it is taken to be treated. This assumption can easily be expanded towards partial treatment on passing the cavitation zone.

Multiple ways to apply an acoustic field to a liquid exist. In our studies we used an ultrasonic horn (sonotrode) penetrating through the liquid surface. The strong acoustic waves generated by the horn resulted in the formation of cavitation bubbles in the liquid. They also produced a mean flow through the mechanism of acoustic streaming. The investigation focused on the jet-flow region and not on the recirculating flow induced by the jet.

6.2 Problem modeling

The potential core is the central region of the jet which is not yet affected by entrainment of the surrounding fluid and does not show the self-similar velocity profile, but rather the velocity profile as it was present at the inflow.

This region of the flow narrows with increasing distance from the source as a result of mixing, however, for flows with a high turbulent intensity the profile is known to develop much faster.

This is due to an increased level of turbulent mixing. The fact that for the current measurements the self-similar profile develops much closer to the source (at approximately 10 mm from the sonotrode the profile is shaped according to the self-similar jet-profile) is therefore attributed to a high entrance turbulent intensity. The source for this high level of turbulence is most probably the cavitation zone: the violent behavior of the cavitation bubbles introduces additional turbulent kinetic energy to the jet.

6.3 Enhancements of focused ultrasound

The idea that stands behind this investigation is to analyze the possibility of relating the focusing method of the ultrasound beam implemented in High-Intensity Focused Ultrasound.

In particular, considering the geometrical technique (with a lens or with a spherically curved transducer) that enables ultrasound waves focusing, it is examined the effect of modifying the shape of the horn of the sonotrode, in order to obtain similar focusing conditions.

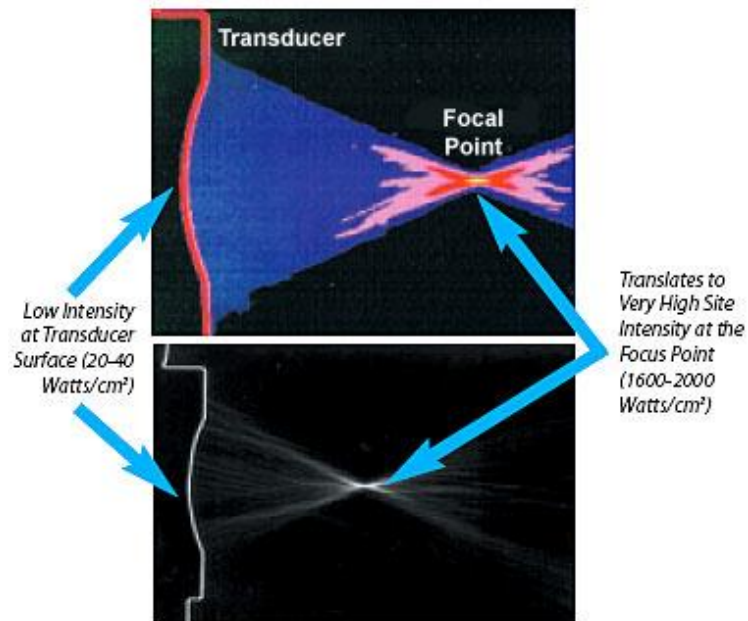


Figure 6.1. Focus point deriving from different geometrical conditions.

6.3.1 State of the art: HIFU

High-Intensity Focused Ultrasound (HIFU, or sometimes FUS for Focused UltraSound) is a highly precise medical procedure that applies high-intensity focused ultrasound energy to locally heat and destroy diseased or damaged tissue through ablation.

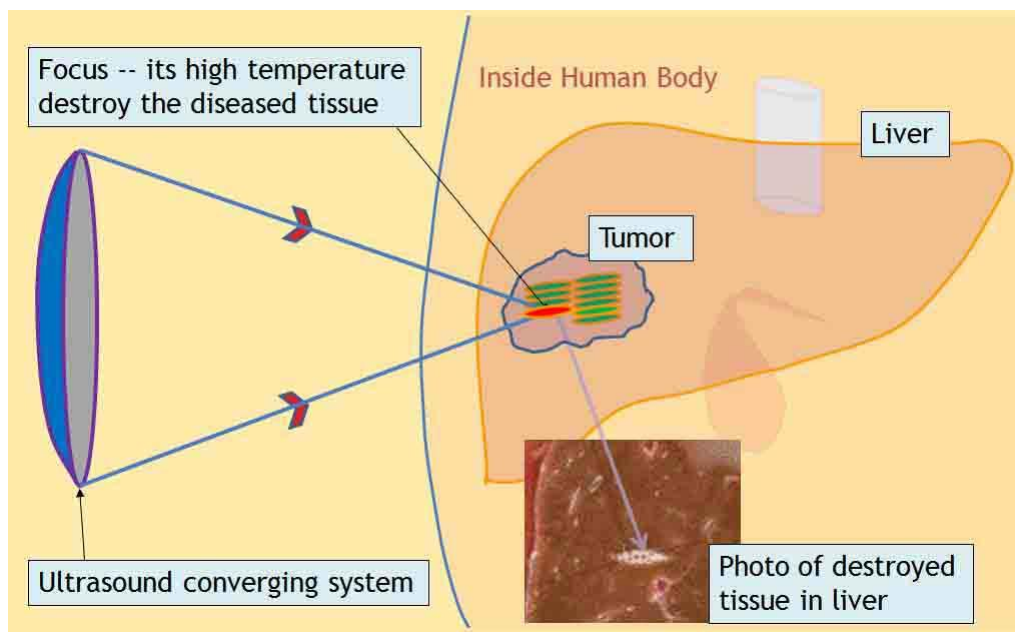


Figure 6.2. HIFU working principle.

This technology, thanks to a variety of biological effects in tissue, enables the treatment of a wide range of clinical conditions.

Much like a magnifying glass focusing multiple beams of light onto a single point, focused ultrasound (FUS) concentrates converging beams of ultrasound energy with extreme precision onto a target deep in the body that can be as small as 1 mm in diameter. As individual beams pass through most intervening tissues, there is no effect; however, when the beams converge, there is a profound effect produced by the thermal and/or mechanical mechanisms of FUS. HIFU has the potential to provide truly non invasive surgery, an alternative or complement for radiation therapy, the means to dissolve blood clots, or a way to deliver drugs in high concentration to a precise point in the body. Treatments can be performed in an outpatient setting without ionizing radiation, general anaesthesia, incisions or scars, therefore resulting in minimal pain and discomfort, and recovery with fewer complications compared with conventional surgery or radiation therapy.

Following more than a decade of basic science research, the first clinical use of HIFU was in the neurosurgical treatment of movement disorders, neuropathic pain and hypersensitivity in 1958. These early experimental treatments were planned with radiographic imaging of the stereotactic-mounted piezoelectric emitters and executed without real-time image guidance or temperature feedback. The treatment was also invasive and required the drilling of burr holes through the skull, allowing ultrasound transmission into the brain tissue. The next documented clinical application of HIFU was in the treatment of glaucoma in the 1980s. These treatments were performed with the first US FDA-approved high-intensity FUS device, which was coupled with a diagnostic ultrasound and fiber optic system for aiming the therapy transducer. The system was not equipped with the capability to monitor temperature.

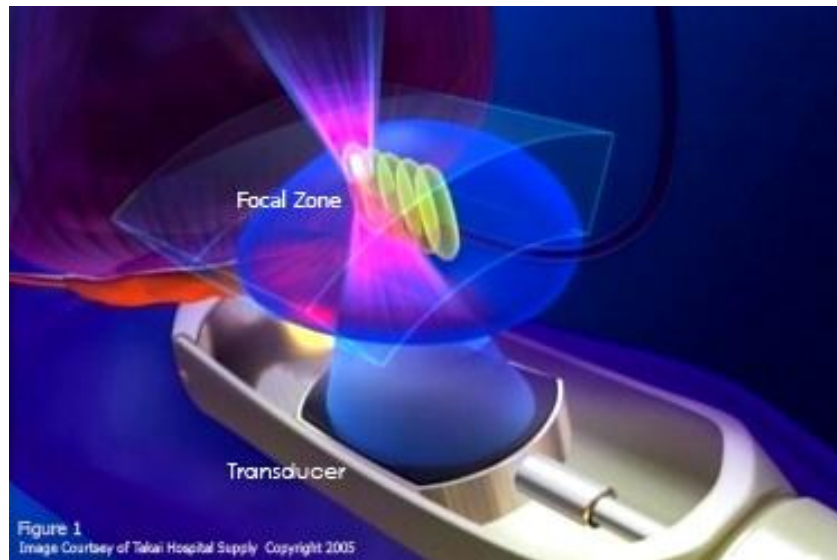


Figure 6.3. HIFU as an alternative treatment for localized prostate cancer.

Vallancien *et al.* conducted a FUS clinical study to treat bladder cancer in five patients in 1991. The investigator moved on the following year to treat the prostate, kidneys and liver. The system used diagnostic ultrasound for planning, but lacked real-time monitoring during the therapeutic application. Temperature was monitored by thermocouples inserted under ultrasonic (in the case of the prostate) or endoscopic guidance.

Shortly after its initial use in the treatment of uterine fibroids, techniques to correct for skull bone acoustic aberration were formally described and proven. This rekindled clinical interest in the original, neurosurgical indications for which FUS saw its first inhuman use. Following the publication of this method, commercial products incorporated the technique and began seeing successful use in clinical trials addressing neuropathic pain in 2009 and other clinical indications in the field of functional neurosurgery.

6.3.2 HIFU mechanisms and bioeffects

Ultrasound can be focused, either via a lens (for example, a polystyrene lens), a curved transducer, or a phased array (or any combination of the three) into a small focal zone, in a similar way to focusing light through a magnifying glass focusing light rays to a point.

With HIFU, for a given transducer there is a direct tradeoff between the frequency of the ultrasound waves, the penetration depth, and the sharpness of the lesion. Ultrasound intensity for a plane-wave beam propagating in an absorbing medium attenuates (scatters and absorbs) exponentially

$$I = I_0 e^{-\mu x}$$

where I is the intensity at any point x and I_0 is the intensity at the origin. The intensity attenuation coefficient, μ , describes the attenuation per unit length.

μ is a power-law function of frequency,

$$\mu = af^b$$

where a and b are constants specific to the medium, and f is the frequency. This relationship means that increasing the ultrasound frequency increases the absorption, i.e., more heating occurs per unit length, and also decreases the possible depth of penetration. The intensity at the focus is reduced due to prefocal absorption. Likewise, a decrease in frequency increases the penetration of the beam, but makes it more difficult to create a sharply defined thermal focus.

The attenuation coefficient also changes in tissue which has been coagulated, making it more difficult to ablate tissue which is located downstream of tissue which has already been ablated.

Thus, the optimal frequency for HIFU varies by treatment and (for a given transducer radius of curvature) is always a balance between penetration depth and the ability to create a focus. It should also be noted that the sharpness of the focus also depends on geometric factors, such as the radius of curvature of the transducer, so there can be a complex set of engineering tradeoffs involved in developing a system.

Also, this demonstrates that tissue heating is proportional to the intensity and the intensity is inversely proportional to the area over which an ultrasound beam is spread, which is why focusing the beam into a sharp point (i.e. increasing the beam intensity) creates a rapid temperature rise at the focus.

However, because ultrasound is a mechanical pressure wave that successively increases and decreases pressure in the tissue, a high pressure change due to the use of high-intensity ultrasound can induce various mechanical effects – from vibration of the target to cavitation. Cavitation describes the interaction of the ultrasonic energy with microbubbles in the tissue. Depending on the clinical application, microbubbles can either be injected into the blood stream or injected directly into the tissue. The sharp change in local pressure caused by FUS transmission can also create

microbubbles in the tissue. Although HIFU remains an early stage technology, significant progress has been made in advancing this medical therapy platform towards clinical adoption for the treatment of a wide range of conditions.

6.4 Sonotrode horn shaping

In the previous chapters we saw that the ultrasound beam can be focused in two ways:

- Electronically, by adjusting the relative phases of elements in an array of transducers (a "phased array").
- Geometrically, for example with a lens or with a spherically curved transducer.

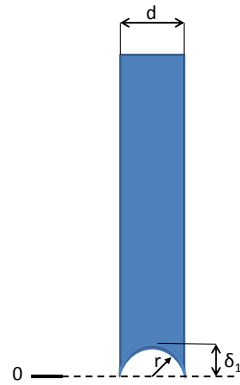
What we would like to do, is to reproduce the geometrical effect in the shape of the horn of the sonotrode.

So using Solidworks, different tip shapes have been created, with different heights and different radius values. The radius selected have been respectively $r_a = \frac{d}{2} = 3,15$ and $r_b = d = 6,3$.

In regard to the heights chosen, here is an explanation of the differences between the physical models, where the zero line represents the initial height of the sonotrode tip:

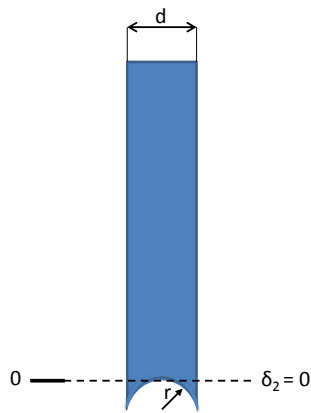
- $\delta_1 = \frac{d}{2} = 3,15$:

this is the maximum positive δ considered.



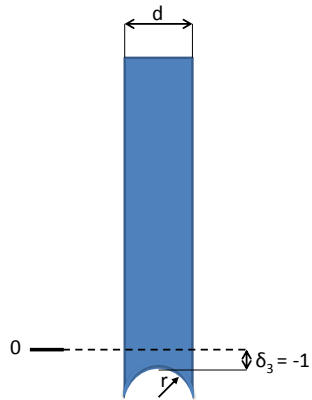
- $\delta_2 = 0$:

in this case the peak of the curvature reaches the zero line.



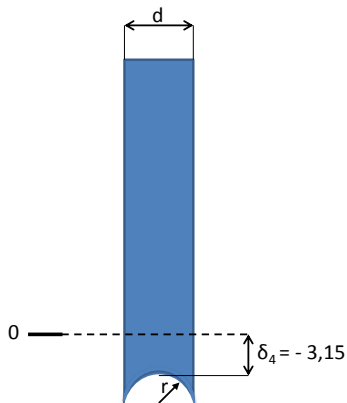
- $\delta_3 = -1$:

this is the case where the mass of the modified sonotrode tip coincide to the initial mass of the original sonotrode tip (73,5 g).



- $\delta_4 = -\frac{d}{2} = -3,15$:

this is the minimum δ value considered.



6.5 FEM analysis

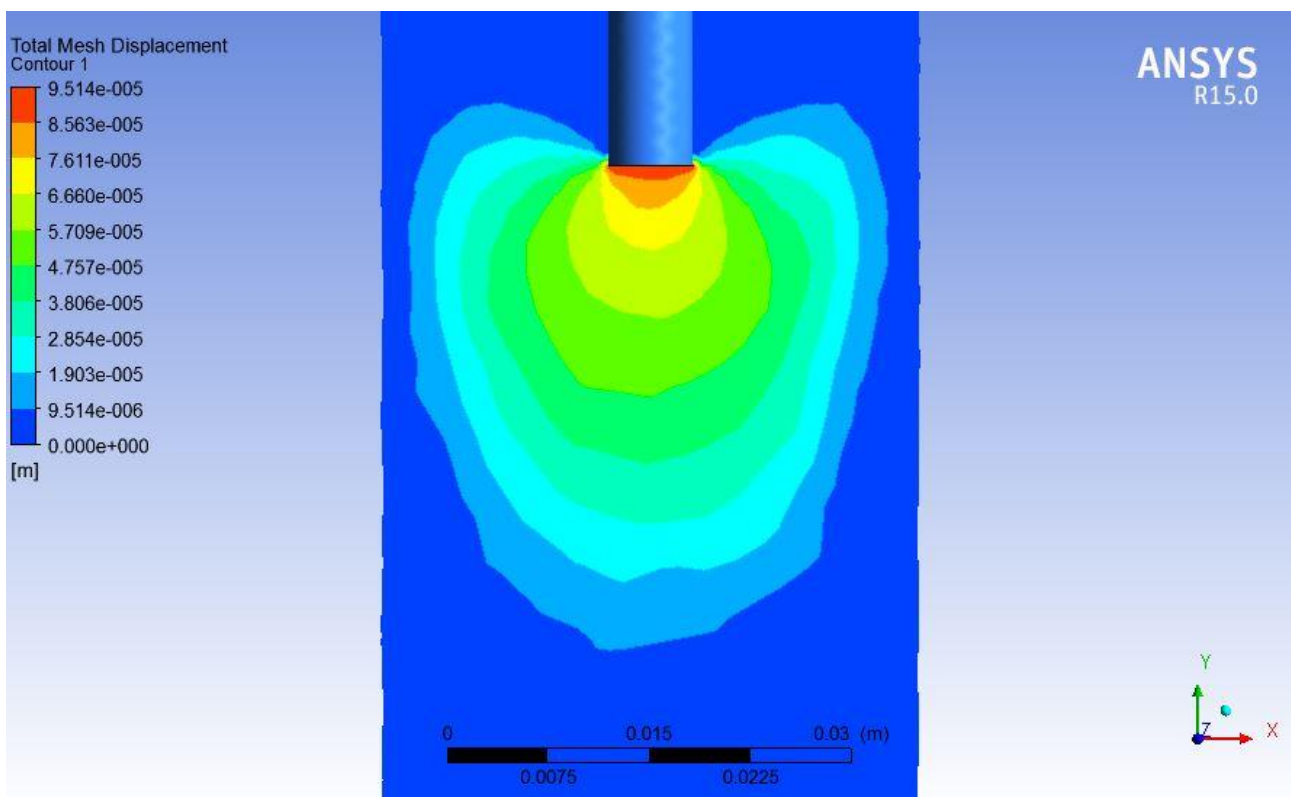
Realized the geometry of the modified sonotrode tip, the effects of the curvature on the ultrasound propagation in water where analyzed. Through the use of Solidworks and Ansys CFX, a water domain has been created, and then a mesh with tetrahedrons has been realized.

In regard to the sonotrode domain, it has been defined as “*immersed solid*”, while for the water domain, standard values of water at 25°C has been selected.

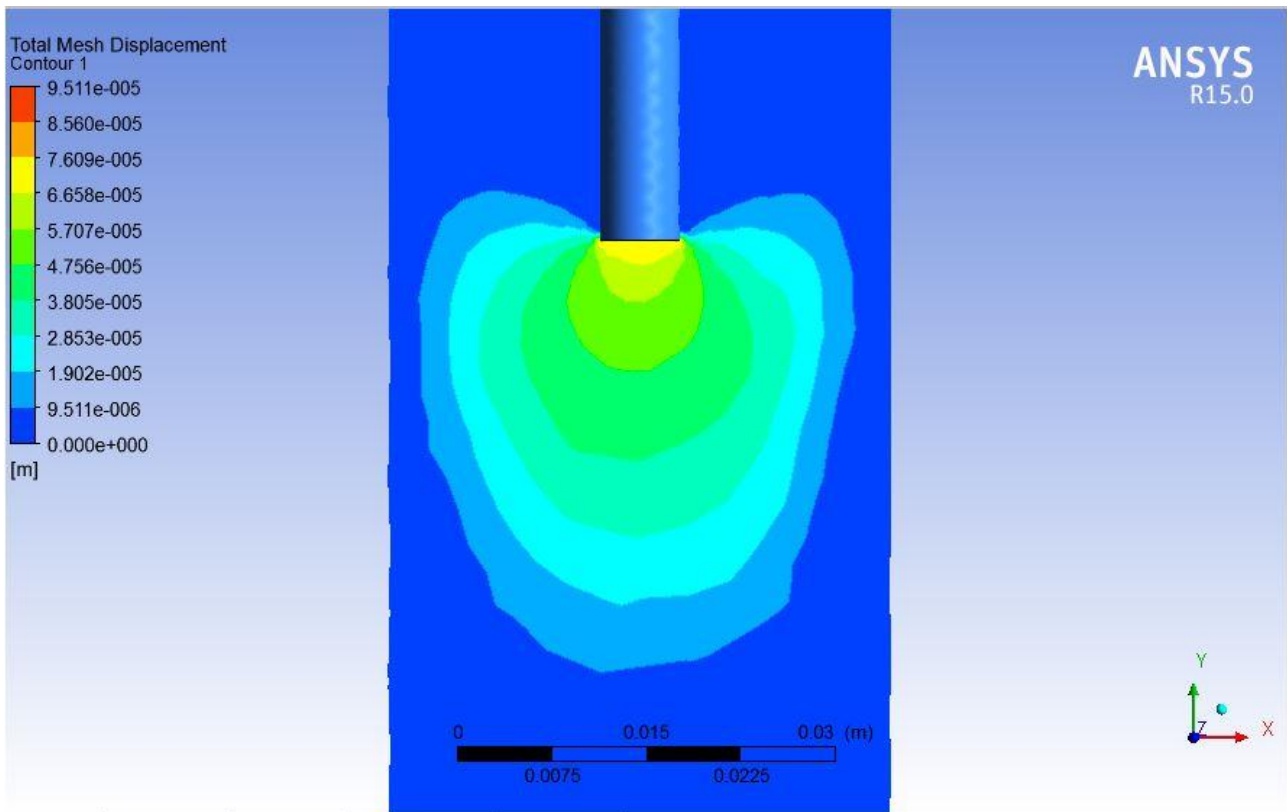
Giving a periodic displacement to the sonotrode extremity, and defining the mesh as a “*region of motion*”, the solution process took place.

6.6 Results

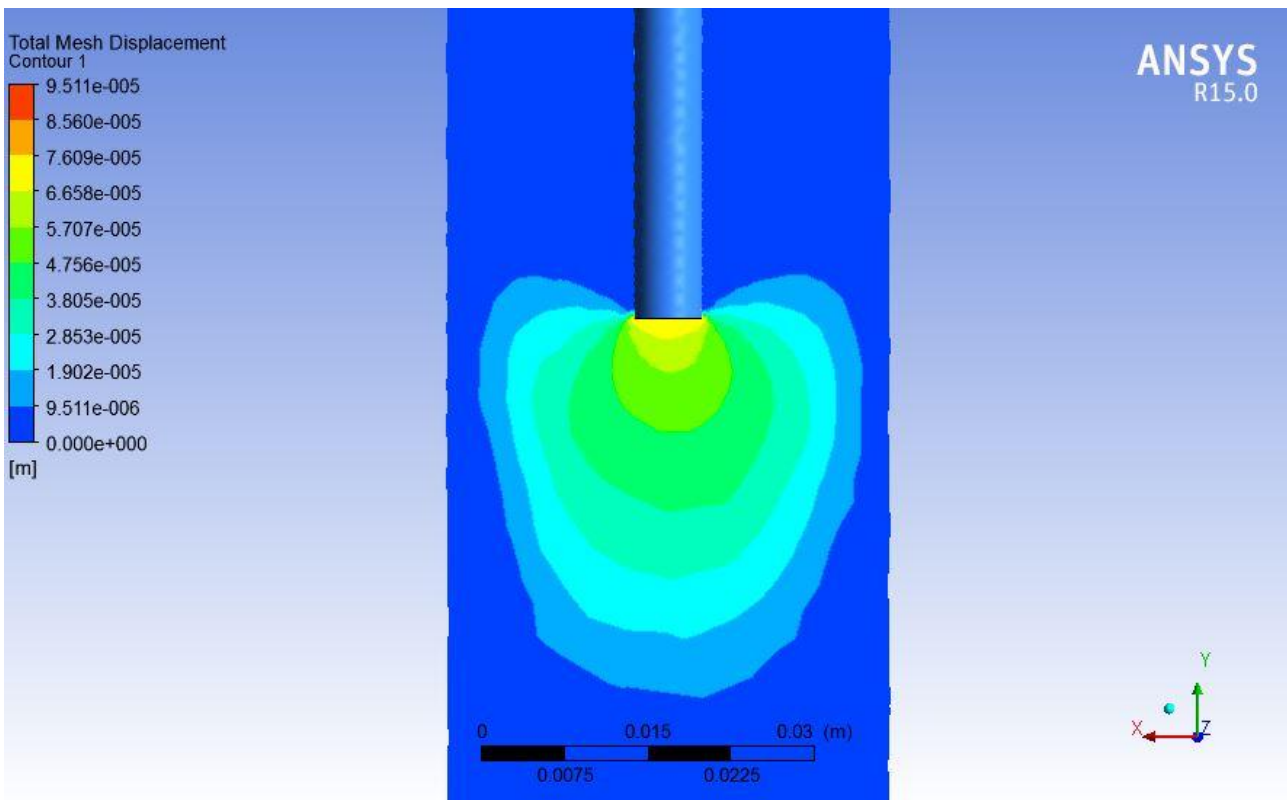
In the “*Results*” section of Ansys CFX, we noticed that the contour analysis confirmed the sound wave focusing, due to the geometrical curvature of the sonotrode tip.



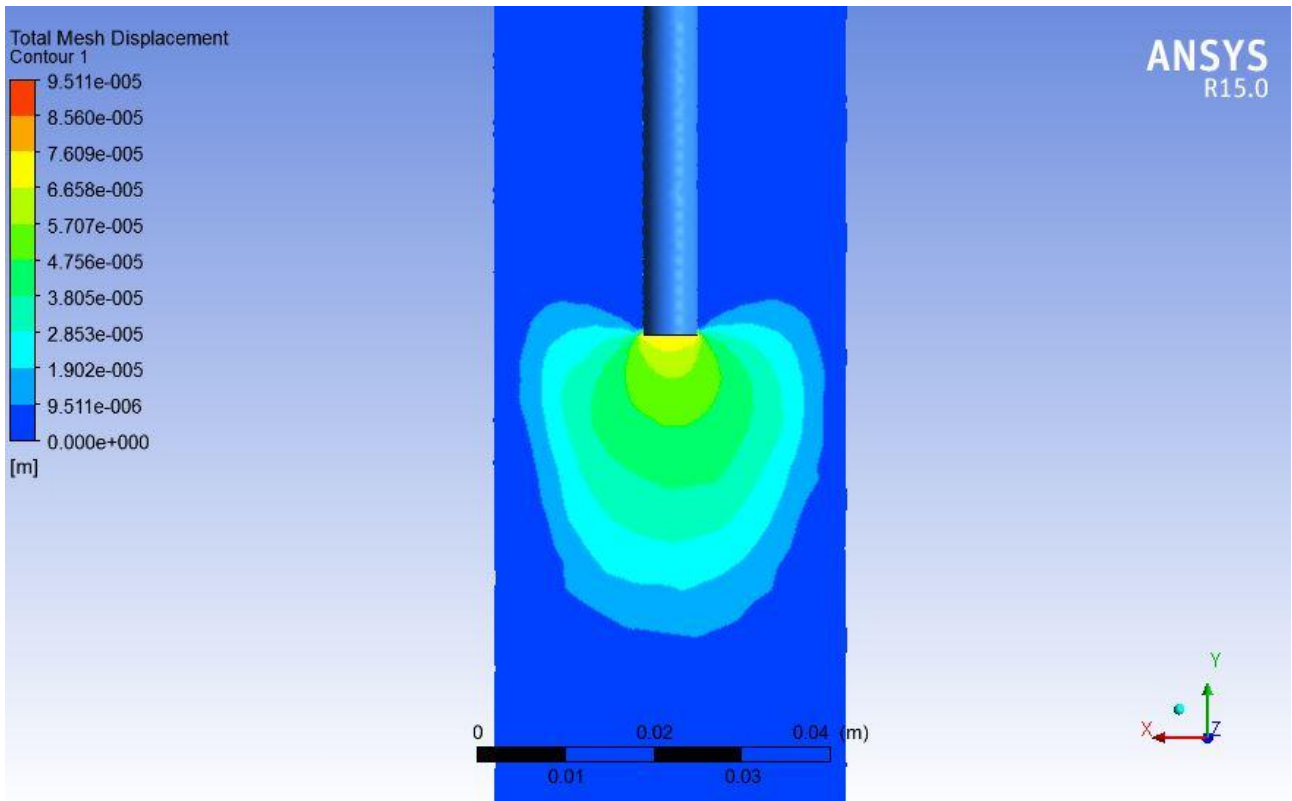
6-1 Mesh displacement of the fluid with r_a and δ_1



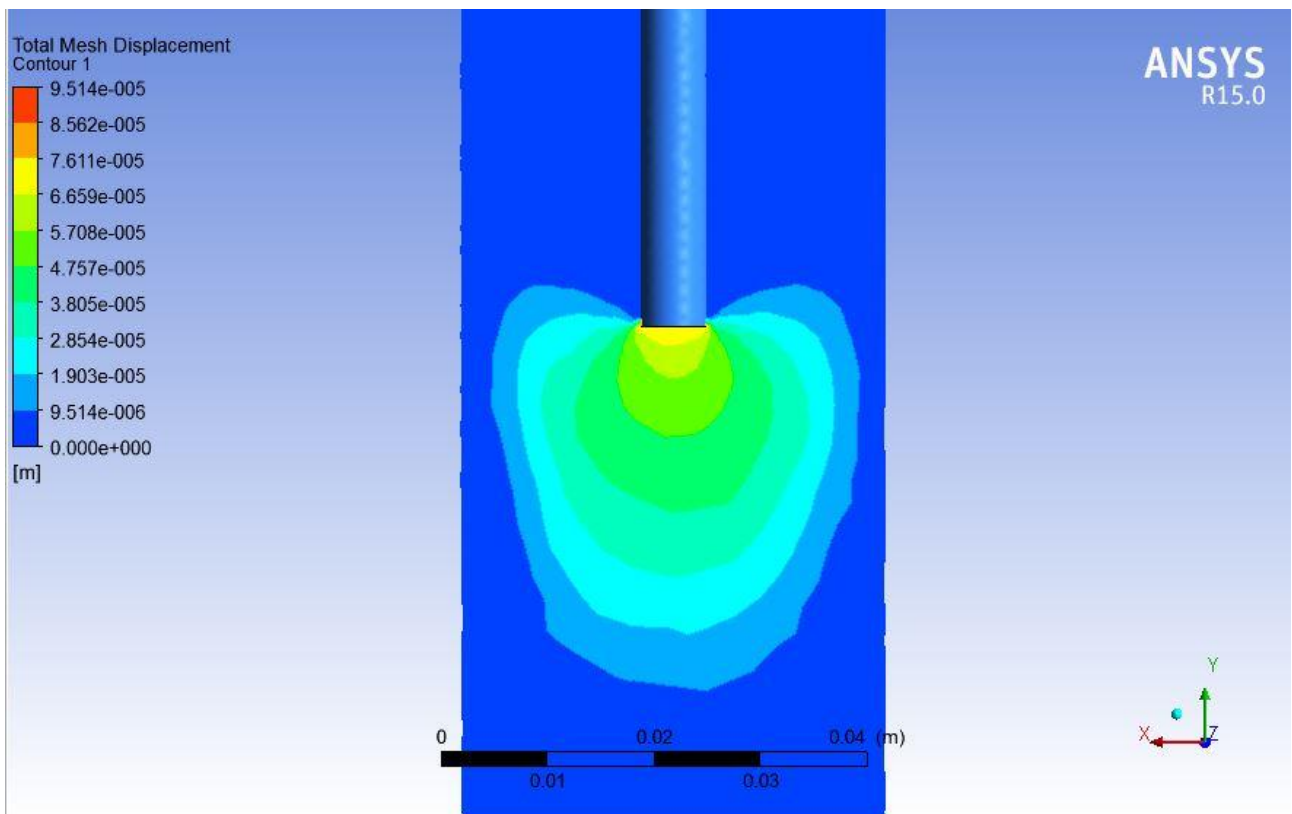
6-2 Mesh displacement of the fluid with r_b and δ_1



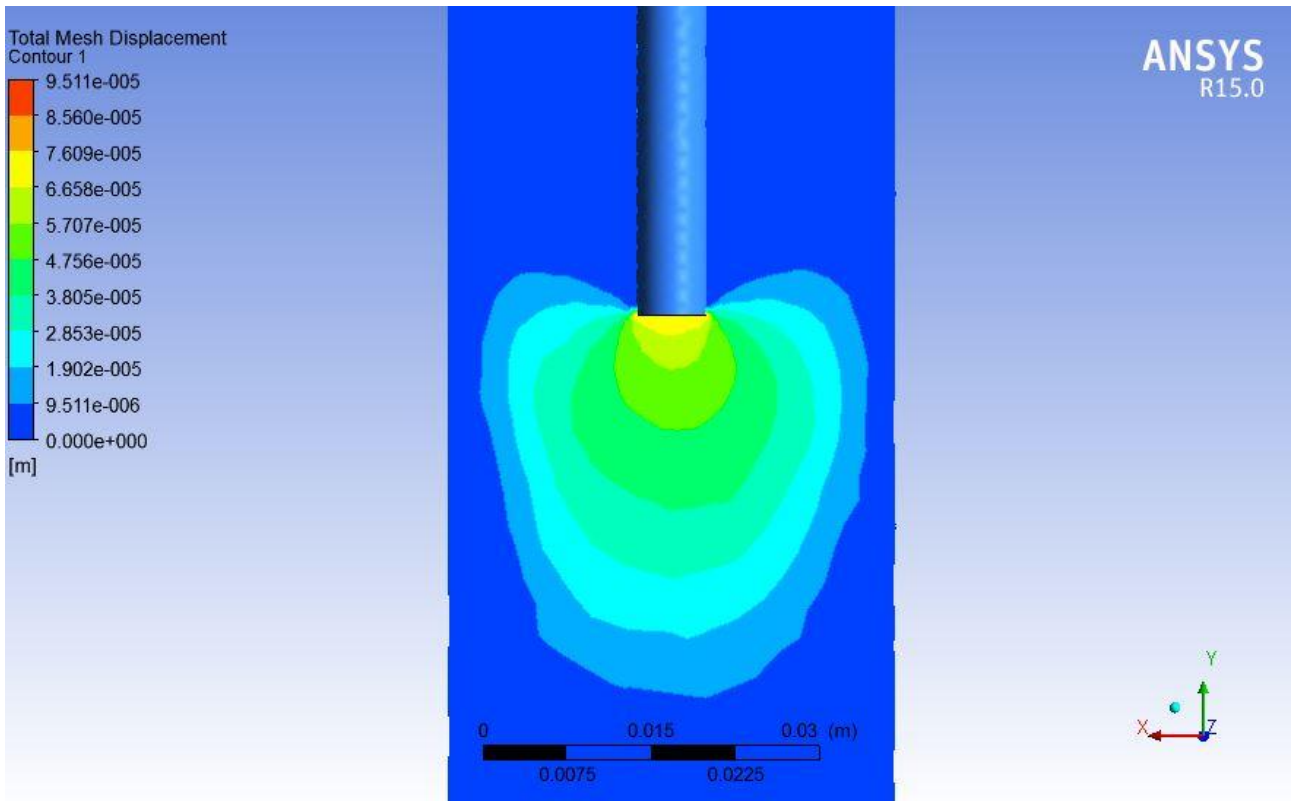
6-3 Mesh displacement of the fluid with r_a and δ_2



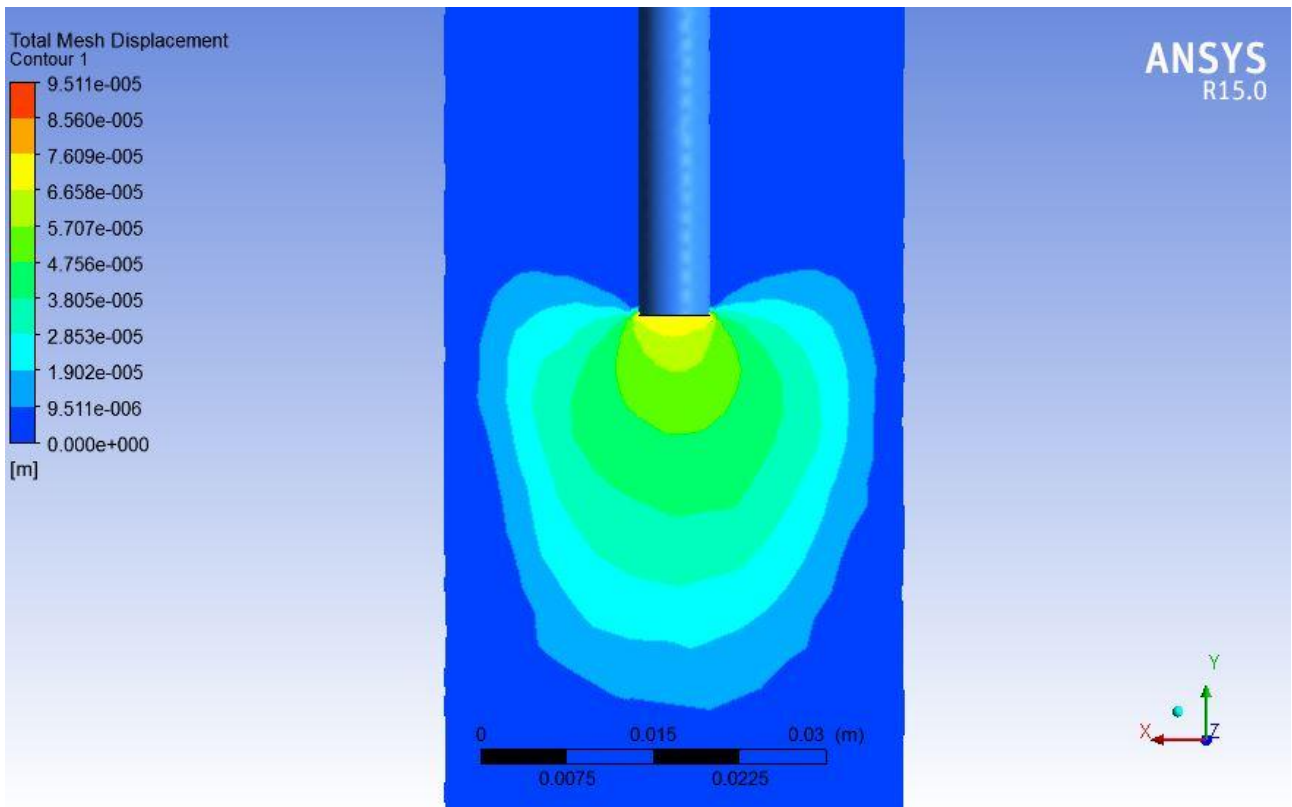
6-4 Mesh displacement of the fluid with r_b and δ_2



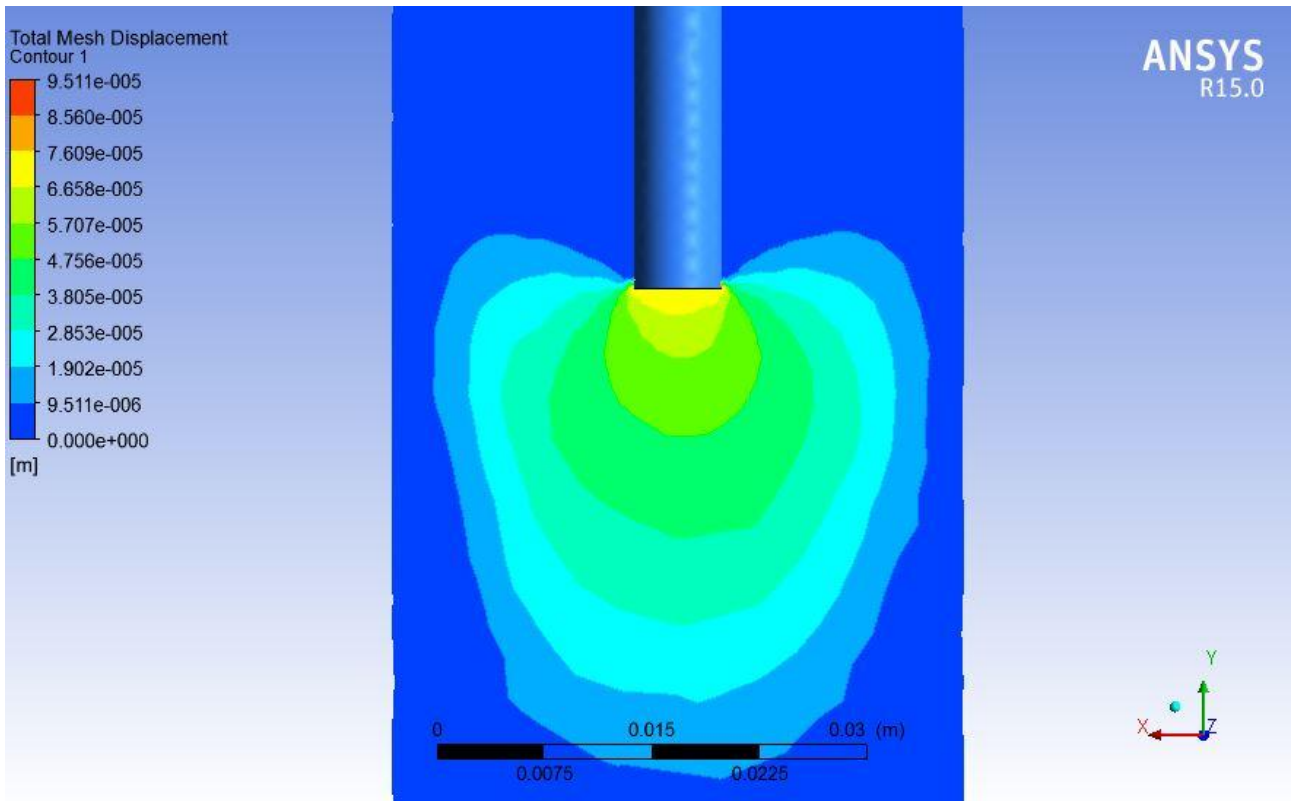
6-5 Mesh displacement of the fluid with r_a and δ_3



6-6 Mesh displacement of the fluid with r_b and δ_3











6-7 Mesh displacement of the fluid with r_a and δ_4



6-8 Mesh displacement of the fluid with r_b and δ_4

Hereafter is a chart clearly showing the focusing points through the mesh displacement of the fluid, depending on the radius of the curvature and the height chosen.

	$\delta_1 = \frac{d}{2} = 3,15$	$\delta_2 = 0$	$\delta_3 = -1$	$\delta_4 = -\frac{d}{2} = -3,15$
$r_a = \frac{d}{2} = 3,15$				
$r_b = d = 6,3$				

7 Conclusion and future works

7.1 Conclusion

The methods proposed in this work represent a valuable alternative to traditional manufacturing methods of foam-like materials like polyurethane, polystyrene and wax.

Furthermore, other foam-like materials can be machined with the operation method proposed in this study, and this could be an alternative 3D modeling, at least for shaping and simple machining operations. In facts, depending both on the input parameters and on the material type, simple traditional operations like drilling of holes can be performed with encouraging results.

This has been confirmed thanks to dimensional analyses comparison and material analyses. The first ones have been helpful for understanding the quality of the manufacturing process, while the second analyses made possible to understand the physics behind the manufacturing process.

The dimensional analyses revealed that grooving operation performed on Polystyrene and Polyurethane has a good precision level, if considered together with the limitations of the physical properties of materials shaped. Vice versa the milling operation has some clear limitations both for Polystyrene and for Polyurethane. The most important limitation lies in the trajectories calculated by the software for the Polystyrene sample, while for Polyurethane the limitation is due to the physical properties of the material itself.

Of particular interest, as regards ultrasound processes, is the absence of dust and debris, which results in a considerable advantage for industries interested in shaping of these types of material.

In underwater tests, the surface finish has also been analyzed showing, for a given combination of working parameters, an improvement with respect to in-air machined samples. The operation is accomplished due to a combination of mechanical effects (contact and cavitation) and thermal effects (heat generation) for what concern Polystyrene and Polyurethane, while heat seems to be the main factor of the manufacturing operation for wax.

Even if the surface quality is not comparable to traditional machining operation on metallic or plastic materials, ultrasound machining can be helpful in some pre-processing phases, where the largest quantity of material has to be removed. By using traditional milling and drilling operation, debris can cause problems, while the proposed methodology does not create dust and debris.

7.2 Future works

This study is still a first step toward enhancing the understanding of procedures for the achievement of well-shaped workpieces. Future works will focus on improving the manufacturing quality of a wider set of materials. It could be interesting to analyze the possibility of using a different type of Polyurethane, commonly known as blue foam, for the creation of workpieces with improved dimensional precision.

In ultrasound machining, it would seem that heat is the main factor of the manufacturing operation, but more detailed studies will be carried out in future research activities. Actually the presence of apertures below the machined surface could seem a symptom of cavitation, but deeper analysis has to be performed.

Other ongoing activities focus on the implementation of force control on the translation speed of the stage, both for drilling and for other manufacturing operations like milling. It will allow the research team to optimize the process also for the case of 3D simple shape manufacturing.

Future works will also study the behaviour of machined materials (especially for wax) in cold water and in other liquid solutions, measuring how the temperature affects loads and surface finishing.

8 BIBLIOGRAFIA

- [1] Medis PS and Henderson HT. "Micromachining using ultrasonic impact grinding." *Journal of micromechanics and microengineering* Vol 15, No .8, 2005, pp 1556.
- [2] Ouyang PR et al. "Micro-motion devices technology: The state of arts review." *The International Journal of Advanced Manufacturing Technology* Vol 38, No .5-6, 2008, pp 463-478.
- [3] Underwood, John R., Jack Robert Auld, and John Christopher Huculak. "Vitreotomy probe with adjustable cutter port size." U.S. Patent Application 13/218,923.
- [4] Dorawa, Klaus, et al. "Device for fixation of bone fractures." U.S. Patent Application 14/012,199.
- [5] Michaeli, Walter, Thomas Kamps, and Christian Hopmann. "Manufacturing of polymer micro parts by ultrasonic plasticization and direct injection." *Microsystem Technologies* 17.2 (2011): 243-249.
- [6] Lanin VL, "Ultrasonic soldering in electronics", *Ultrasonics sonochemistry*, Vol. 8, No. 4, 2001, pp. 379-385.
- [7] Boukerrou, Amar, et al. "Processing of mica/epoxy nanocomposites by ultrasound mixing." *Journal of applied polymer science* 105.3 (2007): 1420-1425.
- [8] Duru, Nicolas, Marion Prunier, and Pascal Tierce. "Spray head including a sonotrode." U.S. Patent No. 8,556,191. 15 Oct. 2013.
- [9] DEKETELE, Lieven, et al. "Enhanced ultrasonic cleaning devices." 2002.
- [10] BÜTTIKER, Albert; KELLER, Holger; BATES, Darren. Sonotrode and device for reducing and eliminating foaming of liquid products. U.S. Patent Application 13/675,638, 2012.

- [11] Eggers G, Klein J, Blank J and Hassfeld S, "Piezosurgery: an ultrasound device for cutting bone and its use and limitations in maxillofacial surgery", *British Journal of oral and maxillofacial surgery*, Vol. 42, No. 5, 2004, pp 451-453
- [12] Underwood JR, Auld JR and Huculak JC, "Vitreotomy probe with adjustable cutter port size", U.S. Patent Application 13/218,923, 2011
- [13] Ouyang PR, Tjiptoprodjo RC, Zhang WJ and Yang GS, "Micro-motion devices technology: The state of arts review", *The International Journal of Advanced Manufacturing Technology*, Vol. 38, No. 5-6, 2008, 463-478
- [14] Moriwaki T, Shamoto E and Inoue K, "Ultraprecision ductile cutting of glass by applying ultrasonic vibration", *CIRP Annals-Manufacturing Technology*, Vol. 41, No. 1, 1992, pp. 141-144
- [15] Lanin VL, "Ultrasonic soldering in electronics", *Ultrasonics sonochemistry*, Vol. 8, No. 4, 2001, pp. 379-385
- [16] Yang Z, Goto H, Matsumoto M and Maeda R, "Ultrasonic micromixer for microfluidic systems", *Micro Electro Mechanical Systems, 2000. MEMS 2000. The Thirteenth Annual International Conference on. IEEE*, 2000, pp. 80-85
- [17] Suslick KS and Gareth JP, "Applications of ultrasound to materials chemistry", *Annual Review of Materials Science*, Vol. 29, No. 1, 1999, pp. 295-326
- [18] Springall EG, "Apparatus for applying adhesive", U.S. Patent No. 5,366,309, 1994
- [19] Medis PS and Henderson HT, "Micromachining using ultrasonic impact grinding", *Journal of micromechanics and microengineering*, Vol. 15, No. 8, 2005, pp 1556
- [20] Benedict GF, "Nontraditional Manufacturing Processes, Manufacturing Engineering and Materials Processing", 3rd Edition, CRC Press, New York, 1987
- [21] Marty C, "Usinages par procédés non conventionnels", Masson, 1971
- [22] Duval DL, Van Hauwermeiren T, Gaaloul S, Deketele LR and Mcdonald MR, "Enhanced ultrasonic cleaning devices", U.S. Patent No. 7,004,182, 2006

- [23] Fantoni G, Tilli J, Belo FA and Ishak R, "Shaping of foam-like materials through the use of A sonotrode", International Conference on Innovative Design and Manufacturing, Montréal, Canada, 2014
- [24] Kraft A, Blaschke M and Kreysig D, "Electrochemical water disinfection Part III: Hypochlorite production from potable water with ultrasound assisted cathode cleaning", *Journal of applied electrochemistry*, Vol. 32, No. 6, 2002, pp 597-601
- [25] Mason TJ, Joyce E, Phull SS and Lorimer JP, "Potential uses of ultrasound in the biological decontamination of water", *Ultrasonics Sonochemistry*, Vol. 10, No. 6, 2003, pp. 319-323
- [26] Jafari SM, He Y and Bhandari B, "Production of sub-micron emulsions by ultrasound and microfluidization techniques", *Journal of Food Engineering*, Vol. 82, No. 4, 2007, pp. 478-488
- [27] Zhou Q, Zhang X and Xiao J, "Ultrasound-assisted ionic liquid dispersive liquid-phase micro-extraction: A novel approach for the sensitive determination of aromatic amines in water samples", *Journal of Chromatography A*, Vol. 1216, No. 20, 2009, pp. 4361-4365
- [28] Phull SS, Newman AP, Lorimer JP, Pollet B and Mason TJ, "The development and evaluation of ultrasound in the biocidal treatment of water", *Ultrasonics sonochemistry*, Vol. 4, No. 2, 1997, pp. 157-164
- [29] Skogsmo JB, Van Reatherford L, Popoola OO, Jahn R and Kiridena VS, "Sonotrode for ultrasonic welding apparatus", *U.S. Patent No. 6,691,909*. Washington, DC: U.S. Patent and Trademark Office, 2004
- [30] Bianchetti F, "Dental hand instrument with incorporated light source for diagnostic purposes", *U.S. Patent No. 6,095,810*. Washington, DC: U.S. Patent and Trademark Office, 2000
- [31] Cardoni A, "Enhancing oral implantology with power ultrasonics", *Ultrasonics, Ferroelectrics and Frequency Control, IEEE Transactions on*, Vol. 57, No. 9, 2010, pp. 1936-1942

- [32] Boy JJ, Andrey E, Boulouize A and Khan-Malek C, “Developments in microultrasonic machining (MUSM) at FEMTO-ST”, *The International Journal of Advanced Manufacturing Technology*, Vol. 47, No. 1-4, 2010, pp. 37-45
- [33] Singh R and Khamba JS, “Ultrasonic machining of titanium and its alloys: a review”, *Journal of Materials Processing Technology*, Vol. 173, No. 2, 2006, pp. 125-135
- [34] Benedict GF, “Nontraditional Manufacturing Processes, Manufacturing Engineering and Materials Processing”, 3rd Edition, CRC Press, New York, 1987
- [35] Moussatov A, Granger C and Dubus B, “Cone-like bubble formation in ultrasonic cavitation field”, *Ultrasonics sonochemistry*, Vol. 10, No. 4, 2003, pp. 191-195

8.1 References

1. Chemat, F. and M.K. Khan, Applications of ultrasound in food technology: processing, preservation and extraction. *Ultrasonics Sonochemistry*, 2011. **18**(4): p. 813-835.
2. Duval, D.L., et al., Enhanced ultrasonic cleaning devices, 2006.
3. Schlottig, F. and U. Werner, Device and method for the amelioration of recesses, 2009, Nexilis Ag.
4. Stoffel, M. and U. Werner, Sonotrode for the introduction of ultrasonic energy, 2012, Nexilis Ag.
5. Babaev, E., Apparatus and methods for pain relief using ultrasound energized polymers, 2006, Babaev, Eilaz.
6. Gehling, S.C., et al., Apparatus for fabricating garments, 1997, Kimberly-Clark Worldwide, Inc.
7. Medis, P.S. and H.T. Henderson, Micromachining using ultrasonic impact grinding. *Journal of micromechanics and microengineering*, 2005. **15**(8): p. 1556.

8. Benedict, G.F., Nontraditional manufacturing processes. Vol. 19. 1987: CRC Press.
9. Shoh, A., Welding of thermoplastics by ultrasound. *Ultrasonics*, 1976. **14**(5): p. 209-217.
10. Marty, C., *Usinages par procédés non conventionnels* 1971: Masson.
11. Fantoni, G., et al., Shaping of foam-like materials through the use of a sonotrode, in *ICIDM 2014* 2014: Montréal, Canada.
12. Tilli, J., G. Fantoni, and S. Currenti, Underwater drilling of foam-like materials and wax using ultrasound technology, in *ICIDM 2014* 2014: Montréal, Canada.
13. Marshall, D.C., G.E. Merz, and W.S. Stewart, Ultrasonic apparatus for forming individual pillowed chips of light lock material, 1995, Eastman Kodak Company.
14. Van Eperen, D.J., Apparatus for mechanically bonding and cutting an article, 2008, Kimberly-Clark Worldwide, Inc.
15. Lee, W. and J. Park, Augmented foam: touchable and graspable augmented reality for product design simulation. *Japanese Society for Science of Design*, 2006. **52**(6): p. 17-26.
16. Barone, S., A. Paoli, and A.V. Razionale, Creation of 3D multi-body orthodontic models by using independent imaging sensors. *Sensors*, 2013. **13**(2): p. 2033-2050.
17. Barone, S., A. Paoli, and A.V. Razionale, Computer-aided modelling of three-dimensional maxillofacial tissues through multi-modal imaging. *Proceedings of the Institution of Mechanical Engineers, Part H: Journal of Engineering in Medicine*, 2013. **227**(2): p. 89-104.

[36] J. Lighthill, Acoustic streaming, *Journal of Sound and Vibration* 61 (3) (1978) 391–418

[37] <http://www.fusfoundation.org/the-technology/overview>

[38] Foley, J., et al., Image-guided focused ultrasound: state of the technology and the challenges that lie ahead. *Imaging Med.* (2013) 5(4), p. 357–370.

- [39] Madersbacher, S., et al., Effect of High-Intensity Focused Ultrasound on Human Prostate Cancer in Vivo. *Cancer research* 55, p. 3346-3351.
- [40] Illing, R. O., et al., The safety and feasibility of extracorporeal high-intensity focused ultrasound (HIFU) for the treatment of liver and kidney tumours in a Western population. *British Journal of Cancer* (2005) 93, p. 890 – 895